12-2017

Experimental and Simplified Analytical Investigation of Full Scale Sandwich Panel Walls

Salam Adil Al-Rubaye
Utah State University

EXPERIMENTAL AND SIMPLIFIED ANALYTICAL INVESTIGATION OF FULL SCALE SANDWICH PANEL WALLS

by

Salam Al-Rubaye

A thesis submitted in partial fulfillment
of the requirements for the degree

of

MASTER OF SCIENCE

in

Civil Engineering

Approved:

_____	_____
Marc Maguire, Ph.D. Major Professor	Joseph A. Caliendo, Ph.D. Committee Member
_____	_____
Paul Barr, Ph.D. Committee Member	Mark R. McLellan, Ph.D. Vice President for Research and Dean of the School of Graduate Studies

UTAH STATE UNIVERSITY
Logan, Utah

2017

ABSTRACT

Experimental and Simplified Analytical Investigation of Full Scale Sandwich Panel Walls

by

Salam Adil. Al-Rubaye, Master of Science

Utah State University, 2017

Major Professor: Dr. Marc. Maguire
Department: Civil and Environmental Engineering

Concrete sandwich wall panels have been used for decades in the precast concrete construction industry because of their thermal efficiency. To achieve full or partial-composite action in concrete sandwich panel walls, the engineer must obtain a percent composite action from a connector manufacturer, making some engineers uncomfortable. Engineers are dependent upon the recommendations given by the connector manufacturers to establish their designs. This project tested six full scale sandwich panel walls to evaluate the percent composite action of various connectors and compare the results to those provided by the composite connector manufacturers.

This project aimed to validate current procedures using these methods, and to develop simpler, more efficient methods for predicting overall strength of this innovative building system. This study concluded that the reported degrees of composite action from each manufacturer are considered conservative in all instances for the connectors tested. Additionally, the intensity and type of connectors are important factors in determining the degree of partial composite action in a panel.

Two methods to predict elastic deformations and cracking were developed (the Beam-Spring model and the Elastic Hand Method) and were compared to the elastic portions of the full-scale testing performed in this study, yielding promising results. Anew method (the Partially-Composite Strength Prediction Method) was also created to predict the nominal moment capacity of concrete sandwich wall panels that is easier to implement than current methodologies and shown to be accurate. The results of this method were also compared to the full-scale testing results in this study. Design and analysis examples using these methods are presented in this report.

(216 pages)

PUBLIC ABSTRACT

Experimental and Simplified Analytical Investigation of Full Scale Sandwich Panel Walls

Salam Adil. Al-Rubaye

Concrete sandwich wall panels have been used for decades in the precast concrete construction industry because of their thermal efficiency. To achieve full or partial-composite action in concrete sandwich panel walls, the engineer must obtain a percent composite action from a connector manufacturer, making some engineers uncomfortable. Engineers are dependent upon the recommendations given by the connector manufacturers to establish their designs. This project tested six full scale sandwich panel walls to evaluate the percent composite action of various connectors and compare the results to those provided by the composite connector manufacturers.

This project aimed to validate current procedures using these methods, and to develop simpler, more efficient methods for predicting overall strength of this innovative building system. This study concluded that the reported degrees of composite action from each manufacturer are considered conservative in all instances for the connectors tested. Additionally, the intensity and type of connectors are important factors in determining the degree of partial composite action in a panel.

DEDICATION

For women and children in wars

For my country

For my family

ACKNOWLEDGMENTS

The author is grateful to the HCED (Higher Committee for Education Development in Iraq) to their financially and emotionally support for his master study.

A very special gratitude goes out to Dr. Maguire for all his guidance, patience, and academically and emotionally support to doing the research. I thank my committee members Dr. Paul Barr and Dr. Joseph Caliendo for all their help.

The author is very grateful to the Precast/Prestressed Concrete Institute and the Daniel P. Jenny Fellowship that funded this work. All connectors and foam was donated by the respective companies, THiN Wall, Thermomass and HK Composites. Mark Lafferty, Maher Tadros (THiN Wall) Jordan Keith, Dave Keith (HK Composites) and Venkatesh Sheshappa (Thermomass) were very helpful. This thesis is not an endorsement by the authors or Utah State University of any manufacturer or system.

Forterra Structural Precast in Salt Lake City, Utah fabricated four of the six panels and Concrete Industries in Lincoln, Nebraska provided the other two. The support from these precast producers was integral to project completion. Several undergraduate and graduate students deserve thanks for their volunteer work: Hannah Young, Parker Syndergaard, Ethan Pickett, Hunter Buxton, Tyson Glover, Mohamed Shwani and Sattar Dorafshan.

Salam Al-Rubaye

CONTENTS

Page

LIST OF TABLES

LIST OF FIGURES

Figure Page

Figure Page

Figure Page

Figure Page

Figure Page

DEFINITIONS AND SYMBOLS

The following symbols are used in this paper.

A_{ps}	area of prestressing steel in wythe
A_s	area of mild steel in wythe
b	slab width
C	compression force in wythe
c	depth to neutral axis of wythe from top of wythe
d_1	effective depth of steel in wythe from furthest compression fiber of concrete
E_c	modulus of elasticity of concrete
E_s	modulus of elasticity of steel
F_E	elastic load limit
F_i, $F(i)$	shear force in connector in connector line i
F_{sum}	total shear force, the sum of connector forces in longitudinal location of interest
F_u	ultimate capacity/strength or peak load
f_c'	concrete compressive strength
f_{ps}	stress in prestressing steel in wythe
f_{pu}	ultimate stress of prestressing strands
f_r	modulus of rupture of concrete (psi)
f_s	stress in mild steel in wythe
f_t	concrete tensile strength

f_y	steel yield stress
I_{test}	experimental moment of inertia of sandwich panel
I_{NC}	theoretical moment of inertia of the non-composite sandwich panel
I_{FC}	theoretical moment of inertia of the fully-composite sandwich panel
i	connector line starting at end of panel
K_d	degree of composite action depending on deflection
K_E	elastic stiffness
K_{Ei}	elastic stiffness of connectors in connector line i
K_{IE}	inelastic stiffness of plastic stiffness
K_{Mcr}	degree of composite action depending on cracking moment
K_{MN}	degree of composite action depending on maximum moment
L	total length of panel
$M_{cr,test}$	experimental cracking moment of sandwich panel
$M_{cr,NC}$	theoretical cracking moment of non-composite sandwich panel
$M_{cr,FC}$	theoretical cracking moment of fully-composite sandwich panel
M_{FC}	fully-composite moment
$M_{n,test}$	experimental maximum moment of sandwich panel
$M_{n,NC}$	theoretical maximum moment of non-composite sandwich panel
$M_{n,FC}$	theoretical maximum moment of fully-composite sandwich panel
$M_{service}$	moment calculated by service loads
M_{wy2}	cracking moment of wythe 2
N_i	number of connectors in connector line i

n	total number of connector rows in half of panel ($L/2$)
P_{we}	equivalent point load
$Span$	unsupported span length (support-to-support distance)
T	tension force in wythe
t_{insul}	thickness of insulation
t_{wy1}	thickness of wythe 1
t_{wy2}	thickness of wythe 2
w_c	unit weight of concrete (pcf)
w_{we}	equivalent distributed load
x_i	location of connector line i from end of panel
x_P	location of point load from end of panel
Z	distance between centroids of wythe 1 and 2
γ	unit weight of concrete (pcf)
Δ_{axial}	slip of wythes due to axial deformation at end connector
Δ_E	deflection corresponding to elastic load limit
Δ_{Rot}	slip of wythes due to bending at end connector
Δ_U	deflection corresponding to the ultimate capacity
δ_{end}	calculated slip at end connector
$\delta(i)$	slip in connector i
δ_{max}	actual slip in end connector
ε_c	strain in concrete
ε_{ps}	strain in prestressing steel

ε_s	strain in mild steel
ε_y	strain of mild steel at yielding
θ	angle of rotation (radians)
θ_{Pwe2}	angle of rotation for given equivalent point load (radians)
θ_{wwe2}	angle of rotation for given equivalent distributed load (radians)
φ	curvature of wythe

CHAPTER 1

INTRODUCTION

1.1. General

Concrete sandwich wall panels (SWPs) are increasing in popularity due to their thermal and structural efficiency and an increasing demand in society for energy-efficient buildings. SWPs are typically a precast concrete product and have all the advantages of precast concrete. In nearly all cases, SWPs consist of three layers: two concrete layers (known as wythes) and a layer of insulation in between. SWPs are designed to act non-composite, fully-composite, or partially composite, depending on the shear connector design used to transfer the shear force between the concrete layers. The connectors can provide varying levels of composite behavior. Although steel connectors have historically been quite common, fiber reinforced polymer (FRP) connectors have become more common due to their significantly superior thermal efficiency. SWPs can be cladding, load bearing or non-load bearing walls.

Some engineers prefer non-composite panels because they have less thermal bowing compared to fully composite panels. However, using non-composite panels does not make use of both wythes structural performance and can be less economical. Fully composite behavior can be achieved at the ultimate state for most proprietary wythe connectors. However, GFRP connectors struggle to achieve high apparent composite action at service loads, and realistically, this may only be accomplished by using the solid concrete zone or steel connectors, both of which create thermal bridging. Hence, partially composite panels are commonly used to avoid the thermal bridging and the thermal bowing load. To design the partially composite panels, the engineers use a given percent

of composite action each limit state, currently provided by the precast company. There are several analytical methods and finite element models used to predict the behavior of partially composite panels. However, most of them are complicated or are only work for specific connector types.

The goal of this thesis is to test full-scale panels with different connector types and wythe thickness to understand their behavior at each limit state. An additional goal of this thesis is to develop simplified methods to predict the behavior of the sandwich panel at the service and ultimate states. Using these methods, the engineers can optimize their design to achieve the desired percent of composite at each limit state.

1.2. Objectives

Several connectors' and SWP's performance was evaluated using different connector types and distributed patterns during full-scale tests. Eight full concrete sandwich panels which were fabricated with XPS insulation and were tested. Two of them had a 4-ft by 16-ft and 3-4-3 in. configuration with prestressed reinforcement in the longitudinal direction. The others were 3ft by 16ft with mild reinforcement and a 4-3-4 in. configuration. In addition, the data from push-off tests was used to accurately and simply predict the flexural behavior of the concrete sandwich panel using hand methods and the results were compared to the experimental full-scale tests. Also, the spring model was used to predict the cracking load. An engineer can easily use these methods to analyze and design sandwich panels with different composite actions in each design stage (service and strength limit state).

1.3. Scope

The scope of this thesis consists of an extensive literature review, which investigates and compares the analytical models developed in the literature. Also, the experimental program consists of eight full-scale sandwich panels subject to flexural loads. The panels' deflection and end slip were monitored and compared to the simplified methods, which the author develops in detail. The simplified methods include a hand method used for the elastic and plastic range and a 2-D finite element model using SAP2000 for the elastic portion only, which is called the beam-spring model (BSM). A parametric study was performed using the hand method and BSM to understand the behavior of the panel using different thickness of foam and distribution patterns for the connectors and span length.

CHAPTER 2

LITERATURE REVIEW

2.1. Introduction

This section includes a brief introduction to some important concepts used to design the sandwich panels. In addition, this section summarizes the analytical methods from the literature.

2.2. Sandwich Panel Components

Sandwich panels consist of several components: the concrete wythes, insulation, flexural and transverse reinforcement, which can be mild reinforcement, welded wire or steel fibers (Morcous et al 2011) prestressing or post-tensioning (Maguire et al. 2015), and the connectors, as shown in Figure 2-1. The only differences between the concrete sandwich panel and other structural concrete components like a concrete solid wall or shear wall are the insulation and the connectors.

2.2.1. Insulation

There are three types of insulation commonly used in sandwich panels. Expanded polystyrene (EPS) is widely used in roofs, walls, and geotechnics because it is economical compared to other rigid insulation types. Extruded polystyrene (XPS) is denser than EPS, and because of that, the modulus of elasticity and the compression strength is higher. XPS contributes very little to the connector shear force. Bunn (2011) performed push off tests with 4 ft by 6 ft specimens which has XPS and EPS insulation without wythe connectors. EPS specimens failed under the average maximum load of 52

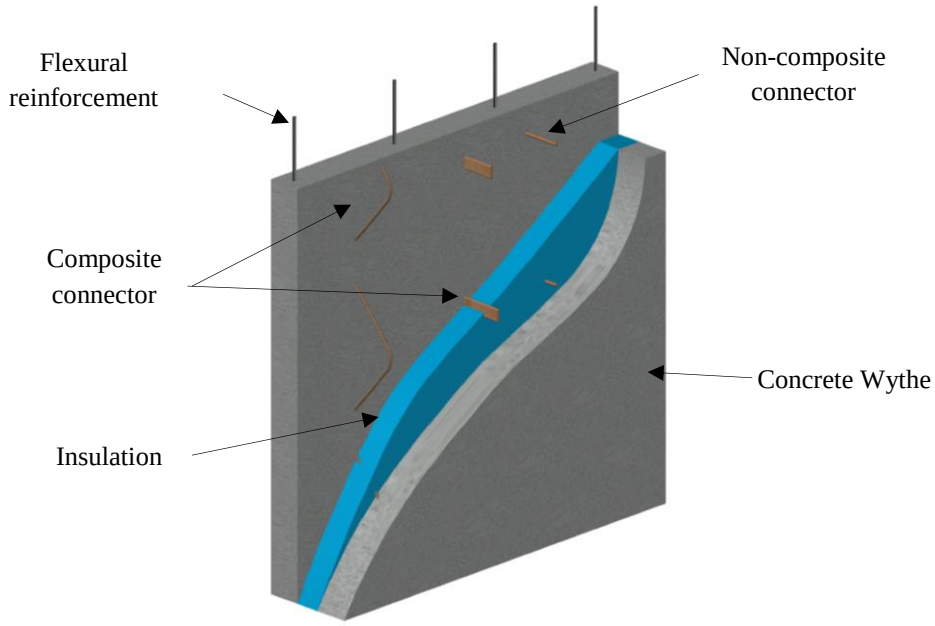

Figure 2-1 Section in typical sandwich panel

kips while XPS specimens failed under their own weight, which made it so the researcher could not test them. In Olsen and Maguire (2016), Olsen et al. (2017) and Al-Rubaye et al (2018), these researchers found that the insulation's contribution to connectors' shear forces depended on the type of connectors used. The reasons for this discrepancy is the apparent differences in bond strengths between EPS (higher bond) and XPS (lower bond) even though the XPS insulation has the better mechanical properties.

The insulation can have a large effect on the connectors mechanical performance depending mainly on truss action and can have a minor effect on the connectors depending on the dowel action (Pin connector); However, this observation requires more statistical evidence and future work for verification (Olsen et al 2017, Bean et al 2017, Chang et al 2017, Maguire et al. 2017). In addition, the ISO insulation contribution is

Table 2-1 Insulation properties (PCI Design Handbook 7th Edition)

	Polystyrene						Polyisocyanurate		Phenolic	Cellular glass
	Expanded			Extruded			Unfaced[a]	Faced[a]		
Density, lb/ft^3	0.7–0.9	1.1–1.4	1.8	1.3–1.6	1.8–2.2	3.0	2.0–6.0	2.0–6.0	2.0–3.0	6.7–9.2
Water absorption, % volume	< 4.0	< 3.0	< 2.0	< 0.3			< 3.0	1.0–2.0	< 3.0	< 0.5
Compressive strength, psi	5–10	13–15	25	15–25	40–60	100	16–50	16	10–16	65
Tensile strength, psi	18–25			25	50	105	45–140	500	60	50
Linear coefficient of expansion, (in./in./°F) × 10^{-6}	25–40			25–40			30–60		10–20	1.6–4.6
Shear strength, psi	20–35			—	35	50	20–100		12	50
Flexural strength, psi	10–25	30–40	50	40–50	60–75	100	50–210	40–50	25	60
Thermal conductivity, (Btu-in.)/[(hr)(ft^2 of area)(°F)] at 75 °F	0.32–0.28	0.26–0.25	0.23	0.20			0.18	0.10–0.15	0.16–0.23	0.35
Maximum use temperature	165 °F			165 °F			250 °F		300 °F	900 °F

also dependent on the surface treatment of the insulation. Table 2-1 shows the insulation properties**.** It should be noted that material properties of polystyrene foam are variable.

2.2.2. Shear Connector

There are two types of connectors: stiff and flexible. Stiff connectors include concrete solid sections that penetrate the insulation, steel and fiber reinforced polymer (FRP) connectors, which are mostly used in partially composite sandwich panels. Flexible connectors refer to non-composite connectors. FRP connectors consist of oriented or random fiber and polymer composites used to achieve the desired properties. These have been used for decades in structural engineering due to their resistance to corrosion and thermal properties. FRP are used in sandwich panels mainly due to their thermal properties.

Many researchers performed push off test on different types of connectors. Naito et al (2012) performed double shear push-off tests on a total of fourteen different connectors (six of them were FRP connectors and the others were traditional steel connectors). The specimens were 18 in. by 18 in. and had a 3-2-6-2-3 configuration. The strength of connectors is highly variable. The distributed connectors have a higher stiffness when compare to pin connectors.

Woltman (2014) used commercially available GFRP bars with various types, diameters, and end treatment of connectors to performed 50 push-through tests. Woltman found that different cross sections did not affect the shear strength. In addition, adhesion has a significant effect on the shear strength; however, it is variable and cannot be used for long term design and under cyclic loading. The researcher did thermal and structural tests and found that the effect of the connector on the R value is small for various cross sections and spacing.

Olsen and Maguire (2016) performed 43 double shear specimen tests on several commercial FRP connectors with various insulated layer thickness, types, and bond conditions. They found that increasing the insulated layer thickness affects the strength and the stiffness of connectors. Moreover, foam type and bond condition have little effect on the pin connector, which mainly failed in dowel action and has a significant effect on the truss connectors.

Tomlinson et al. (2016) introduced a new type of shear connector that combined vertical and angled connectors made from basalt fiber reinforced polymer (BFRP). They performed 38 push-off tests for different angles, connector diameters, and bond

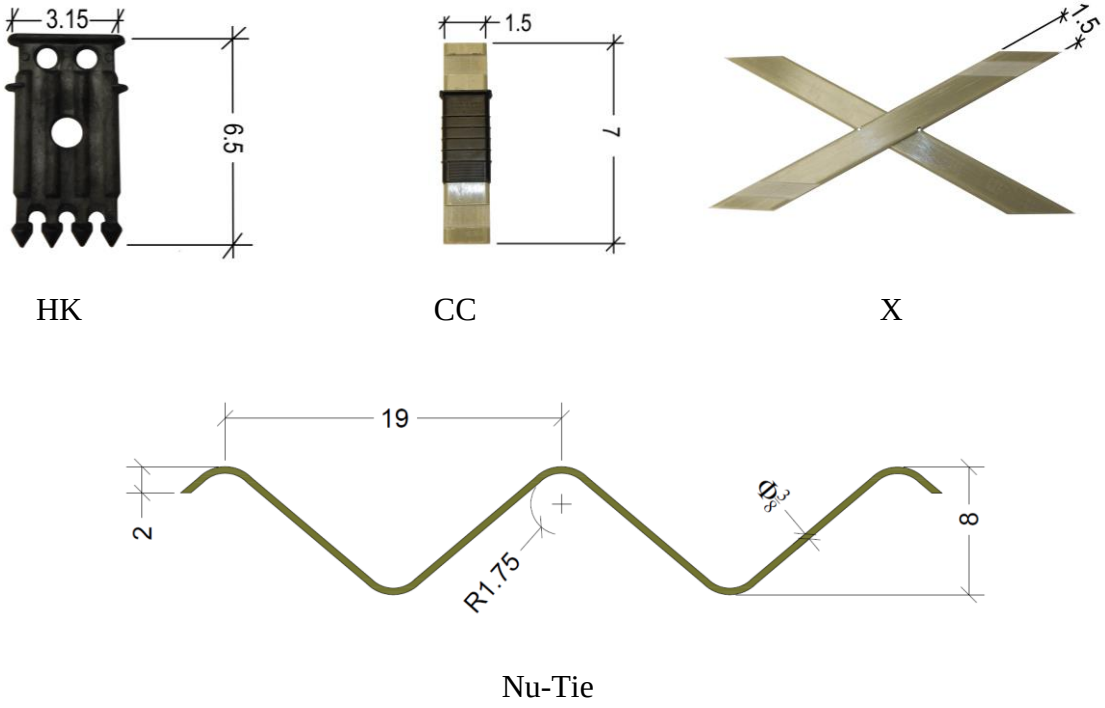

Nu-Tie

Figure 2-2 Connector types that used in this research (all dimensions is in inches)

condition. In addition, Tomlinson et al. proposed an analytical model, which depends mainly on the connector, dowel, and truss action to estimate the connector shear strength and failure mode.

The research in this thesis focuses on four proprietary types of FRP composite connectors which are commonly used in industry. Figure 2-2 shows the connectors' shapes and dimensions.

2.2.2.1. HK connector

HK connectors are fabricated using mold injection of a proprietary short fiber GFRP. This type of GFRP is brittle compared to other manufacturer processing due to

short fiber length and matrix stiffness. Figure 2-3 shows shear load versus the slip curve (Olsen 2016).

2.2.2.2. Nu-Tie connector

Einea (1992) began development of the Nu-Tie connector to achieve a high structural and thermal efficiency. Figure 2-4 shows the Nu-Tie generation from 1992 until now. Nu-Tie connectors mainly depend on truss action to provide the shear stiffness. Figure 2-3 presents the shear load versus slip (Olsen et al 2017).

2.2.2.3. Thermomass (CC, X)

CC and X connectors are from the Thermomass company. Jacobs (1987) performed push-off and pull-off tests to determine the properties of GFRP non-composite connectors. Later, the company developed composite connectors for different insulations and wythe thickness. Figure 2-5 shows the shear load versus slip for CC and X connectors (Olsen et al 2017, Al-Rubaye et al 2018).

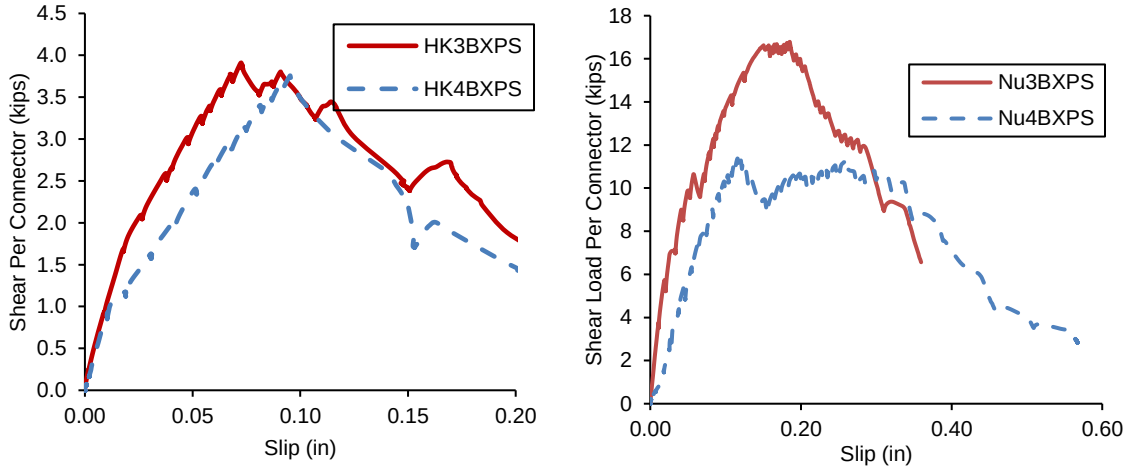

Figure 2-3 Load versus Slip for 3 and 4 in XPS insulation for HK (left) for Nu-Tie (right)

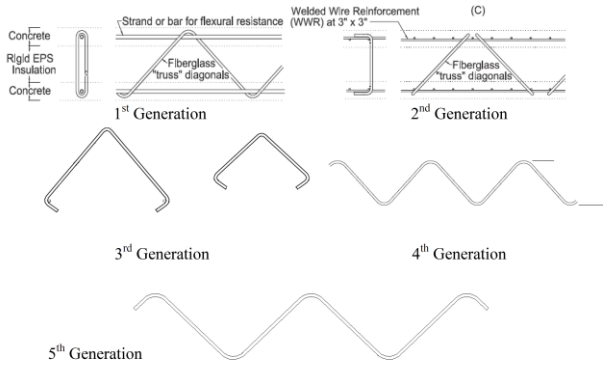

Figure 2-4 Nu-Tie Version (Morcous et al 2011)

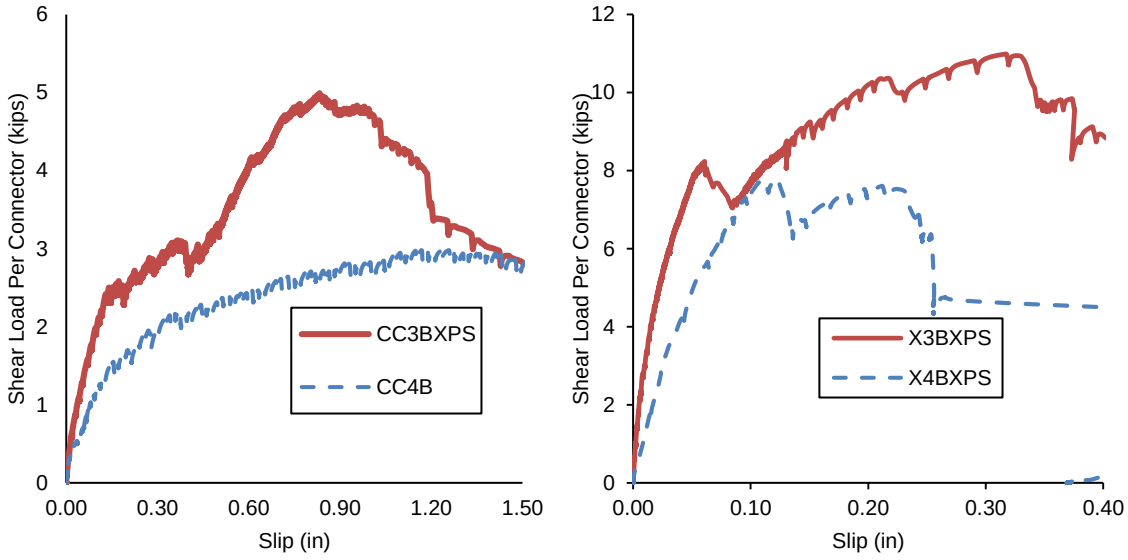

Figure 2-5 Load versus Slip for 3 and 4 in. XPS insulation for CC connector (left) for X connector (right)

2.3. Composite Action

Composite action is often expressed as a percentage of apparent composite behavior as compared to non-composite and fully composite panel behavior. Non-composite panels consists of a structural wythe and a nonstructural wythe with an insulating layer between them. The structural wythe, which is commonly thicker than the nonstructural one, will

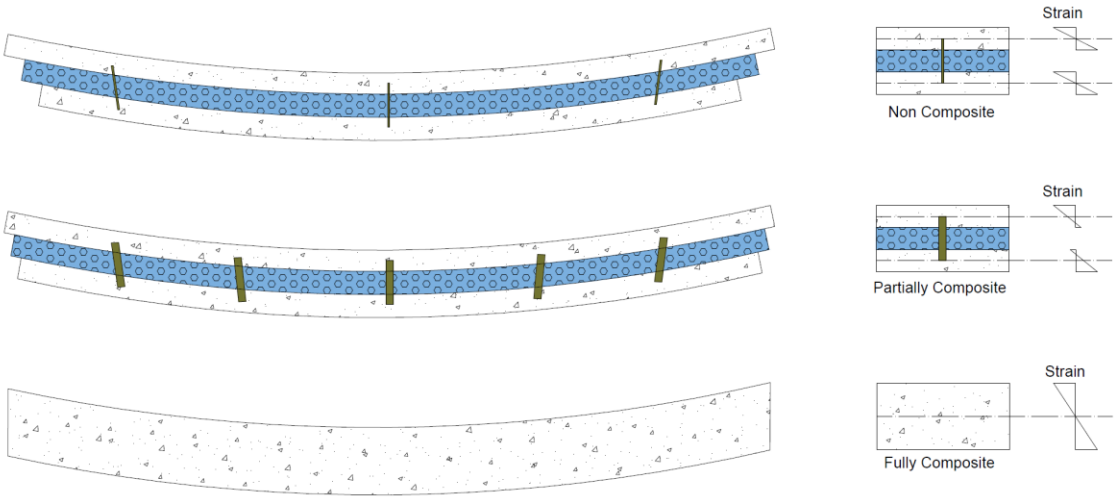

Figure 2-6 Composite action

take all the load, including the self-weight of the nonstructural layer, through the connector. The concrete layers are connected using non-composite connectors. Fully composite panels consist of two concrete layers acting together as single beam and foam layer. Partial composite action will occur when shear connectors are used to transfer the load between each wythe and full composite action is most commonly achieved with steel truss connectors or large solid concrete zones.

Pessiki and Mlynarczyk (2003) define the composite action of the sandwich panel using the stiffness properties of the fully and non-composite panels, as shown in equation (2-1).

$$\kappa = \frac{I_{exp} - I_{nc}}{I_c - I_{nc}} \qquad (2\text{-}1)$$

2.4. Thermal Efficiency

One of the advantages of sandwich panels is their thermal efficiency. The majority of thermal resistance comes from the insulation layer between the concrete

wythes. However, using the steel connector or concrete solid zone to transfer the load between the wythe or just to connect them will cause another problem, which is thermal bridging, because of the low thermal resistance of the steel connector and the concrete. Thermal bridging is the heat escape through high conductivity material compared to surrounding materials such as steel connectors or the concrete solid zone. To minimize this problem, Calvin McCall (1985) recommended that the shear steel should be kept to a minimum. One solution for the thermal bridging is to use a material that has low thermal conductivity such as FRP. Figure 2-7 shows a thermal image of two sandwich panel buildings: one with steel connectors (right) and one with FRP connectors (left) (see Sorensen et al (2017) for more details of the heat loss in sandwich panels). Woltman stated that the idea of using connectors made of the FPR composite came from Jacobs (1987). Jacobs used different samples of GFRP connectors with different end treatments to achieve a high bond with the concrete. Jacobs also did push-off and pull out tests to verify their results. He concluded that the embedment length of a connector is dominated the results of pull out tests. Einea (1992) evaluated different FRP connectors to improve the thermal and structural behavior of sandwich panels. Einea used different connector shapes depending on their thermal and structural efficiencies. The connectors were I-shaped FRPs with a wide flange, bone shaped, straps with Steel pins, and fabricated bent FRP bars. Einea performed push off tests on the connectors, which and led to choosing bent FRPs. In addition, Einea also performed small scale tests on sandwich panel specimens with the bent connector.

In 2004, Lee and Pessiki proposed a new sandwich panel type consisting of five wythe layers with staggered foam and concrete sections to improve the thermal and structural performances. However, this type of sandwich panel is difficult to construct and never became popular.

2.5. Theoretical Approaches to Predicting Sandwich Panel Behavior

For decades, researchers tried to predict the behavior of sandwich panels using analytical or numerical methods. In this section, a brief summary of their methods is presented.

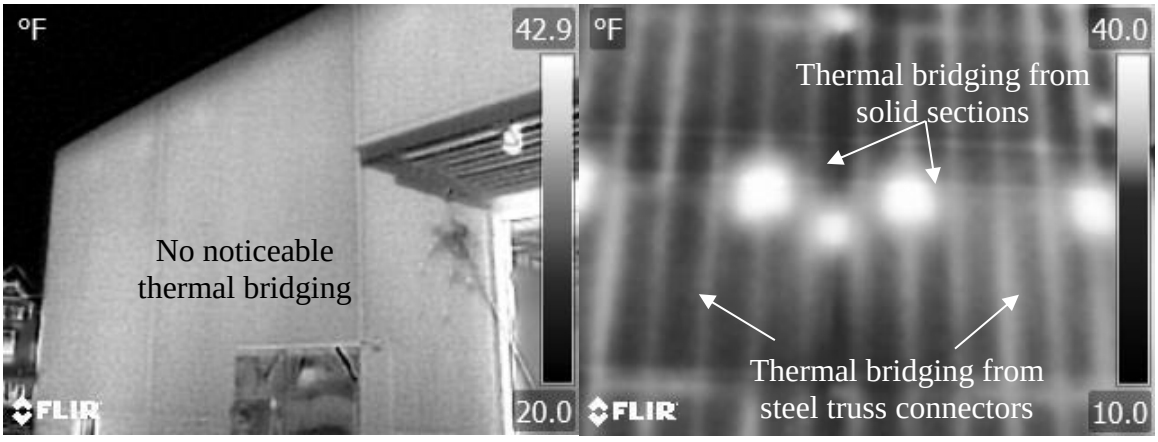

Figure 2-7 Thermal Images of PCSWPs using FRP connectors (left) and steel truss connectors (right)

2.5.1. Analytical Approaches for flexural composite behavior

There are several analytical approaches used to predict the behavior of concrete sandwich panels. Most of them are complicated or developed for certain connectors only.

Prior to development of sandwich panel partial composite action, Newmark, Siess, and Viest (1951) proposed a theoretical analysis to predict the behavior of partially

composite steel beams consisting of two elements: a steel beam and a concrete slab. The researcher performed double shear push-off and full-scale flexural tests to verify their analytical approach. They provided an expression for the slip, deflection, and strain for partially composite beams under concentrated loadings. There are several assumptions and principles that they used in their methods:

1. The shear connection is continuous along the length.
2. The slip is proportional to the load and can be determine by integrating the rate of change of the slip along the length, which is equal to the strain difference between the beam and slip as shown in equation (2-2).

$$Slip = \int \frac{d\gamma}{dx} = \int \epsilon_b - \epsilon_s \qquad (2\text{-}2)$$

Where: ϵ_b *and* ϵ_s *are the strain of the beam and the slab at the connection surface as shown in* Figure 2-8.

3. The external moment can be calculated using equation (2-3).

$$M = M_s + M_b + F * Z \qquad (2\text{-}3)$$

Where: M_s*= the moment from the slab*

M_b*= the moment from the beam*

F= the shear force from the connector

Z= the distance between the center of the slab and the beam

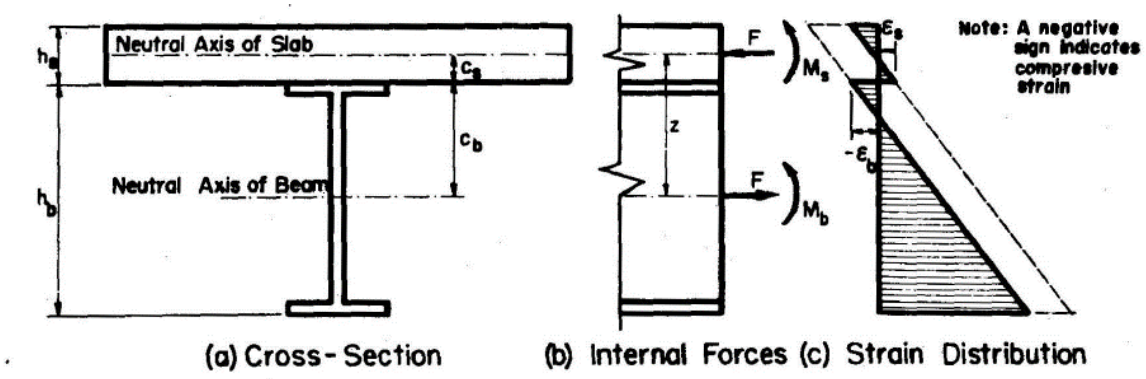

Figure 2-8 Composite Beam (Newmark, Siess, and Viest 1951)

4. Deflection can be calculated by double integrating equation (2-4).

$$\frac{d^2y}{d^2x} = -\frac{M}{\sum EI} + \frac{F * Z}{\sum EI} \qquad (2\text{-}4)$$

In 1965, Holmberg and Plem published a book about the behavior of sandwich panels, which provided examples of those behaviors. The researchers proposed analytical methods to predict the behavior of sandwich panels under bearing loads, longitudinal loads, transverse loads, thermal loads and differential shrinkage. The researchers depended on the Granholm (1949) basis of their procedure for the sandwich panel. Using Granholm (1949), Holmberg and Plem used equations (2-5) through (2-7) to predict the behavior of the sandwich panels.

$$\varphi'' - \chi^2\varphi = 2rv''' \qquad (2\text{-}5)$$

$$v'' - \frac{\alpha^2}{2r}\varphi' = -\frac{M_x}{EI} \qquad (2\text{-}6)$$

$$M_x = 2M + 2rN \qquad (2\text{-}7)$$

Where: φ = *Slip between the wythes*

v = *Deformation in y direction (deflection)*

r = *The distance between the centers of each wythe*

χ = $d^2/(d^2+12*r^2)$

α^2 = $2Ar^2/I$ *(see* Figure 2-9*)*

M = *internal moment in each of the wythes*

N = *Axial Force in each wythes*

For sandwich panels under a uniform loading, the external moment can be calculated for static loads as shown in equation (2-8) and Figure 2-9.

$$M_x = \frac{1}{8} * q * b * l^2 * [1 - \left(\frac{2x}{l}\right)^2] \qquad (2\text{-}8)$$

Where: q = *external load (force per unit area)*

b =*width of the sandwich panel*

l = *Span length*

By substitute equation (2-7) into equation (2-5) and solving the differential equation, the equation becomes

$$\varphi = -2 * \frac{qrb}{EI} * \frac{1}{\chi^2} x + C_1 \sinh\frac{\chi}{\beta} x + C_2 \cosh\frac{\chi}{\beta} x \qquad (2\text{-}9)$$

Using the boundary conditions of the simple support beam where deflection is zero at the support and the slope is zero at midspan, deflection, moment, shear, and axial force can be express as shown equations (2-10), (2-11), (2-12), and (2-13), respectively.

$$\nu = +\frac{5}{384}\frac{qbl^4}{EI} * \left[1 - \frac{24}{5}\left(\frac{x}{l}\right)^2 + \frac{16}{5}\left(\frac{x}{l}\right)^4\right] + \frac{1}{16}\frac{qbl^4}{EI}\frac{\alpha^2}{\beta^2}\left(\frac{2\beta}{xl}\right)^2 \left[\left(\frac{2\beta}{xl}\right)^2 \left(\frac{\cosh\frac{\chi}{\beta} x}{\cosh\frac{\chi l}{2\beta}} - 1\right) + \frac{1}{2}\left(1 - \left(\frac{2x}{l}\right)^2\right)\right] \qquad (2\text{-}10)$$

Where: β^2 = *1-* α^2

$$M = \frac{1}{8} qbl^2 \left[\alpha^2 * \left(\frac{2\beta}{xl}\right)^2 \left(1 - \frac{\cosh\frac{\chi}{\beta} x}{\cosh\frac{\chi l}{2\beta}}\right) + \frac{1}{2}\beta^2 \left(1 - \left(\frac{2x}{l}\right)^2\right)\right] \qquad (2\text{-}11)$$

$$\tau = \frac{1}{4}\frac{ql}{r}\,\alpha^2[\frac{2\beta}{xl} * \frac{\sinh\frac{\chi}{\beta}x}{\cosh\frac{\chi l}{2\beta}} - \frac{2x}{l}] \qquad (2\text{-}12)$$

Where: τ = *Shear Stress*

$$-N_{ex} = N_{in} = \frac{1}{8}\frac{qbl^2}{r} * \alpha^2[-\left(\frac{2\beta}{xl}\right)^2 * \left(1 - \frac{\cosh\frac{\chi}{\beta}x}{\cosh\frac{\chi l}{2\beta}}\right) + \frac{1}{2}\left(1 - \left(\frac{2x}{l}\right)^2\right)] \qquad (2\text{-}13)$$

In addition, Holmberg and Plem proposed a formula to calculate the stiffness of the truss connector as shown in Figure 2-10 and equation (2-14)

$$K = \frac{E_a * A_a}{4r^2 b} * \sin^2\gamma\cos\gamma \qquad (2\text{-}14)$$

Where: E_a = *Modulus of elasticity of the connector*

A_a = *Cross section area of the connectors over the width.*

γ = *Angle of the connector, see* Figure 2-10.

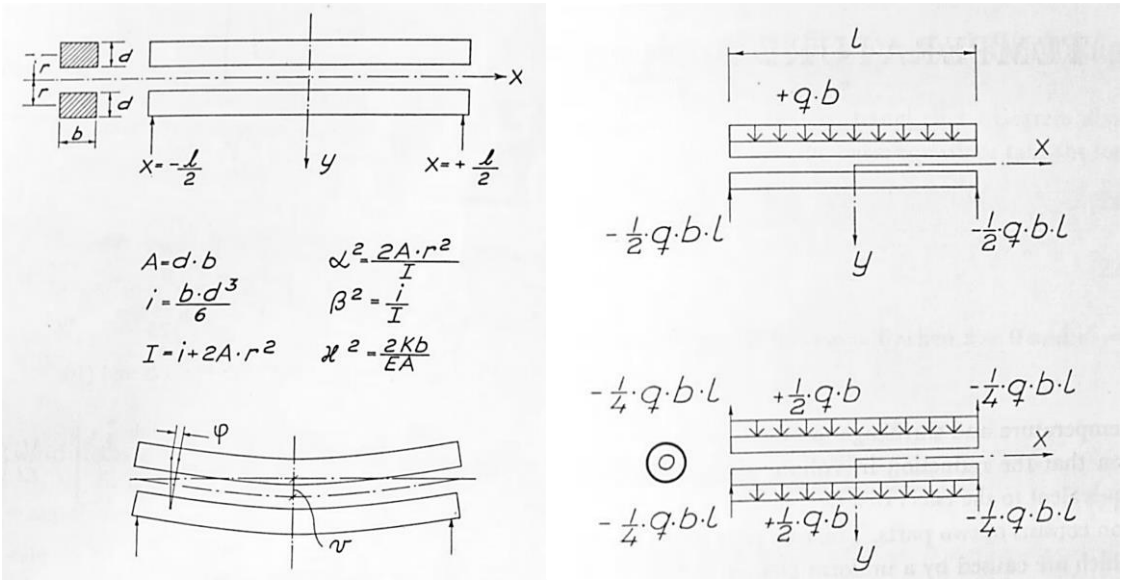

Figure 2-9 Sandwich panel diagram (left) sandwich panel under uniform load (right) (Holmberg and Plem 1965)

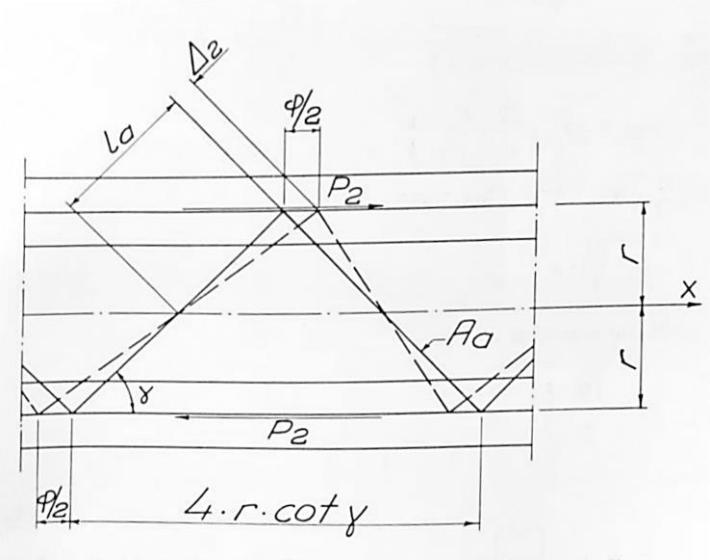

Figure 2-10 The connector deformation under shear force (Holmberg and Plem 1965)

Allen (1969) proposed a method for Sandwich Beam with Antiplane Core ($\sigma_x = \sigma_y = \tau_{xy} = 0$.) with various wythes thickness and load conditions to predict stresses and deflection. Allen assumed that there are two conditions applied in this case:

$$6\frac{E_{wythe}}{E_{ins}}\frac{t}{c}\left(\frac{d}{c}\right)^2 > 100 \qquad (2\text{-}15)$$

$$4\frac{E_{wythe}}{E_{ins}}\frac{t}{c}\frac{d}{c} > 100 \qquad (2\text{-}16)$$

Where: E_{wythe} = *Modulus of elasticity of the wythe*

E_{ins} = *Modulus of elasticity of the insulation*

t = *Wythe thickness*

c = *Insulation thickness*

If these conditions are satisfied, the shear stress can be assumed to be constant over the thickness of the core. The flexural rigidity of the beam consists of the flexural rigidities of the two wythes and the insulation, as shown in Equation (2-17).

$$D = E_{wythe}\frac{bt^3}{6} + E_{wythe}\frac{btd^2}{2} + E_{ins}\frac{bc^3}{12} \qquad (2\text{-}17)$$

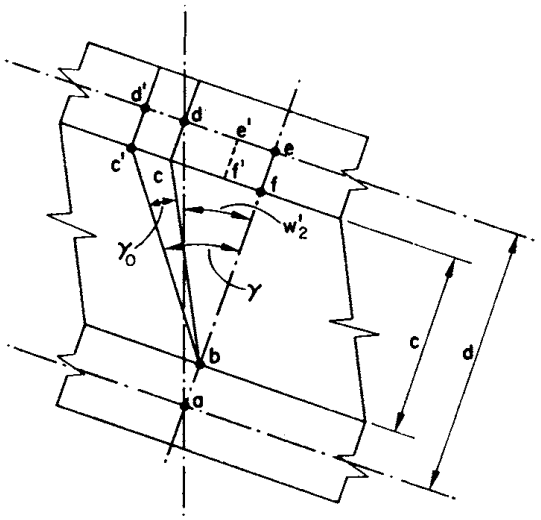

Figure 2-11 Shear Deformation (Allen 1969)

If the conditions in equation (2-15) and (2-16) are satisfied, the flexural rigidity from the insulation in neglected (less than 1% of the wythes flexural rigidity). Allen stated that the deflection consists of two components, which are the deflection from the bending associated with the shear forces Q_1 and the shear deflection of the core due to Q_1, as shown in Figure 2-11. The differential equation for the equally thick wythes is shown in equation (2-18) and its solution is shown in equation (2-19).

$$Q_1'' - a^2 Q_1 = a^2 Q \qquad (2\text{-}18)$$

Where: $a^2 = \frac{AG}{EI_f(1-\frac{I_f}{I})}$

Q_1 = *Modulus of elasticity of the insulation*

$$-Q_1 = C_1 \cosh ax + C_2 \sinh ax + qx \qquad (2\text{-}19)$$

Where: q = *Load per unit length*

By applying the support condition, the deflection and stress can be calculated from the following equations:

$$w_{max} = -\frac{5qL^4}{384\,EI} - \frac{qL^2}{8AG}\left(1 - \frac{I_f}{I}\right)\Psi_4 \qquad (2\text{-}20)$$

$$\sigma_{max} = \frac{qL^2}{8}\left\{\frac{c + 2t}{2I}\Psi_6 + \frac{t}{2I_f}(1 - \Psi_6)\right\} \qquad (2\text{-}21)$$

Where: w_{max} = *Maximum deflection*

σ_{max} = *Maximum stress*

$$\Psi_4 = 1 + \frac{2\beta_2}{\theta}(1 - cosh\,\theta)$$

$$\Psi_6 = 1 - \frac{2}{\theta^2}(1 - \beta_2\theta)$$

$$\beta_2 = \frac{\frac{1}{\theta} + tanh\,\phi}{cosh\,\theta + sinh\,\theta\ tanh\,\phi};\ \theta = \frac{aL}{2};\ \phi = aL_1$$

Salmon and Einea (1995) developed a displacement prediction using a finite element model (FEM) for FRP connected panels, which analyzed both mechanical and thermal loading. The model derivation follows that of Holmberg and Plem. They assumed that the deformation was similar to that described by Allen (1969), which consists of two components: the panel curvature and the offset due to the shear deformation between the wythes, as shown in Figure 2-12. The displacement of the panel can be expressed in equation (2-22) for small deformation after summing the moment due to the deformation of each component.

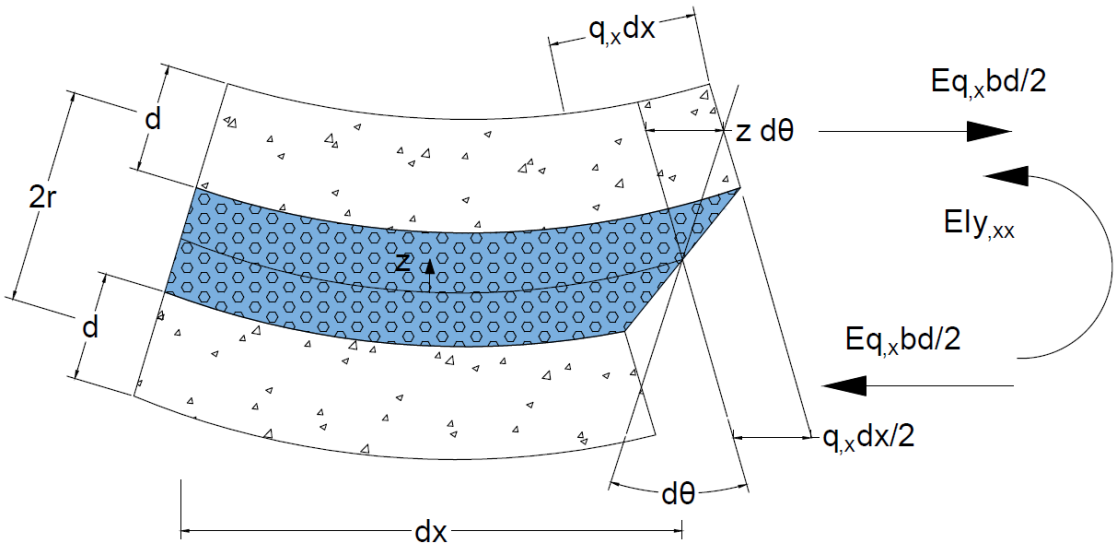

Figure 2-12 Salmon and Einea Differential panel element

$$y_{,xx} = \frac{M}{EI} + \frac{\alpha^2}{2r} q_{,x} \qquad (2\text{-}22)$$

Where: $\alpha^2 = \frac{I - 2I_w}{I}$

I = *moment of inertia of entire section*

I_w = *moment of inertia of each wythe.*

y = *Upward displacement*

q = *Slip between wythes*

The researchers proposed that the stiffness of the connector is computed from three conditions, which are truss action, full embedment fixity, and later embedment restrain as shown in Figure 2-13. Each of these conditions may dominate depending on

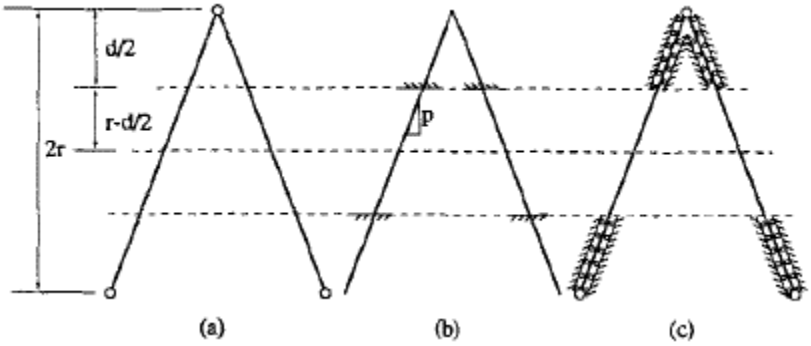

Figure 2-13 Salmon and Einea connector embedment types: (a) Truss action; (b)Fixed at wythe Embedment; (c) Laterally Supported with in Wythe (Salmon and Einea 1995)

the connector's geometric and material properties. In addition, the researchers used Truss action only for their bent FRP connectors to calculate connector stiffness because it is simplified and the other conditions contribute little to connector stiffness.

Truss action, Full embedment fixity, and later embedment restrain condition can be calculated using equations (2-23), (2-24), and (2-25), respectively.

$$K = \frac{A_c E_c p^2 m}{4r^2 b(1+p^2)^{\frac{3}{2}}} \tag{2-23}$$

$$K = \frac{E_c p^2 m}{2rb(1+p^2)^{\frac{5}{2}}(2r-d)^3}[(1+p^2)+(2r-d)^2 A_c + 12p^4 I_c] \tag{2-24}$$

$$K = \frac{E_c p^2 m}{2rb(1+p^2)^{\frac{3}{2}}}\left[\frac{A_c}{r} + \frac{24p^4}{(1+p^2)(2r-d)^3}\right] \tag{2-25}$$

Where: A_c = *cross section area of connector*

E_c = *modulus of elasticity of connector*

m = *Number of connectors along the width*

p = *slope of the connector as shown in Figure 2-13*

I_c = *Moment of inertia of the connector*

Using this model a design equation, termed the continuum model, was developed that could analyze the FRP shear connected panels using equation (2-26):

$$\delta = \frac{M_T L^2}{8EI}\left[1 - \frac{2}{\psi^2}(1 - \operatorname{sech}\psi)\right] \qquad (2\text{-}26)$$

Where: M_T = *External moment*

$\psi = \frac{\chi L}{2\beta}$

$\beta^2 = (1 - \alpha^2)$;

$\chi^2 = \frac{2K}{Ed}$

K = *Stiffness of the connector*

Salmon and Einea validated their model with short and long panels that had the same number of connectors and predicted deflections to within 0.5% and 1% of a FEM, respectively, although there was no comparison to test values. The researcher found that the long panel with weak connector stiffness experienced 82% of thermal bowing of the full composite. In addition, that long non-composite panel experienced some thermal bowing.

In "State of the Art of Precast/Prestressed Concrete Sandwich Wall Panels" (1997), flexural design for sandwich panels was divided into three categories: non-composite panel design, composite panel design, and partially-composite panel design. For non-composite panel design, the flexural design for the non-composite panel is the same as for solid panels, and the applied loads are distributed to each wythe depending on the stiffness for the individual wythe. Equations (2-31) through (2-33) show the percentage of total load carried by the individual wythes.

$$M_T = M_1 + M_2 \qquad (2\text{-}27)$$

$$M_1 = M_T \frac{I_1}{(I_1 + I_2)} \qquad (2\text{-}28)$$

$$M_2 = M_T \frac{I_2}{(I_1 + I_2)} \qquad (2\text{-}29)$$

Where: M_T = Total cracking moment

M_1 = Cracking moment for the wythe 1

M_2 = Cracking moment for the wythe 2

I_1 = moment of inertia for the wythe 1

I_2 = moment of inertia for the wythe 2

Wythe 1 is considered the wythe that would be in compression during positive bending and wythe 2 is considered the wythe that would be in tension during positive bending.

For P-δ effects from the axial load and self-weight, only the properties of the structural wythe are used for the stiffness-reduction factor. For a composite panel, the sandwich panel is assumed to be composite if the shear connectors provide forces greater than or equal to the lesser of the maximum compressive forces for the concrete or the tensile capacity for the steel at ultimate.

$$V \leq \min \begin{Bmatrix} 0.85 * f_c' * t_{wythe1} * b \\ A_s * f_y + A_{ps} * f_{py} \end{Bmatrix} \qquad (2\text{-}30)$$

Where: V = shear force provided by connectors

t_{wythe1} = thickness of the wythe 1

In the second edition of the State-of-the-Art report, the flexural design is kept the same, with the exception of partially-composite panels. Partially-composite panels are assumed to obtain a percentage of composite action based on known similar existing panels, relying on shear connector manufacturer recommendations.

Bush and Wu 1998 proposed a modified model of Allen's methodology to account for the partially composite panel with the truss connector. Their model predicted the service load and deflection under uniform load. In the model, the modified shear modulus was used in Allen's equation.

$$G_{eff} = G_{ins} + G_{truss} = G_{ins} + \frac{N\, E_s A_t \sin^2\theta \cos\theta}{bS} \qquad (2\text{-}31)$$

Where: N = *Number of the truss connector over the width*

E_s = *Modulus of elasticity of the connector.*

A_t = *Cross section area of the connector.*

S = *Tributary width of the diagonal connector (mid-length to mid length)*

θ = *Vertical angle of the connector see Figure 2-14*

The model was compared to a 3D FEM and experimental data. Additionally, the model results using the 3D FEM was promising, with a deflection measured-to-prediction ratio equal to 1.05 and 1.04 for a Two-truss and Three-truss, respectively. However, the results of the model and the 3D FEM were conservative when compared to the experimental data, which may be because they did not account for the shear forces from handling and stripping conditions.

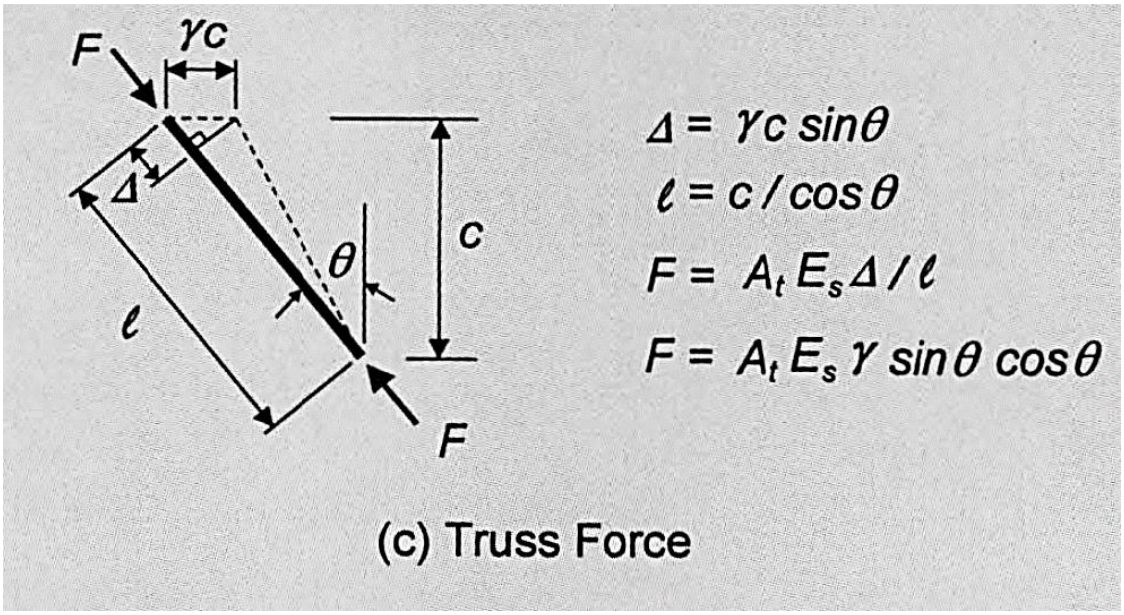

Figure 2-14 Truss connector deformation (Bush and Wu 1998)

Hassan and Rizkalla (2010) modified the original theory of Newmark et al. for the composite steel beam to be suitable to predict the flexural behavior of partially composite concrete sandwich panels. Their method focuses on concrete sandwich panels that are reinforced with carbon FRP (CFRP) grid connectors; however, it can be applied to sandwich panels with different shear mechanisms. Hassan and Rizkalla developed charts to simply design.

Naito et al. (2012) found that the connector stiffness affects the flexural sandwich panel behavior. In addition, it highly affects the behavior after the sandwich panel has cracked. They proposed a numerical method to estimate the sandwich panel behavior under uniform static loading by using the degree of composite action and moment curvature. The researchers used the slip that is calculated using the load-slip curve of a

connector to estimate the percent of composite action. The procedure for their model is as follows:

1. Calculate the moment-curvature using a trilinear curve (cracking, yield, and ultimate moment) for non-composite and fully composite panels.
2. Calculate the static moment along the panel from load W_i.
3. Calculate the shear force transfer between the wythes at each division using equation (2-32).

$$V_{ij} = \frac{(M_{i+1} - M_i)_j}{(d - \frac{a}{2})} \qquad (2\text{-}32)$$

Where: M_{i+1}-M_i = *change in moment in each division*

d = *depth of tensile reinforcement*

a = *Depth of Whitney stress block.*

4. Determine slip at each section using the shear force from step 2 and load-slip curve for the connector and insulation. Category the section to non-composite, partially composite, and fully composite if the slip is higher than s_2, between s_1 and s_2, and less than s_1, respectively. s_1 and s_2 limits are from push-off test experiments. s_1 is the midpoint between the yield slip and the ultimate slip. s_2 is $1.2s_1$.
5. Calculate percent of composite action
6. Interpolate the moment-curvature from step 1 to determine the moment-curvature for partially composite panels.
7. Integrate the curvature using virtual work or other methods to calculate the deflection.

8. Go to step 2 and repeat for a new load.

Tomlinson (2015) used an analytical model that depends on the composite action as defined by Naito et al. (2012); however, the researcher used the analytical approach to estimate the shear in the connector and the foam. In addition, this model is more complicated and involves integrating the strain in the panel to estimate the slip, which requires a computer program. The model's predictions were accurate. Tomlinson found that insulation affects the strength, but this effect is decreased when a high number of connectors is used. The Tomlinson (2015) model procedure is outlined below:

1. Calculate the moment curvature under load from W_i (1 to n) assuming fully composite and non-composite properties.
2. Calculate the moment diagram along the panel under F load.
3. Assume the slip profile along the panel. The slip profile can be linear or similar to calculated slip from the previous load.
4. Calculate the shear forces V_L along the panel using slip from step 3 and the load-slip curve for the insulation and the connectors.
5. Calculate the percent of composite depending on the shear force V_L and strain discontinuity along the panel length as shown in Figure 2-15.
6. Integrate the strain discontinuity profile to determine the revised slip profile.
7. Compare the difference between the calculated slip and assumed slip in step 3 and go to step 4 if the difference is not within the tolerance.
8. Interpolate the moment-curvature from the non-composite and fully composite moment-curvature in step 1 using the percent of composite.

9. Use moment area or other methods to calculate the deflection from the interpolated moment curvature.

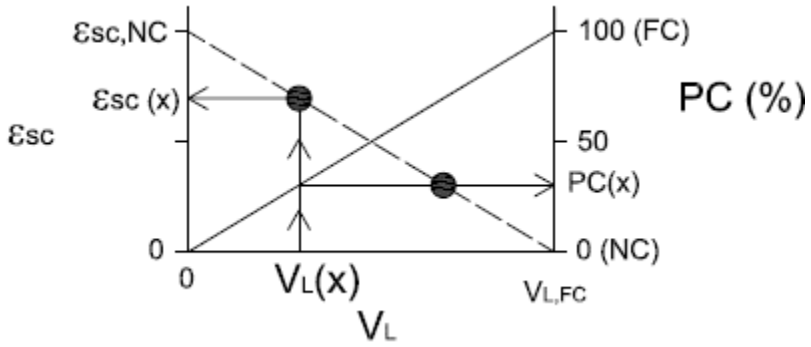

Figure 2-15 Percent of Composite Action

Bai and Davidson (2015) presented and compared the Allen and Holmberg methods about sandwich beams and. In addition, they proposed Allen and Holmberg methods using a discrete model for the shear connectors rather than continuous. The discrete connector function is defined as a rectangular waved function obtained using a Fourier Transform that can only be solved numerically as shown in equation (2-33) and Figure 2-16:

$$K_f(x) = K_{in}\left\{\frac{t}{T} + \sum_{n=1}^{\infty}\frac{1}{n\pi}\sin\left(\frac{2\pi n}{T}\right)\cos\left(\frac{2\pi n}{T}x\right) + \sum_{n=1}^{\infty}\frac{1}{n\pi}\left(1-\cos\left(\frac{2\pi n}{T}\right)\right)\sin\left(\frac{2\pi n}{T}x\right)\right\} \quad (2\text{-}33)$$

Where: K_f = *Stiffness of whole structure*

K_{in} = *Stiffness of individual connector*

t = *Length of positive length*

T = *Period length*

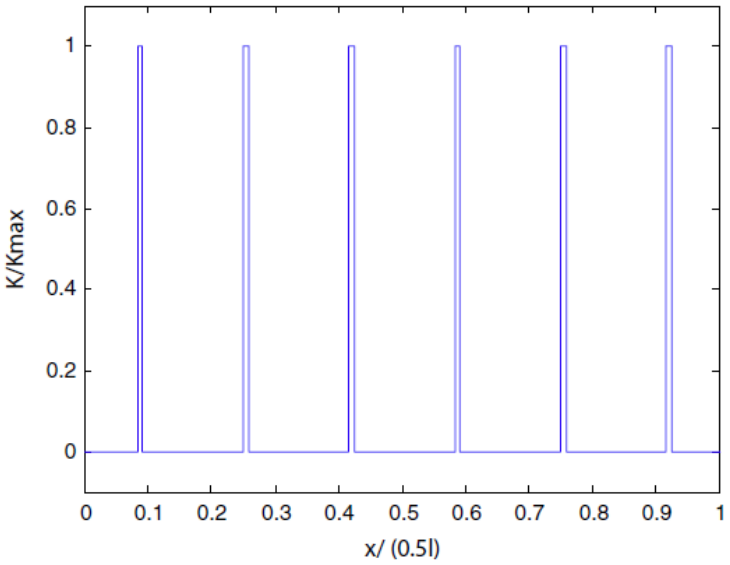

Figure 2-16 Shear stiffness function. (Bai and Davidson (2015))

Matthew et al. (2017) proposed a simplified model for the partially composite concrete sandwich panel. The model is complicated and consists of three major stages: Fully composite, non-composite, and partially composite panels. The procedure for the model is as follow:

1. Calculate the moment curvature under the load from W_i (1 to n) assuming fully composite and non-composite properties.
2. Use virtual work, moment area, or other methods to calculate deflection for each increment using the moment curvature information.
3. Assume the percent of composite action depending on the previous step. Additionally, use % composite to Interpolate moment-curvature from non-composite and fully composite curvature (step 1).
4. Utilize virtual work or other methods to calculate the rotation of the sandwich panel at each connector to determine its slip from equation (2-34).

$$Slip_i = \theta_i * e \quad (2\text{-}34)$$

Where: θ_i =*Rotation of the sandwich panel*

e $= (\frac{t_{wythe1}}{2} + t_{ins} + \frac{t_{wythe2}}{2})$

t_{wythe1} = *Thickness of wythe 1*

t_{ins} = *Thickness of insulation*

t_{wythe2} = *Thickness of wythe 2*

5. Determine the connector force using Slip from step 4 and the load-slip curve of the connector.
6. Calculate the moment using equation (2-35).

$$M_{PCi} = \min(M_{Ci}, M_{NCi} + F_i * e) \quad (2\text{-}35)$$

Where: M_{PCi} =*Partially composite moment*

M_{Ci} =*Fully composite moment*

M_{NCi} =*Non-composite moment*

F_i = *Summation of shear connector force for current increment*

7. Calculate the percent of composite using equation (2-36). And compare the difference between the calculated and assumed percent composite in step 3 and go to step 3 if the difference is not within tolerance.

$$PCA_i = \frac{M_{PCi} - M_{NCi}}{M_{Ci} - M_{NCi}} \quad (2\text{-}36)$$

Tomlinson, Nathan Teixeira, and Amir Fam developed a theoretical model to predict the shear strength of the connectors. The researchers stated that there are two things that contribute to the shear strength of a connector: dowel action and truss action. The dowel action of a connector can be found using equation (2-37). The truss action contribution, which is dominant in angled connectors like truss connectors, can be found

from equation (2-38). It should be noted that the tension and compression connectors may fail at the bond and in buckling, respectively.

$$V_{dw} = \frac{12\ E_{sc} * I_{sc}}{X^3}\delta \qquad (2\text{-}37)$$

$$V_{tr} = E_{sc} * \varepsilon_{sc} * A_{sc} \tan^{-1}\left(\frac{X \tan\theta + \delta}{X}\right) \qquad (2\text{-}38)$$

Where: E_{sc} =*Modulus of elasticity of connector*

I_{sc} =*Moment of inertia of connector*

δ =*Slip of connector*

X =*Span of connector (thickness of the insulation)*

ε_{sc} $= \frac{\Delta L_{ac}}{L_{ac}} = \frac{\sqrt{(X \tan\theta + \delta)^2 + X^2} - L_{ac}}{L_{ac}}$

A_{sc} =*cross section of connector*

2.5.2. Finite Element Approaches

There are several methods that were used to predict the flexural behavior of partially composite concrete sandwich panels. Most methods can accurately predict the composite action for different load levels.

Einea et al. (1994) performed a linear and nonlinear FEA to predict the behavior of the full-scale sandwich panel. They used a quadrilateral element for the insulation and a concrete and beam element for the FRP connector and the steel reinforcement. The FEA is in good agreement with the analytical model; however, this did not compare well to experiment data.

Salmon et al. (1997) used a computer program to compute the capacity of the FRP connector. They used beam elements for the concrete and a truss element pinned in the

centroid of the wythes as the connectors. The FEA is in good agreement with the experimental data and they recommended this model to compute the capacity of connectors.

Hodicky et al. (2014) used a 3D FEA to predict the shear capacity of the C-Grid connector. The model is complicated and included an interface element between the concrete and foam and the bond between the connector and concrete. The FEA was in good agreement with the measured data.

Olsen and Maguire (2016) performed a beam spring model using a commercial finite element program to predict the elastic behavior of the sandwich panels with variations of concrete strength and shear distribution. The beam represents the concrete wythe, and the spring stiffness represents the shear stiffness from the double shear push-off tests. They found that the model was accurate when predicting the cracking load and deflection. In addition, providing more connectors near the end in a triangular distribution increased the cracking moment.

Teixeira, Tomlinson, and Fam (2016) used a two-dimensional finite element computer program that consisted of two parts, beam element and link element, to predict the flexural behavior of partially composite sandwich panels. The properties of the link element are the stiffness of connectors from the push-off test. The model accounts for the nonlinear behavior of the materials. The model's results were promising; however, it is highly variable when predicting the ultimate load.

CHAPTER 3

EXPERIMENTAL PROGRAM

3.1 Introduction

The experimental portion of this research was to test several different proprietary and non-proprietary FRP shear connector systems by fabricating and testing eight full-scale sandwich panel walls. The purpose of this testing was to develop a general methodology to calculate partial composite action elastic behavior and capacity. This chapter of this thesis contains an outline of the experimental program including specimen configuration and testing setup.

3.2 Full-scale tests

3.2.1 Full-scale Specimen Configurations and Test Matrix

Two 16-ft long and six 15-ft long concrete sandwich wall panels were tested to evaluate their flexural strength and the composite action of different shear connectors. This part of the study included 4 different connectors (presented in Figure 3-1). For convenience of data presentation, each connector was assigned a letter descriptor as follows: Nu-Tie connector (Connector A), Thermomass CC Connector (Connector B), Thermomass X Connector (Connector C), and HK Composite Connector (Connector D). Two panels were tested with Connector A (NU-Tie 3/8 in. diameter connectors), two with only Connector B (Thermomass CC connectors), two with a combination of Connectors B and C (Thermomass CC and X connectors), and two with only Connector D (HK Composite connectors). All connectors were a type of glass fiber reinforced

polymer (GFRP). Connector A was a GFRP rebar fabricated into a “zig-zag” pattern, 3/8-in. diameter rebar with longitudinally aligned fibers. Connectors B and C were also an aligned fiber flat bar of GFRP (like Connector A) that were either oriented in an X shape or orthogonal to the concrete wythes. Connector D was a mold-injected product with randomly aligned fibers. The manufacturing process and alignment of the fiber significantly changes the failure mode and ductility of the connectors (Olsen and Maguire 2016).

Figure 3-1 Shear Connectors Tested, Left to Right: Connector A, B, C, and D

All panels were fabricated with XPS insulation, and utilized shear connectors to attain some degree of composite action by transferring shear between the both wythes through the insulation.

Connector A panels had a 3-4-3 in. configuration with prestressed reinforcement in the longitudinal direction and shear connectors as shown in Figure 3-2 and Figure 3-3. The prestressing consisted of three low-relaxation 270 ksi strands with a 3/8-inch diameter tensioned to $0.70f_{pu}$. The panels were designated A-2 (Figure 3-2) and A-4 (Figure 3-3) with the 2 and 4 designating the number of shear connectors in each row. Shear connectors were distributed uniformly with a total of eight in the A-2 panel and

sixteen in the A-4 panel. The difference in the number of connectors was intended to demonstrate the dependence of the panel performance upon the number of connectors within the panel. At the authors' request, the A-2 panel used connectors at a lower level than typically used by the manufacturer for this panel configuration.

The B, BC, and D panels had mild reinforcement and a 4-3-4 in. configuration. The reinforcement of these panels included four Grade 60 #3 bars in the longitudinal direction for each wythe and three shear connectors in each row. In the B panels, only Connector B shear connectors were distributed uniformly for a total of 12 in each panel (see Figure 3-4). In the BC panels, 33 Connector B shear connectors were uniformly distributed with an additional six Connector C shear connectors spread throughout the panel (see Figure 3-5). D panels had Connector D shear connectors distributed uniformly at sixteen-inch spacing for a total of 33 in each panel (see Figure 3-6).

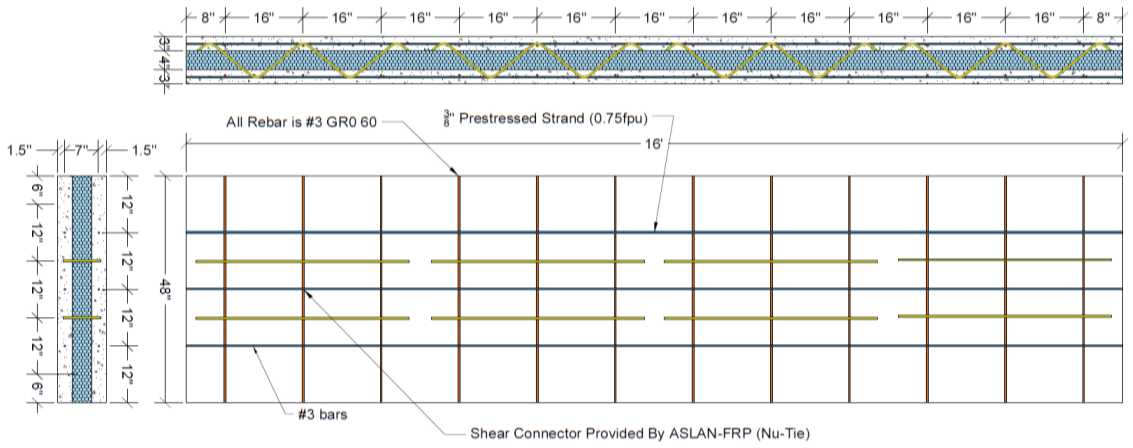

Figure 3-2 A-2 panel details

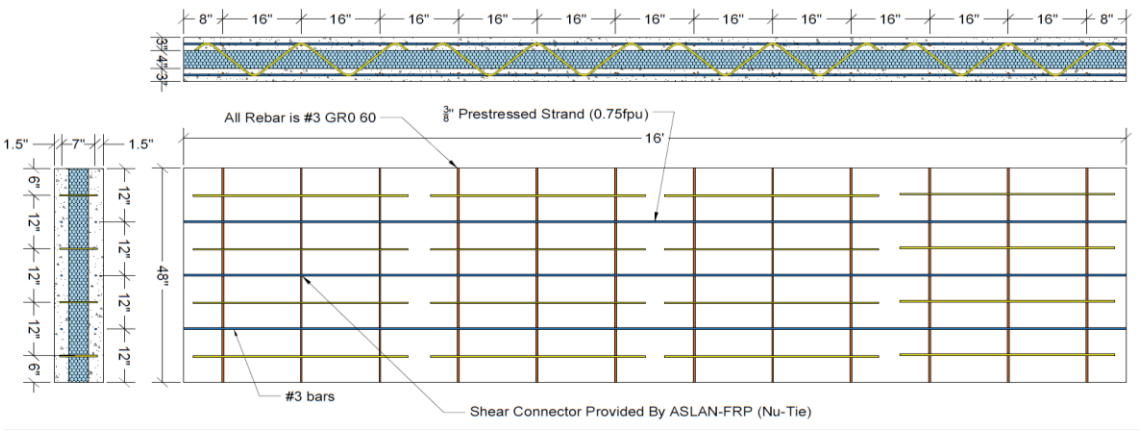

Figure 3-3 A-4 panel details

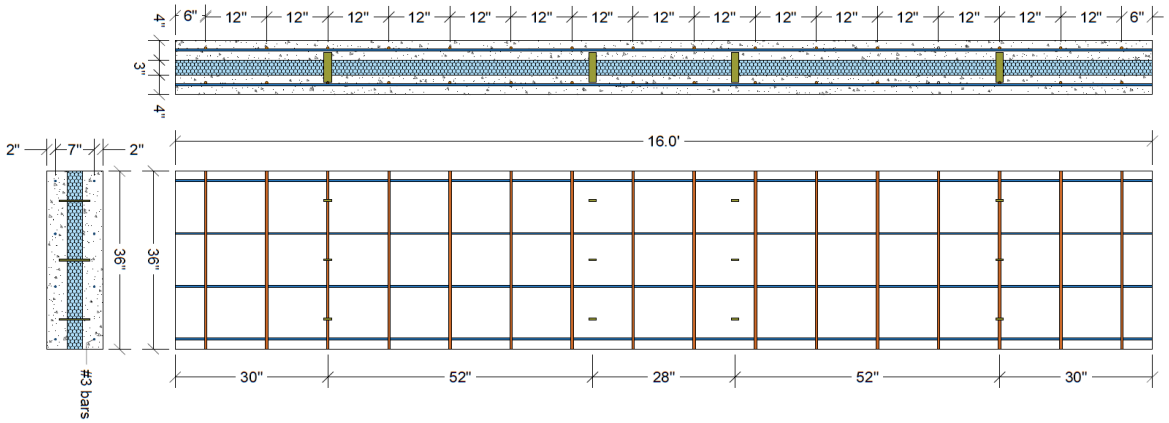

Figure 3-4 B panel details

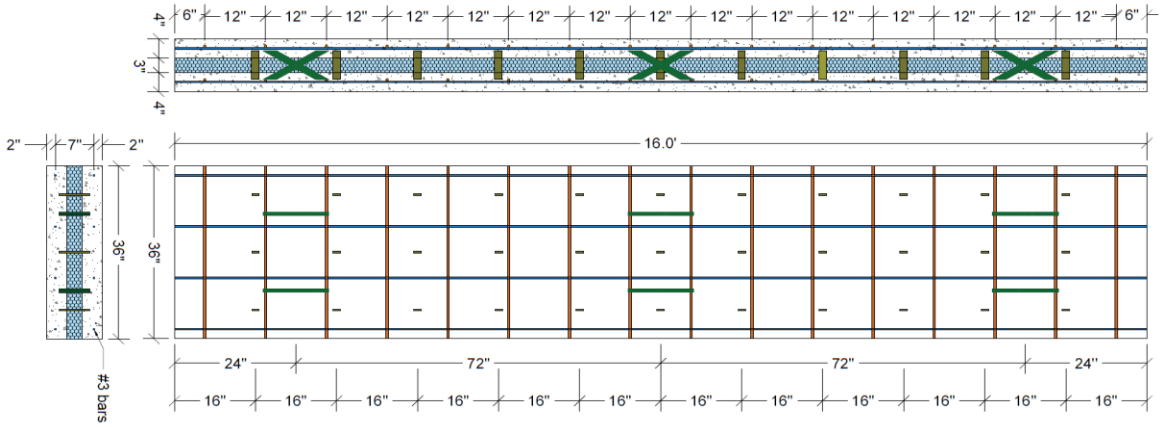

Figure 3-5 BC panel details

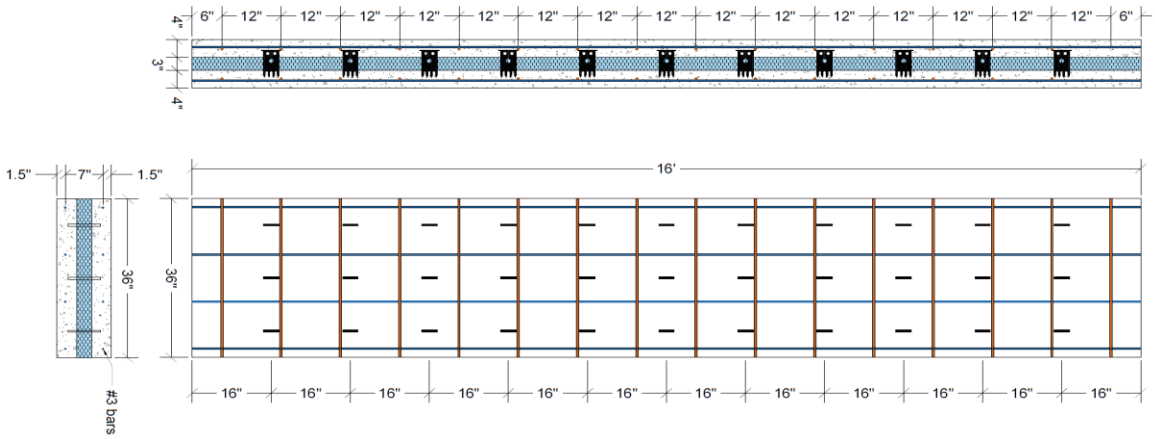

Figure 3-6 D panel details

3.2.2 Construction of Wall Panels

All panels were fabricated with XPS insulation, and utilized shear connectors to attain a certain degree of composite action by transferring the shear flow between the both wythes through the insulation. The design of the panels was performed in conjunction with representatives from Forterra Structural Precast (Salt Lake City, Utah) and Concrete Industries (Lincoln, Nebraska).

3.2.3 Full-scale Test Setup

Each 16-ft long panel was placed on simple supports with a 15-ft span for A-2 and A-4 panels, and a 14-ft span for the B, BC, and D panels. A single hydraulic actuator applied four point loads with a spreader beam assembly to simulate a distributed load, as shown in Figure 3-7.

Deflection was measured at midspan on both edges (north and south) of the panel. Relative slip between concrete wythes was measured using LVDTs at each panel corner (northeast, southeast, northwest and southwest). Prior to testing, dead load deflection was

measured at midspan with a total station and high accuracy steel ruler by finding the elevations of the supports and at midspan. This procedure provided a dead load midspan deflection with an accuracy of 1/32 in.

Concrete compression strengths were measured using ASTM C39 procedures from 4 in. x 8 in. concrete cylinders sampled and provided by the precasters. Rebar and prestressing steel samples were obtained from each panel after testing by breaking out the concrete from the ends, where there was no plasticity.

Rebar were tested according to ASTM A370 and the full stress strain curved developed using a 2-in. extensometer. Because of gripping limitations of the tensile testing machine available, standard reusable chucks were used to test the 3/8 in. prestressing strand. Using chucks during tensile testing is known to limit both elongation and provide slightly lower ultimate stresses (Morcous et al. 2012; Maguire 2009). Only ultimate tensile stress was recorded for the prestressing strand because a proper (24 in. gauge length, rotation capable) extensometer was not available.

3.2.4 Full Scale Test Sensors

The data acquisition, LVDTs for slip measurement and load cell for ram load measurement were newly calibrated. The deflection measurements were made with LX-PA-20 (UniMeasure) string potentiometers with calibration verified on a NIST traceable Tinius Olsen Universal Testing Machine to an accuracy of 0.001 in.

3.3 Material Testing

Concrete cylinder compressive tests were performed for all specimens tested. For full-scale tests, concrete cylinders were provided by the respective precaster to be tested on the day of specimen testing. Cylinders were created from the concrete midway through each pour. All cylinders were 4-inch diameter, with compressive tests performed according to ASTM C39.

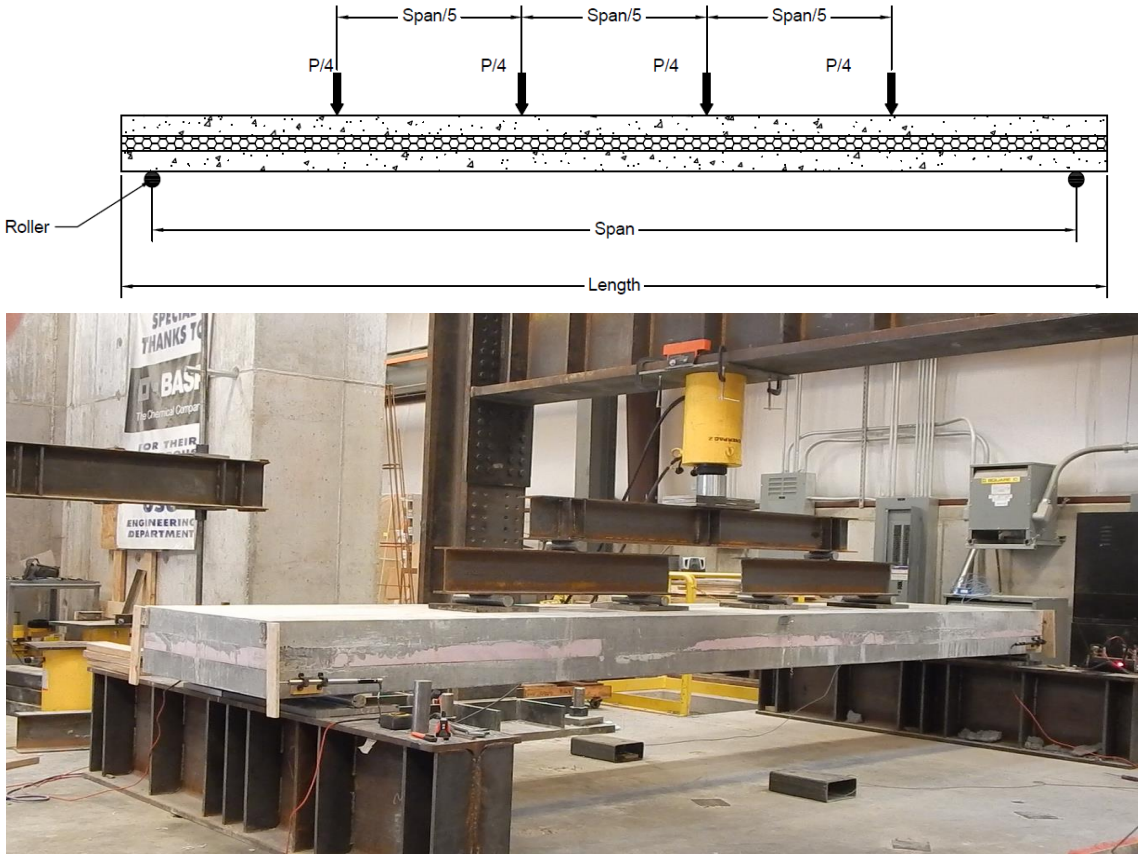

Figure 3-7 Full-scale specimen test setup

3.4 Summary

The preceding chapter described the test setup for the experimental program. The full-scale specimens were fabricated by Concrete Industries and Forterra Precast and

tested at the Utah State University SMASH lab. The following chapters present the results and analysis of the full-scale tests.

CHAPTER 4

TEST RESULTS FOR FULL-SCALE PANELS

4.1 Material Testing

Concrete cylinder compressive tests were performed for all specimens tested. For full-scale tests, concrete cylinders were provided by the respective precaster to be tested on the day of specimen testing. The results of the ASTM C39 compression testing is presented in

Table 4-1. Each value presented in

Table 4-1 is the average of three cylinders from the compression wythe taken on the day of testing. For convenience of data presentation, each connector was assigned a letter descriptor as follows: Nu-Tie connector (Connector A), Thermomass CC Connector (Connector B), Thermomass X Connector (Connector C), and HK Composite Connector (Connector D). Two panels were tested with Connector A (NU-Tie 3/8 in. diameter connectors), two with only Connector B (Thermomass CC), two with a combination of Connectors B and C (Thermomass CC and X connectors), and two with only Connector D (HK Composite connectors).

Figure 6-9 presents the stress vs strain curves for the rebar in the B, BC, and D sandwich panels. The average yield stress was 72.2 ksi and the ultimate stress was 110 ksi. The average ultimate capacity for the prestressing strands was 259 ksi. It is likely the testing method described in **Section 3.2** above affected the ultimate capacity of the strands.

Table 4-1 Concrete Compression Strength for Full-scale Specimens

Specimen	**Average f_c'** *(psi)*	**Split tension** *(psi)*	**Modulus of Elasticity** *(psi)*
A-2	10,400	766	6,191,000
A-4	10,400	766	6,191,000
B-1	9,230	691	5,824,000
B-2	8,000	699	5,986,000
BC-1	9,230	691	5,824,000
BC-2	8,000	699	5,986,000
D-1	9,230	691	5,824,000
D-2	8,000	699	5,986,000

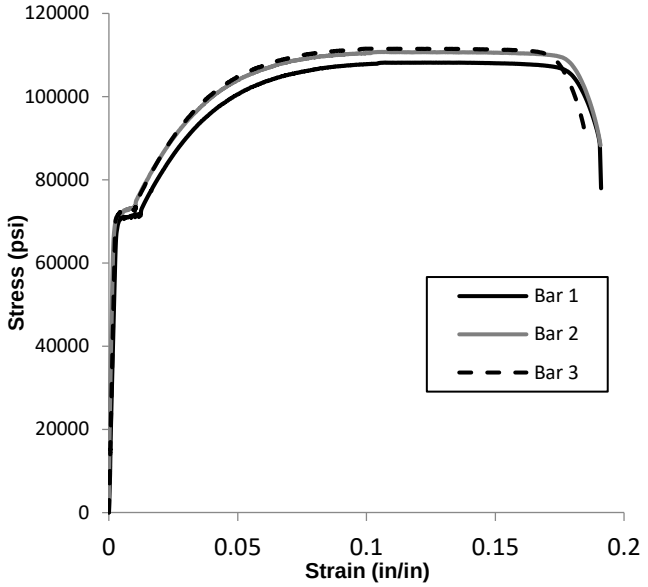

Figure 4-1 Stress vs. Strain for rebar in B, BC, and D panels

4.2 Full-scale Test Results

4.2.1 Load vs. Deflection entire data set

All loads shown herein include self-weight, and all deflections include deflection due to self-weight as measured by a total station. Figure 4-2 presents the load versus deflection plot for A-2 and A-4 panels. The maximum loads attained by the two panels were considerably different. The maximum loads attained were 30% different (compare 463 psf to 333 psf in Figure 4-2). Observed slip at the maximum load in the A-4 panel was 0.18 inches, whereas the slip at maximum load observed in the A-2 panel was 0.24 inches at failure. Clearly the shear tie intensity, at the level tested in these two panels, had a large effect on maximum load and slip.

The load vs. deflection results of B-1 and B-2 panels are presented in Figure 4-3. The maximum loads for these panels were also very similar with a difference of only 13% (comparing 355 psf for B-1 and 307 psf for B-2 in Figure 4-4). The amount of slip measured in the panels at maximum capacity was 0.74 in.

The load vs. deflection results of BC-1 and BC-2 panels are presented in Figure 4-4. The maximum loads for these panels were also very similar with a difference of only 8% (comparing 528 psf for BC-1 and 485 psf for BC-2 in Figure 4-4). The amount of slip measured in the panels at maximum capacity was 0.05 in.

Figure 4-5 presents the Load versus Deflection plots for the D-1 and D-2 panels. The maximum loads attained by the two panels were similar. The maximum loads attained had only a 6% difference (comparing 529.5 psf to 498.8 psf in Figure 4-5). The amount of slip measured in the panels at maximum capacity was 0.08 in. in both panels.

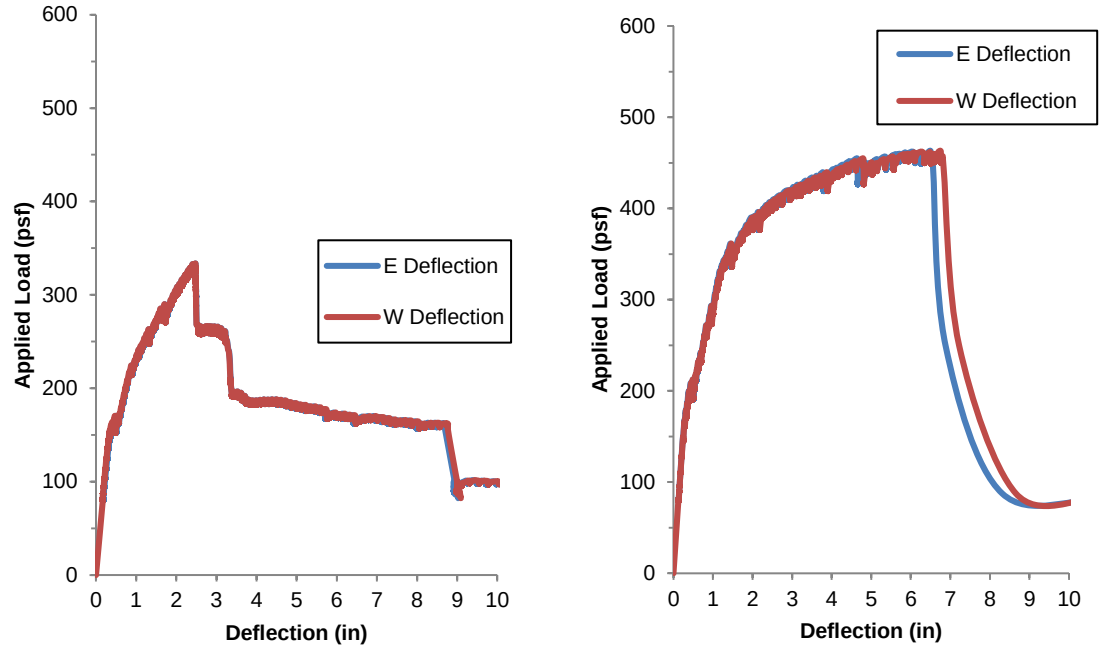

Figure 4-2 Load vs Deflection for A-2 (left) and A-4 (right)

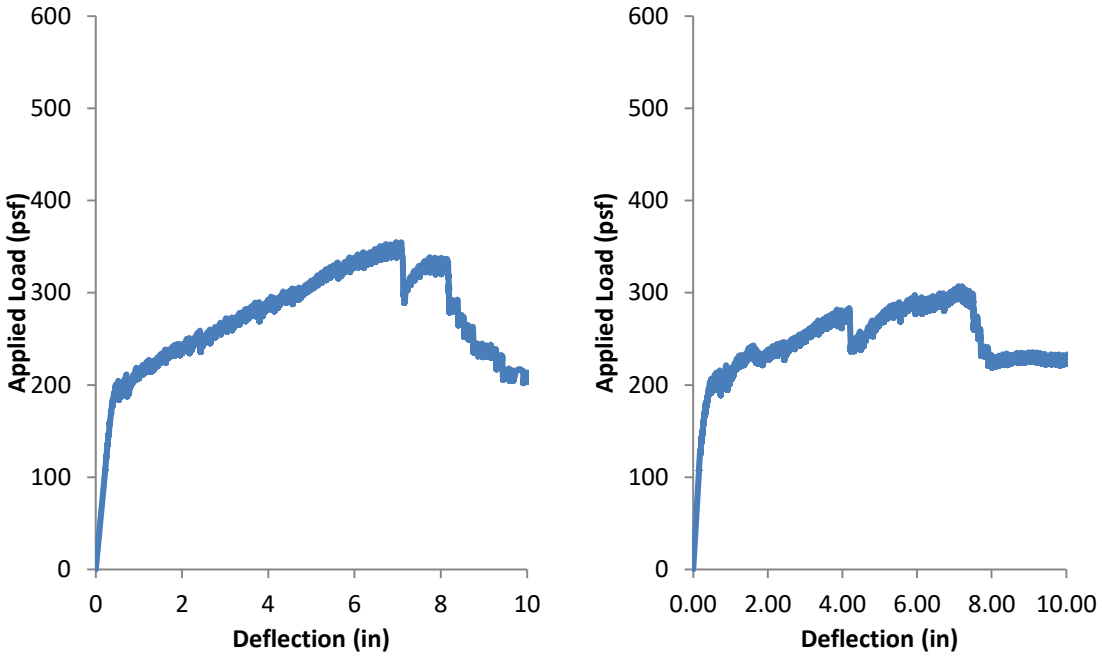

Figure 4-3 Load vs. Deflection for elastic only for B-1 (left) and B-2 (right) panels

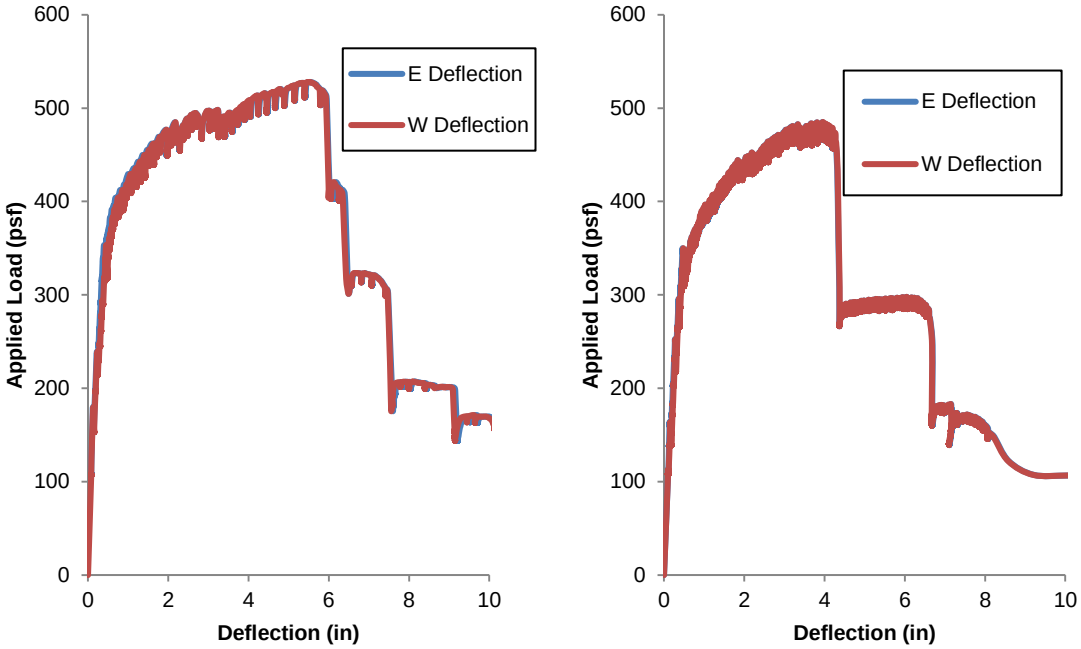

Figure 4-4 Load vs. Deflection for BC-1 (left) and BC-2 (right) panels

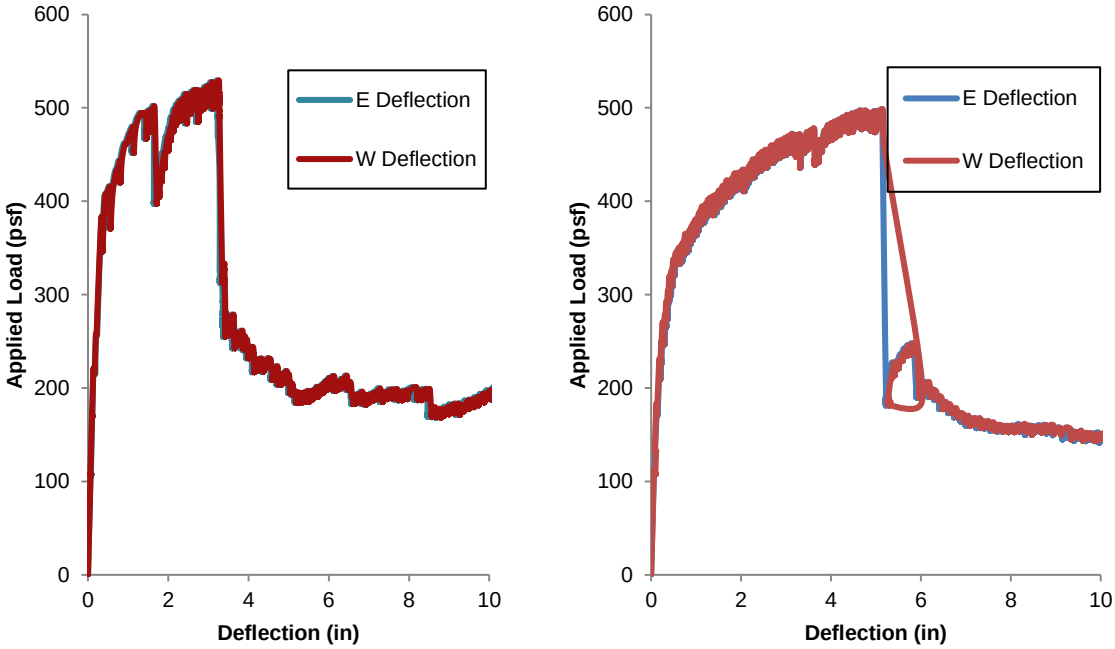

Figure 4-5 Load vs Deflection for D-1 (left) and D-2 (right) panels

The maximum loads and slip values are also summarized numerically later in Table 4-2 of Section 4.2.3.

4.2.2 Load vs. deflection for elastic only

Figure 4-6 through Figure 4-9 show the load vs deflection for the elastic only.

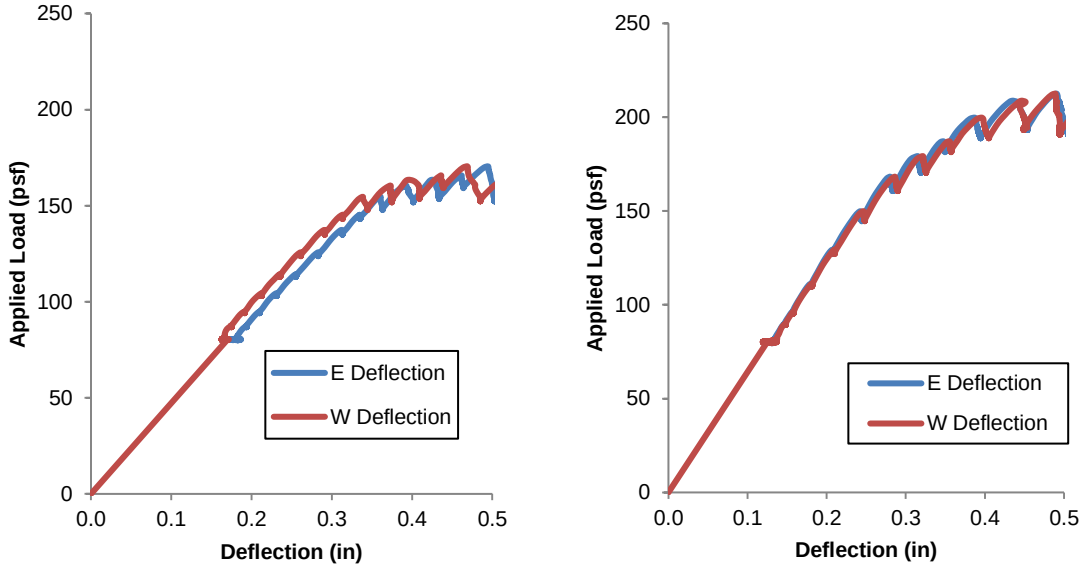

Figure 4-6 Load vs Deflection for elastic only for A-2 (left) and A-4 (right)

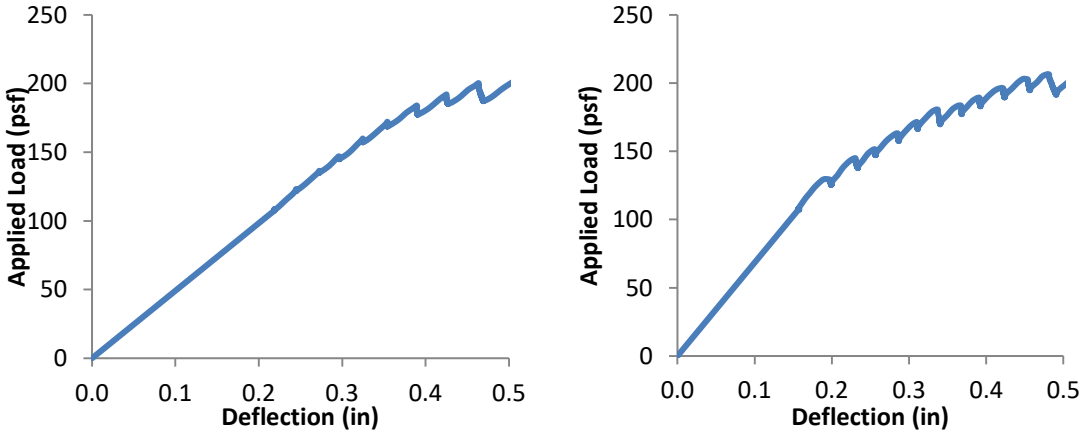

Figure 4-7 Load vs. Deflection for elastic only for B-1 (left) and B-2 (right) panels

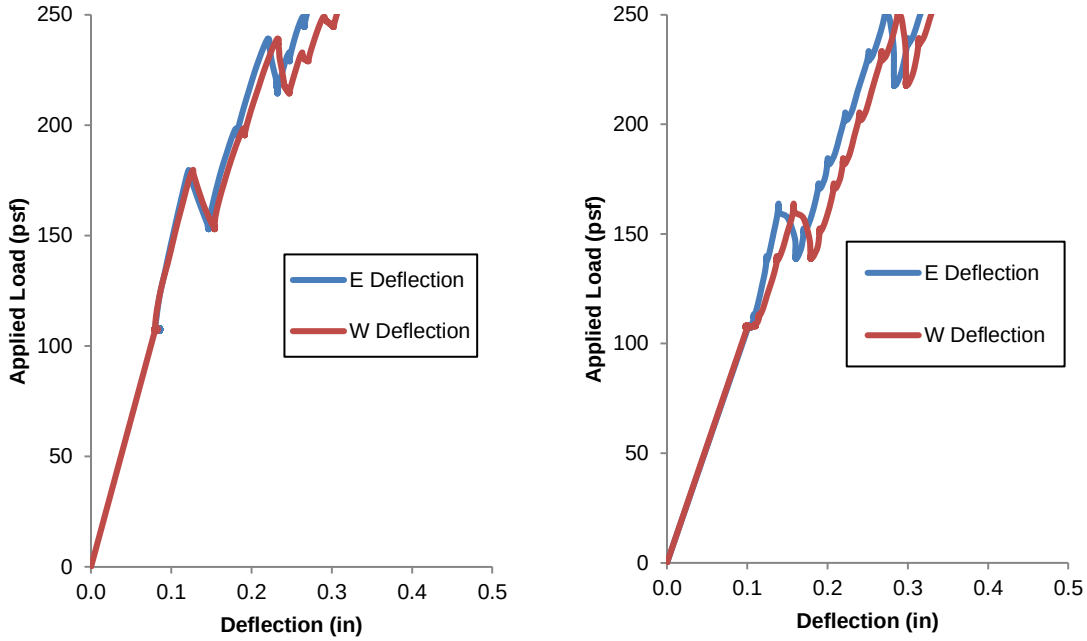

Figure 4-8 Load vs. Deflection for elastic only for BC-1 (left) and BC-2 (right) panels

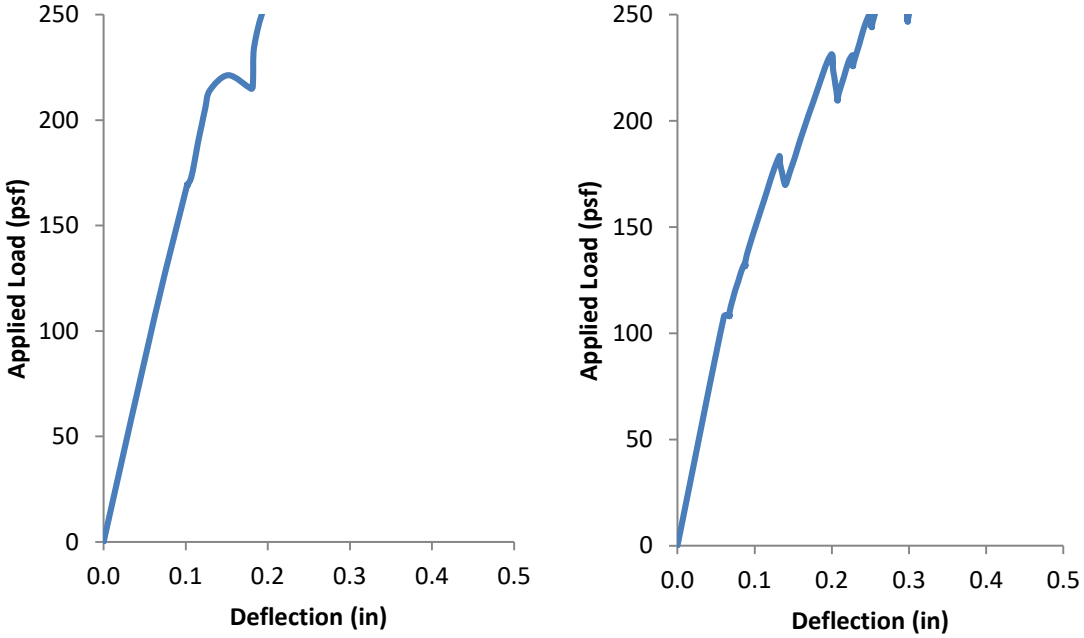

Figure 4-9 Load vs Deflection for elastic only for D-1 (left) and D-2 (right)

4.2.3 Load vs. slip for entire data set

Slip of the wythes was measured during testing to calculate the composite action within each panel. Table 4-2 summarizes the maximum loads and slips measured for all tested panels.

Table 4-2 Full-scale Specimen Panel Test Results

Specimen	**Wythe configuration** *(in)*	**Span length** *(ft)*	**Maximum Load** *(psf)*	**Slip at Maximum Load** *(in)*
A-2	3-4-3	15.0	334	0.26
A-4	3-4-3	15.0	463	0.18
B-1	4-3-4	14.0	355	0.74
B-2	4-3-4	14.0	307	0.74
BC-1	4-3-4	14.0	528	0.11
BC-2	4-3-4	14.0	485	0.05
D-1	4-3-4	14.0	530	0.08
D-2	4-3-4	14.0	499	0.08

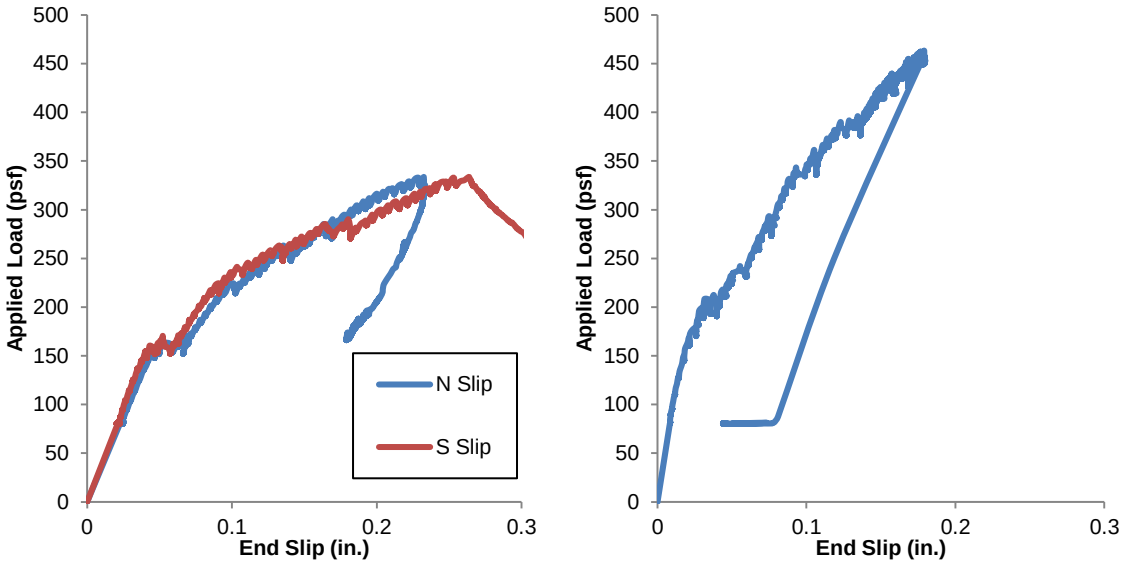

Figure 4-10 Load vs. slip for A-2 (left) and A-4 (right) panels

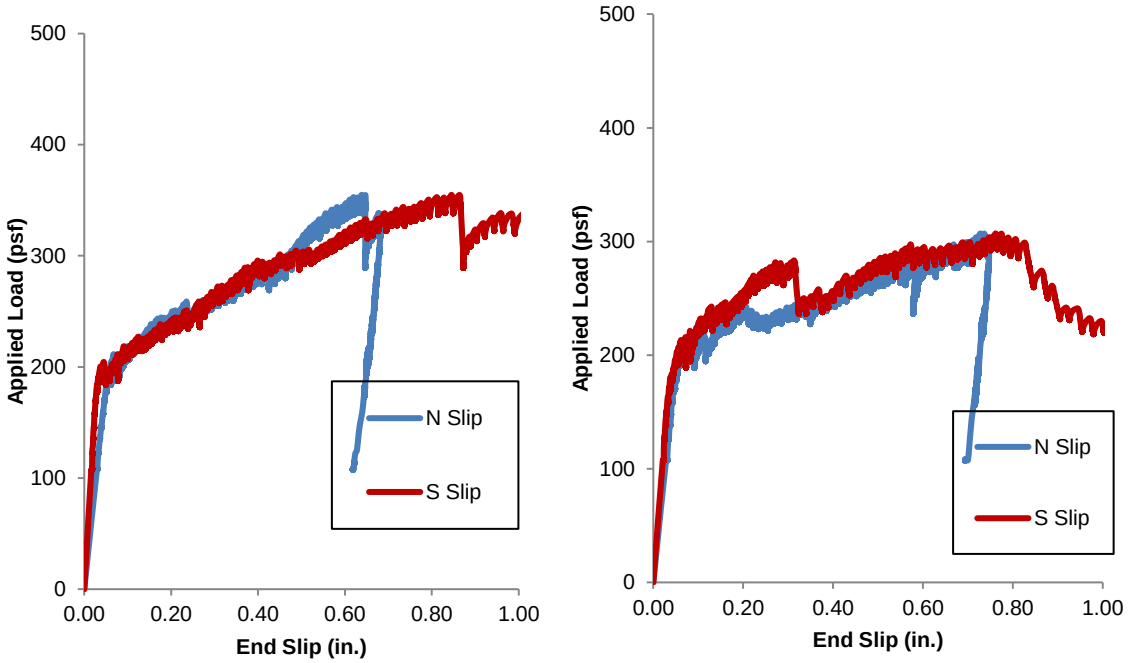

Figure 4-11 Load vs. slip for B-1 (left) and B-2 (right) panels

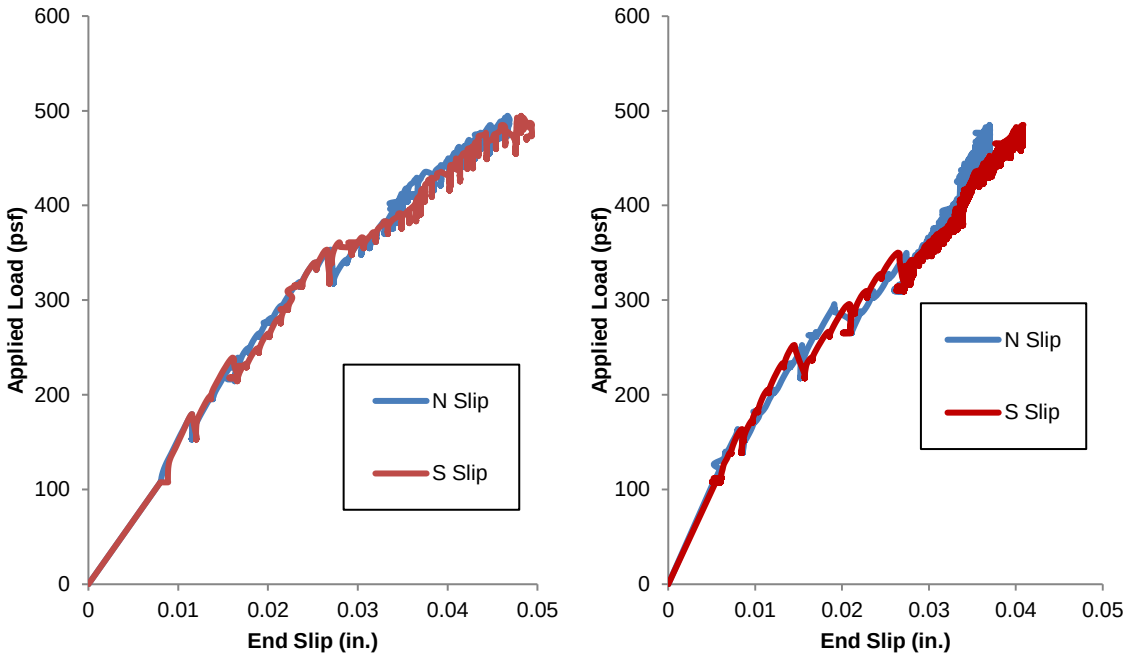

Figure 4-12 Load vs. slip for BC-1 (left) and BC-2 (right) panels

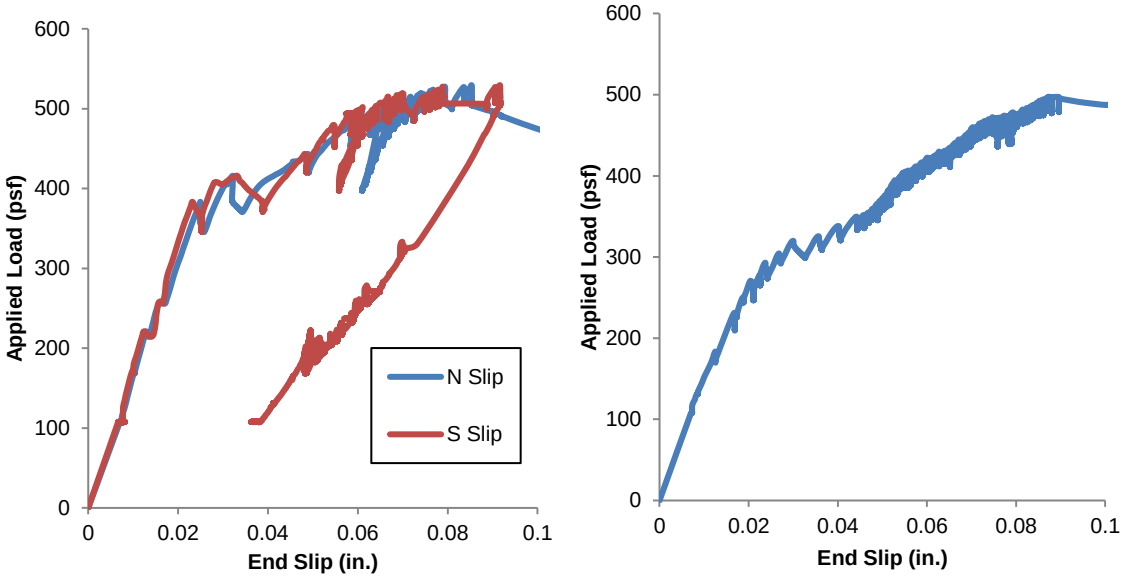

Figure 4-13 Load vs. slip for D-1 (left) and D-2 (right) panels

4.2.4 Composite Action Results

Utilizing the theoretical fully-composite moment, theoretical non-composite moment, and the actual measured moment from the test results, the degree of composite action, K_{Mn}, can be determined as shown in for different panels using Eq. (4-1).

$$K_{Mn} = \frac{M_{n,test} - M_{n,NC}}{M_{n,FC} - M_{n,NC}} \qquad (4\text{-}1)$$

Where Mn_{test} = experimental maximum moment of the sandwich panel

Mn_{NC} = theoretical maximum moment of the non-composite sandwich panel

Mn_{FC} = theoretical maximum moment of the fully composite sandwich panel

For the degree of composite action depending on cracking moment using Eq. (4-2).

$$K_{Mcr} = \frac{M_{cr,test} - M_{cr,NC}}{M_{cr,FC} - M_{cr,NC}} \quad (4\text{-}2)$$

Where Mcr_{test} = experimental cracking moment of the sandwich panel

Mcr_{NC} = theoretical cracking moment of the non-composite sandwich panel

Mcr_{FC} = theoretical cracking moment of the fully composite sandwich panel

For the degree of composite action depending on deflection using Eq. (4-3).

$$K_d = \frac{I_{test} - I_{NC}}{I_{FC} - I_{NC}} \quad (4\text{-}3)$$

Where I_{test} = experimental moment of inertia the sandwich panel

I_{NC} = theoretical moment of inertia of the non-composite sandwich panel

I_{FC} = theoretical moment of inertia of the fully composite sandwich panel

Figure 6-2 graphically demonstrates the degree of composite action shown in Eq. (4-1), (4-2), and (4-3).

Table 4-3 presents the midspan moment comparisons for the full-scale panels. The measured maximum moments of the sandwich panels were used to evaluate the composite action achieved. The measured maximum moment was calculated at midspan, using the self-weight of the panel (a distributed load) and the four point loads. The fully composite nominal moment was calculated using strain compatibility and actual material properties for the concrete and steel as presented above, assuming the entire cross section

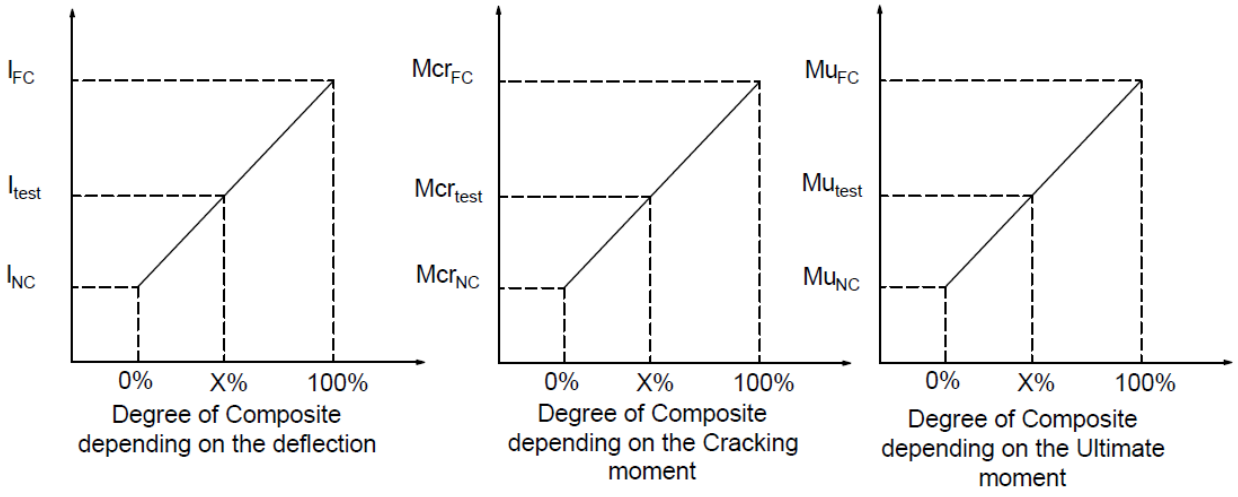

Figure 4-14 Visual demonstration of degree of composite action

was active. The non-composite moment strength was calculated in the same manner using only the properties of a single wythe and multiplying by two.

The A-4 panel resulted in 115% composite action. Other programs have noticed over 100% in the past, which is likely due to material variability as it would be impossible for a panel to be stronger than theoretically composite. Had the manufacturer designed this panel, it would have been designed at 100% composite. The A-2 panel would not have been a design coming from the manufacturer, but was prepared to demonstrate what would come from under-detailing such a panel. Doubling the number of connectors resulted in a 30% increase in composite action at ultimate.

The Connector B panels had a lower connector number due to manufacture error. This resulted in an average of 50% composite action, and is not realistic of actual design used in the field.

The Connector BC panels resulted in a composite action of 103% and 93% (Table 4-3). However, the manufacturer would recommend only 70% composite action at nominal strength for these connectors

Table 4-3 Measured Composite Action vs. Manufacturer Reported Composite Action for maximum moment

Specimen	**M_{nFC} (lb*ft)** *(lb*ft)*	**M_{nNC} (lb*ft)** *(lb*ft)*	**Measured Composite Action** *(%)*	**Manufacturers Reported Composite Action** *(%)*
A-2	55,000	15,800	70%	-*
A-4	55,000	15,800	115%	100%
D-1	44,100	12,800	104%	80%
D-2	43,400	12,200	97%	80%
BC-1	44,100	12,800	103%	70%
BC-2	43,400	12,200	93%	70%
B-1	44,100	12,800	41 %	-*
B-2	43,400	12,200	57 %	-*
* Purposely reinforced lower than usual – not a typical panel				

The D-1 and D-2 panels at the as-built 16 in. spacing would have resulted in a panel designed at 80% composite action per manufacturer recommended guidelines. Both panels achieved far more that 80% composite (see 104% and 97% in Table 4-3).

From the panels tested with the recommended connectors, it is clear that the manufacturer recommended empirically based composite actions are accurate and conservative.

4.3 Conclusions

Eight concrete sandwich panels were tested to failure at the Utah State University Structures Lab. The purpose of the testing was to evaluate the percent composite action for the connector configurations and compare the results to those reported by composite connector manufacturers. The following conclusions can be made from the experimental program:

- The type and intensity of shear connectors significantly affect the degree of composite action achieved in a concrete sandwich wall panel. Doubling the number of shear connectors in the Connector A panels (Nu-Tie connector) resulted in a large gain in percent composite action. (Note that the A-2 panel is reinforced much lighter than would be detailed for an actual building)
- The manufacturer-reported degree of composite action can be considered conservative for the panel configurations and connectors and connector patterns tested in this paper.

CHAPTER 5

PREDICTING ELASTIC BEHAVIOR

5.1 Introduction

Predicting concrete sandwich panel elastic stresses and deformations is paramount for design to prevent cracking and limit second order effects. Several researchers have developed techniques to predict sandwich panel deformations (e.g. Bunn 2011; Frankl et al. 2011; Bai and Davidson 2015; Woltman et al. 2013). Prediction methods vary significantly in complexity and accuracy. This section presents two proposed methods that were developed and used during this testing that may give engineers a quick and accurate prediction of the elastic behavior of PCSWPs in the future: the Beam Spring Model, and the proposed Elastic Hand Method.

5.2 Beam Spring Model

The first model investigated was an analytical model created using a commercial matrix analysis software package and is a more general variation of what many connector manufacturers do currently using usually specialized techniques for their connector shape/configuration. This model could easily be replicated using any commercial or personally written matrix analysis software, and could also be easily built into commercial wall panel analysis and design software and should work for any connector type. This approach modeled the PCSWP using only beam and spring elements (Figure 5-1) combined with the appropriate material values, boundary conditions, and shear connector stiffnesses (attained from literature review). Other research programs (e.g.,

modified truss and beams and springs [Teixeira et al. 2016]) have described similar methods using matrix software. This concept has been around for decades when discussing multi-wythe masonry (Drysdale, Hamid, and Baker 1994). Similar models have also been used in the literature for prediction of dynamic response of coupled structures (Behnamfar et al 2016). Many connector manufacturers use a truss analysis with matrix software, usually a Vierendeel truss, but some angled connectors, like Connector A (Nu-Tie connector), use angled truss elements. The purpose of developing a simple model that relies only on springs and beam elements is that it can be used to model a panel with any connector type, repetitively, with little to no change between analyses, and relies only on shear testing data, which most connector companies already have from ICC-ES acceptance criteria, specifically ICC-ES AC320 and ASTM E488-96. The proposed two-dimensional model consists of two frames with cross-sectional areas equal to the area of the wythes of the panel they represent. These beam elements can be assigned the individual gross properties of each wythe and separated by a distance equal to the distance between the centroids of the wythes. Shear and axial spring elements are then used to model the transfer of shear force between wythes, and are assigned shear stiffnesses corresponding to the actual stiffnesses of the connectors as measured in (Olsen et al 2017 and Al-Rubaye et al 2018). Support conditions are modeled as pin (translation fixed, rotation free) and roller (longitudinal translation free, transverse translation fixed, rotation free) and should be placed at the appropriate location on the panel.

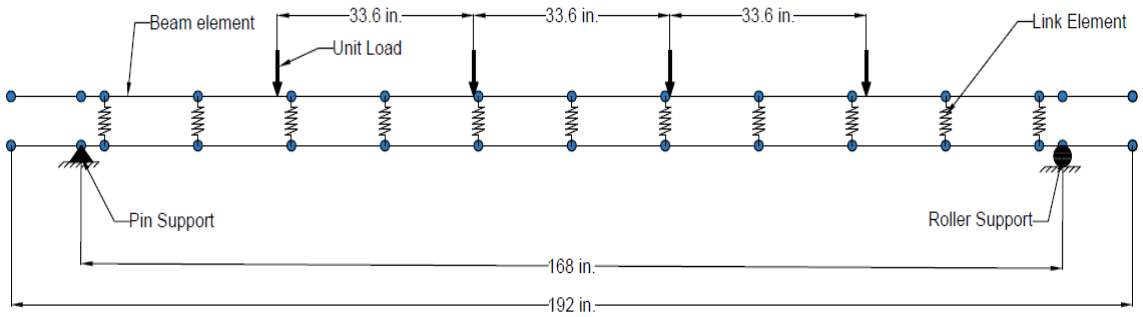

Figure 5-1 Example of Full-scale specimen modeled using the Beam Spring Model

To verify this method, each test specimen was modeled from the previous chapter, and elastic deflections and stresses were compared to the test results. Because each test specimen had a different connector configuration and spacing, links connecting the beam elements were placed at locations corresponding to each of the shear connectors. The values of shear stiffness, K_E, used in each model are shown in Table 5-1. These shear connector stiffnesses from the push-off tests included both the stiffness of the connector and the lumped insulation stiffness. For design, it may be prudent to use the unbonded values, but to verify the accuracy of the panels in this study the bonded values for K_E were used.

The model included four point loads applied to the top face of the model, imitating the full-scale testing performed in this study. In addition, self-weight was added to the total load. Links were also assigned longitudinal stiffnesses based on the tributary geometry and on an assumed Young's modulus of XPS insulation (since XPS was the only insulation used for the full-scale specimens). Tension/compression values for the

Table 5-1 Panel Properties

Panel	Width *in.*	Configuration *in.*	Span *in.*	Modulus of Elasticity of Concrete *psi*	Concrete Split Tension *psi*	Connector Stiffness (K_E) *kips/in*	Insulation Modulus of Elasticity *psi*
A-2	48	3-4-3	180	6,191,000	766	118	670
A-4	48	3-4-3	180	6,191,000	766	118	670
B-1	36	4-3-4	168	5,824,000	691	17.9	670
B-2	36	4-3-4	168	5,986,000	699	17.9	670
BC-1	36	4-3-4	168	5,824,000	691	17.9 205	670
BC-2	36	4-3-4	168	5,986,000	699	17.9 205	670
D-1	36	4-3-4	168	5,824,000	691	94.8	670
D-2	36	4-3-4	168	5,986,000	699	94.8	670

connectors were not measured in this study, but most connector companies have tension testing performed according to ICC-ES AC320. With this model, the deformations and deflections were easily predicted along with axial forces and bending moments in the concrete wythes, which can be resolved into stresses. The results will be discussed later in **Section 5.3.**

5.3 Elastic Hand Method Analysis Procedure

5.3.1 Elastic Hand Method Description

The proposed Elastic Hand Method for predicting deflections and cracking requires a sectional analysis as well as a full member analysis in order to incorporate panel geometry and connector forces. This method was based on the following assumptions:

1. Standard Euler-Bernoulli beam theory applies to the individual wythes (i.e. plane sections remain plane and normal to the deflected axis)
2. Linear elastic material behavior (including the shear connectors).
3. The Principle of Superposition is valid
4. The slip varies linearly along the length of the panel as shown in Figure 5-2. This implies that the shear forces will vary linearly too if the connectors are identically distributed. This is not always true, but is a reasonable simplification as will be demonstrated below.

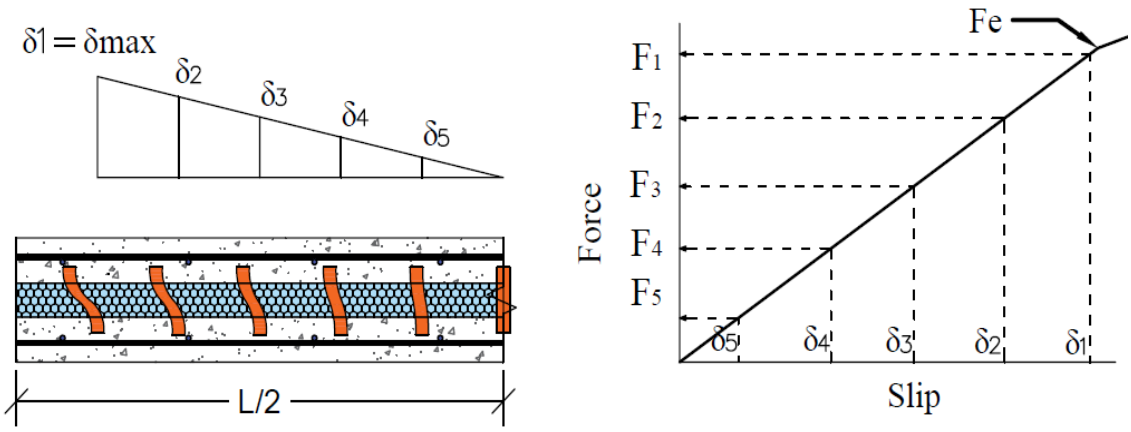

Figure 5-2 Slip Diagram Along the Length of the Panel

Using the above assumptions, the engineer must perform an iterative procedure due to the nature of determining slip for various connector patterns. Once the connector force is determined based on the end slip, a sectional analysis is performed for the controlling wythe (the cracking wythe) and deflections can be easily determined using elastic beam equations. The guessed slip will need to be checked using slip kinematic

relationships, but this is accomplished using familiar mechanics equations and equivalent loads.

5.3.2 Elastic Hand Method Procedure

The cracking moment and deflection predictions of the Elastic Hand Method depend mainly on the section geometry, modulus of rupture of the concrete, the elastic modulus, and the connector forces. For the purposes of discussion, wythe 1 is considered the wythe that would be in compression during positive bending of a fully composite sandwich panel and wythe 2 is considered the wythe that would be in tension during positive bending of a fully-composite sandwich panel. The following steps comprise the procedure for the Elastic Hand Method.

1. Calculate the material and section properties assuming the sandwich panel acts non-compositely. The following equations are an example. These may vary depending on the type of reinforcement.

$$E_c = 33.0 * \gamma^{1.5} * \sqrt{f'c} \qquad (5\text{-}1)$$

$$f_r = 7.5 * \sqrt{f'c} \qquad (5\text{-}2)$$

$$I_{NC1} = \frac{bt_{conc_1}^3}{12}$$

$$I_{NC2} = \frac{bt_{conc_2}^3}{12} \qquad (5\text{-}3)$$

$$Z = \frac{t_{conc_1} + t_{conc_2}}{2} + t_{insul} \qquad (5\text{-}4)$$

Where E_c = modulus of elasticity of the concrete (psi)

γ = unit weight of the concrete (pcf)

f_c' = concrete compressive strength (psi)

f_r = modulus of rupture of concrete (psi)

I_{NC1} = moment of inertia of non-composite wythe 1 (in^4)

I_{NC2} = moment of inertia of non-composite wythe 2 (in^4)

b = slab width (in)

t_{conc1} = thickness of wythe 1 (in)

t_{conc2} = thickness of wythe 2 (in)

Z = distance between compression and tension wythe centroids (in.)

t_{insul} = insulation thickness (in)

2. Assume an end slip, which is the slip at the end connector line (see Figure 5-2). Calculate the slips in the other connectors using similar triangles or Eq. (5-5).

$$\delta(i) = \delta_{max} * \frac{\left(\frac{L}{2} - x_i\right)}{\left(\frac{L}{2} - x_1\right)} \qquad (5\text{-}5)$$

Where $\delta(i)$ = slip in connector i (in)

δ_{max} = Slip in the end connector (in), also assumed to be the max. slip in the panel

L = total length of the sandwich wall panel (in)

x_i = location of the connector from the end of the panel (in)

3. Calculate the forces in each connector and connector line using Equations (5-6) and (5-7).

$$F_i = \delta(i)\ N_i * K_E \qquad (5\text{-}6)$$

$$F_{sum} = \sum F_i \qquad (5\text{-}7)$$

Where $F(i)$ = is the force in connector line i (in)

N_i = is the number of connectors in connector line i

K_{Ei} = is the elastic stiffness from shear testing for the connectors in connector line i

F_{sum} = is the sum of the connector forces at the longitudinal location of interest

4. Calculate the cracking moment for a mild reinforced non-composite wythe (assuming wythe 2 will crack before or simultaneously with wythe 1) as shown below, with appropriate addition of prestressing forces if necessary (not shown), and including the axial force generated by the connector forces from Equation (5-7) and as demonstrated by Figure 5-3:

$$\frac{M_{wy_2} * \frac{t_{conc_2}}{2}}{I_{NC2}} + \frac{F_{sum}}{b * t_{conc2}} = f_r$$

$$M_{wy_2} = 2 * I_{NC2} * \left(\frac{f_r}{t_{conc_2}} - \frac{F_{sum}}{b * {t_{conc2}}^2} \right) \qquad (5\text{-}8)$$

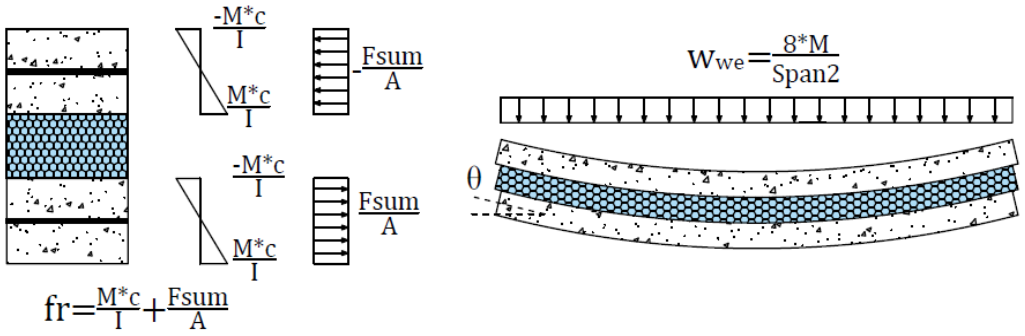

Figure 5-3 Load and stress profile of sandwich panel (left) equivalent load (right)

5. Now, the applied load that causes this cracking moment can be back calculated which will aid in determining deflections and rotations. Calculate the equivalent load that wythe 2 can carry using equations (5-8) and (5-9). Figure 5-3 shows the stress profile and the equivalent distributed load to produce the cracking moment in a reinforced concrete section. An equivalent load can be a distributed load, a point load, four point loads etc. depending on load condition. Equation (5-9) demonstrates the equivalent distributed load for the moment carried by only the bottom wythe at cracking assuming the wythes share load equally ($t_{conc1} = t_{conc2}$).

$$M_{wy_2} = \frac{w_{we2} Span^2}{8}$$

$$w_{we2} = \frac{8 * M_{wy_2}}{Span^2} \qquad (5\text{-}9)$$

To determine if the above assumption of slip is correct, the slip needs to be recalculated for verification. This iteration is deemed necessary only

because solving for the slip (in a closed form) directly is very cumbersome (but possible). Slip calculation is accomplished by finding the different components of slip (axial and rotational, see Figure 5-4) at the end connector line and comparing it to the assumptions using the equivalent load above. For additional accuracy, the same process could be used at each connector line (with additional iteration), but will be shown to be unnecessary with respect to accuracy.

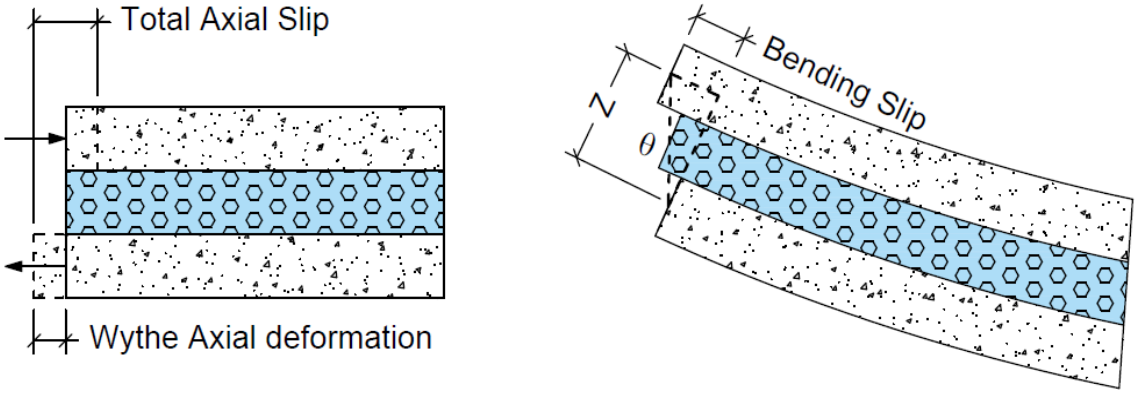

Figure 5-4 Axial and Bending Slip

6. Using the equivalent load from the previous step, calculate axial and rotational displacement at the end connector. Rotation (θ) of the wythe at the end connector location can be calculated using published equations (available in the PCI Design Handbook) or an elastic structural analysis method (e.g. Castiglione's Theorem, Virtual Work) for the applied load (e.g., distributed, point loads). For this explanation, it is assumed a distributed load is most common and is presented in Equation (5-10).

Equation (5-10) uses the moment of inertia of only wythe 2 and the equivalent load calculated in the previous step for wythe 2.

$$\theta = \frac{w_{we2} * Span^3}{24 * E * I_{NC2}} \qquad (5\text{-}10)$$

$$\Delta_{Rot} = \theta * Z \qquad (5\text{-}11)$$

Where w_{we} = equivalent distributed load of the wythe (lb/in)

θ = angle of rotation (radians)

Span = support to support distance (in)

Δ_{Rot} = slip of the wythes due to bending (in) at the end connector

n = total number of connector rows on *L*/2

To calculate the axial slip, one must account for each of the connector forces along the beam based on the assumed slip distribution. Then the axial forces from the connectors combined with their locations on the panel are used with the well-known elastic axial deformation equation (*PL*/*AE*) for both wythes. This process is demonstrated in Figure 5-5 for a single wythe. Equation (5-12) below could be simplified for direct solution of standard connector patters (e.g., uniform, triangular) if desired.

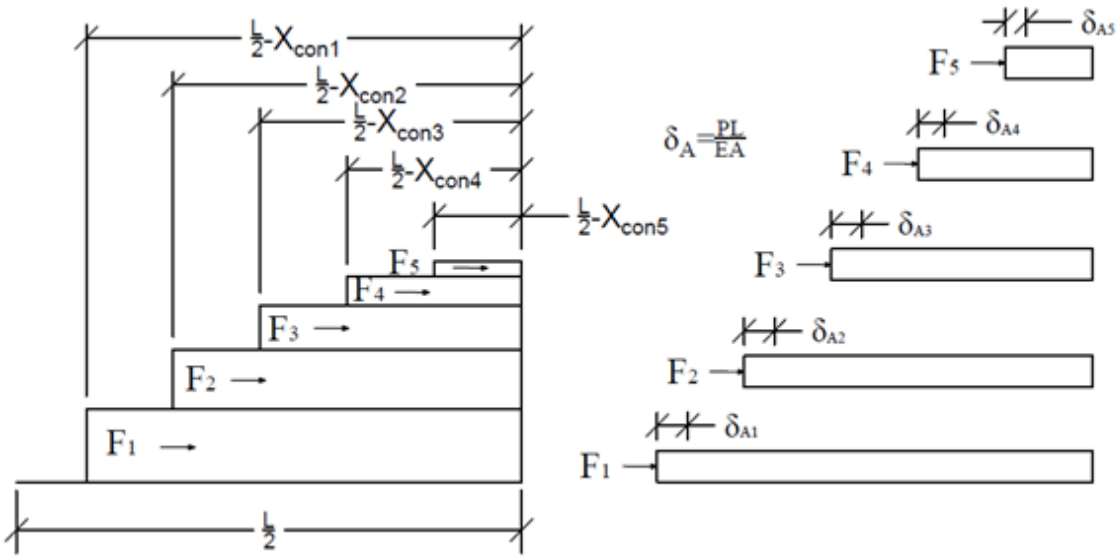

Figure 5-5 Axial slip

$$\Delta_{Axial} = \left[\left(\frac{1}{b * E * t_{conc_1}}\right) + \left(\frac{1}{b * E * t_{conc_2}}\right)\right] * \sum_{i=1}^{n} F_i * \left(\frac{L}{2} - x_i\right) \quad (5\text{-}12)$$

Where Δ_{Axial} = slip of the wythes due to axial deformation at the end connector (in)

n = total number of connector lines on the half span

i = connector line starting at the end of the panel

F_i = force in connector i (lb)

x_i = location of connector line i

7. Finally, using Equation (5-11) and (5-12), the slip at the end connector can be calculated as

$$\delta_{end} = \Delta_{Rot} - \Delta_{Axial} \qquad (5\text{-}13)$$

Total slip at every connector is the result of two components: the axial deformation and the bending slip, as shown in Figure 5-4. I may also be noted that the axial slip and the rotation slip act in different directions. Because they are calculated as absolute deformations in Equation (5-11) and (5-12), they lose their sign and Equation (5-13) requires the negative sign.

Compare this slip value to that assumed in Step 2, and repeat Steps 2 through 6 until δ_{end} assumed (Step 2) is equal to δ_{end} calculated (Step 6). This is most easily accomplished using a spreadsheet or computer program.

8. Calculate the cracking moment using equation (5-14).

$$M_{cr} = M_{wy_2} * 2 + F_{sum} * Z \qquad (5\text{-}14)$$

Where M_{cr} = applied moment (lb-in)

Calculate deflection using Equation (6-1) for a uniform distributed load. For different loading pattern, a different formula should be used.

$$\Delta = \frac{5 * w_{we2} * Span^4}{384 * E_c * I_{NC2}} \qquad (5\text{-}15)$$

Where Δ = predicted overall deflection of the midspan of the sandwich wall panel (in)

The above steps and explanation outline the approach using only first principles and equations most engineers are familiar with. Below, this methodology will be checked against the experimental results in previous chapters which include panels with prestressing only, mild reinforcing only, different depths, different concrete strengths, different connectors, and different connector patterns. In theory, this method could also be used to predict behavior of panels with holes and at any location along the length of the panel, with some modifications.

5.4 Validation of the Beam-Spring Model and Elastic Hand Method

Predictions of cracking moment, deflection, and slip of the eight full-scale test panels were made using the Beam-Spring Model and Elastic Hand Method above, and then compared to the actual measured values to validate these predictions. Both methods returned very favorable results. Figure 5-6 presents the actual results and predictions of both models for the full-scale A-2 sandwich panel. In this figure and those similar in the following, the Beam Spring and Elastic Hand Method (labeled as HM), are plotted up

through cracking, which is the last point at which they are valid. In the plots, a slightly bi-linear relationship for the HM and the Beam-Spring model can be observed (which is counterintuitive for an elastic method) this is because the method was applied for a uniform load to simulate dead load and then four point loads (as it was tested).

Both models show excellent agreement with the observed behavior. The cracking moment differs only by 0.5% and 0.8% for the Beam-Spring Model and Elastic Hand method, respectively. Deflection at the cracking moment differs by 14% and 4% for the Beam-Spring model and Elastic Hand method, respectively. The actual slip of the A-2 panel was measured to be 0.05 inches, with the Beam-Spring Model predicting 0.045 inches and the Elastic Hand Method predicting 0.0423 inches. Furthermore, in the below figures, it is easy to see the experimental load deformation plots and the slip plots become non-linear just as the HM and beam spring model predict cracking.

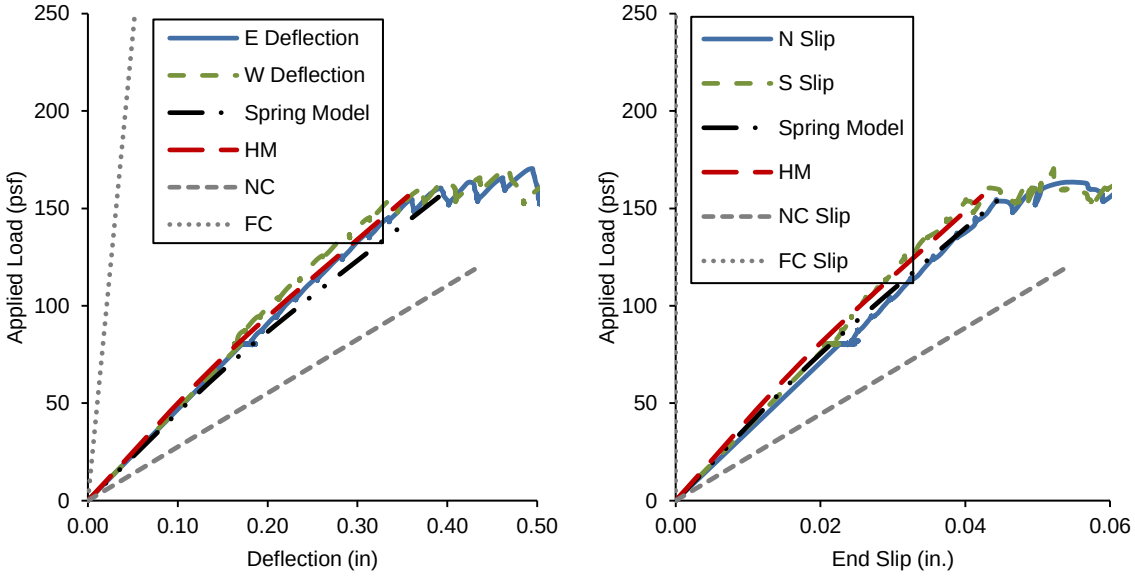

Figure 5-6 Load versus Deflection (left) and Load versus End Slip (right) for A-2 Panel

The Beam-Spring Model and the Elastic Hand Method underpredicted the cracking moment of the A-4 panel by 5% and 4% percent respectively. Figure 5-7 shows that the applied load at cracking was around 200 psf, which differed slightly from the predictions of both methods. Both methods overpredicted the slip in this specimen, the Beam-Spring Model doing so by 11% and the Elastic Hand Method by 14%.

The Connector B specimens are included in this section only for completeness. The full-scale Connector B specimens were fabricated incorrectly and transported improperly, arriving to the USU facility cracked. As such, deflection and cracking predictions are not valid by the methods presented here and are not indicative of a real-life panel reinforced per manufacturer recommendations. The load vs. deflection and load vs. slip for the Connector B specimens are shown in Figure 5-8 and Figure 5-9. The Beam-Spring Model and Elastic Hand Method for this case predicted the same cracking load and slip values. A comparison of the actual values to the predicted values was not possible for these specimens since the panels had cracked during transportation.

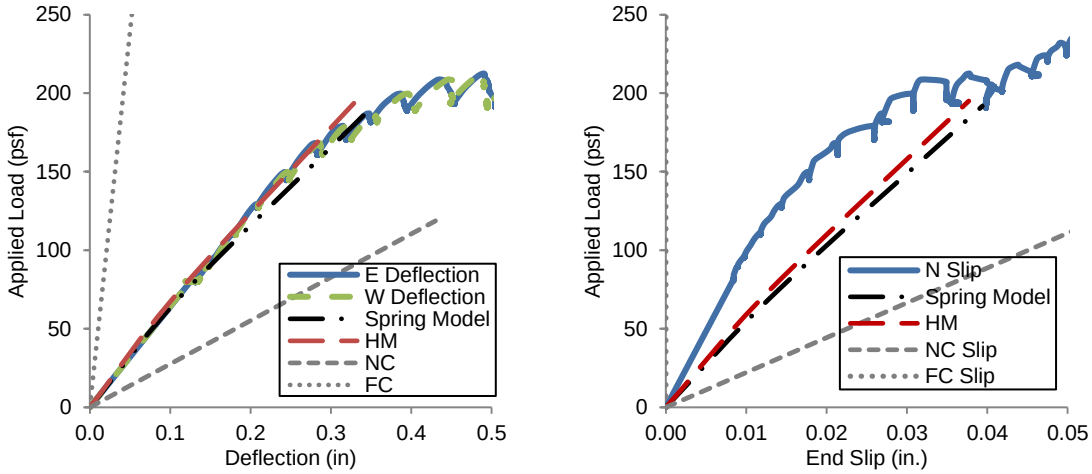

Figure 5-7 Load versus Deflection (left) and Load versus End Slip (right) for A-4 Panel

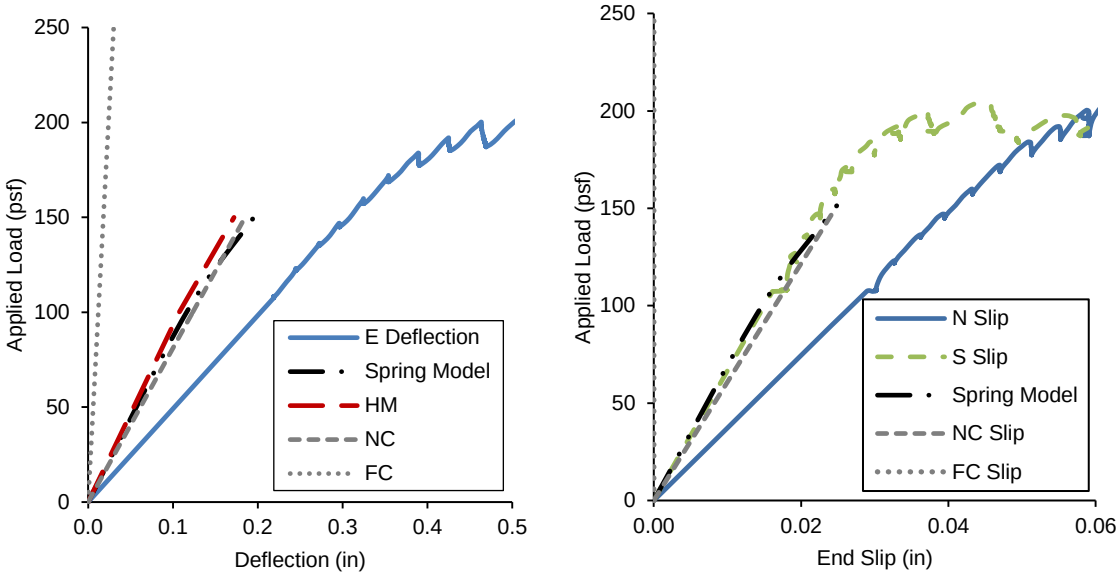

Figure 5-8 Load versus Deflection (left) and Load versus End Slip (right) for B-1 Panel

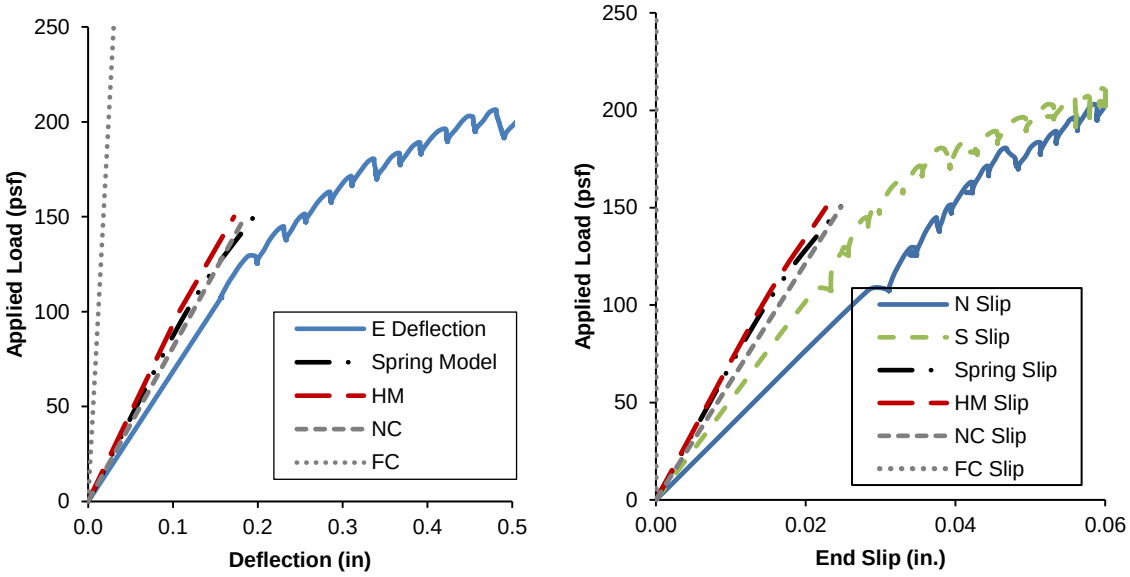

Figure 5-9 Load versus Deflection (left) and Load versus End Slip (right) for B-2 Panel

Both methods overpredicted the cracking load, the Beam-Spring Model by 10% and the Elastic Hand Method by 10% as shown in Figure 5-10 and Figure 5-11 for the

BC-1 and BC-2 panels. The slip for the BC specimens was overpredicted by 80% for both methods.

Figure 5-12 and Figure 5-13 display the predicted values vs. the actual values for the D-1 and D-2 specimens. The cracking load predicted by the Beam-Spring Model matched the average result of the full-scale D panel specimens. However, the Elastic Hand Method overpredicted the cracking load by 9%. The Beam-Spring Model overpredicted the slip by 18%, and the Elastic Hand Method overpredicted the slip by 40%.

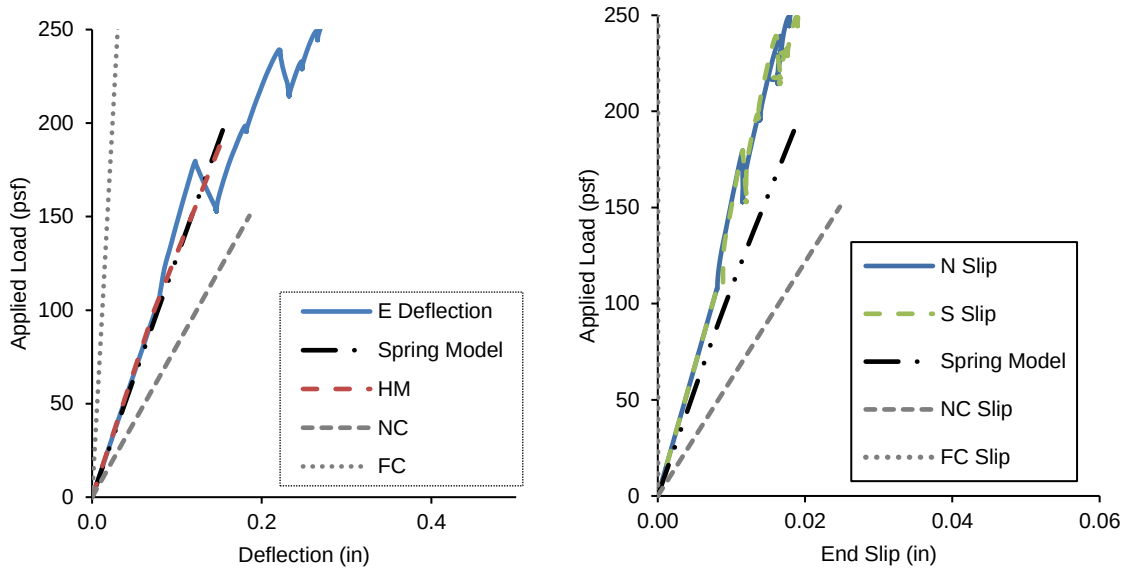

Figure 5-10 Load versus Deflection (left) and Load versus End Slip (right) for BC-1 Panel

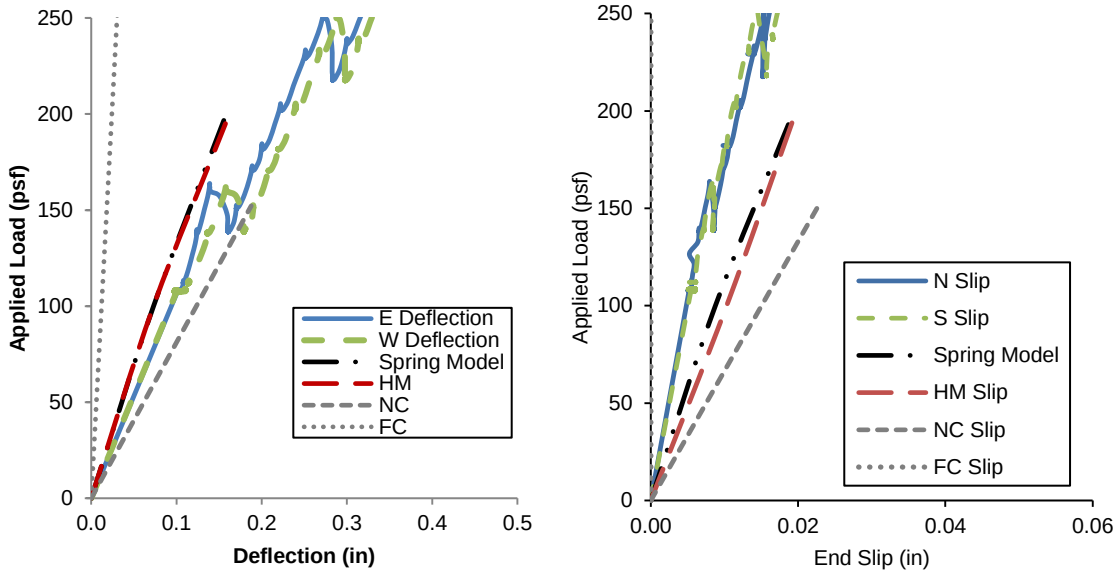

Figure 5-11 Load versus Deflection (left) and Load versus End Slip (right) for BC-2 Panel

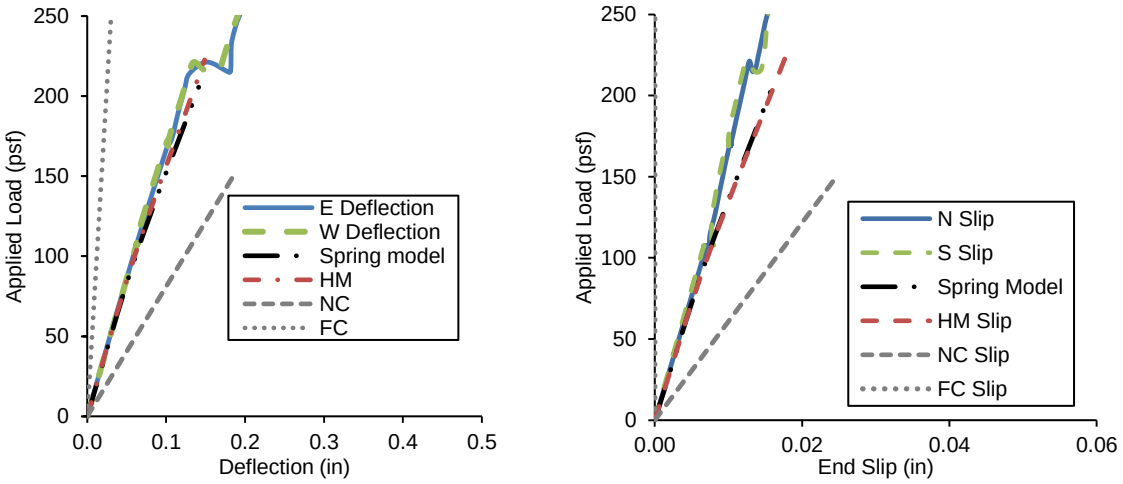

Figure 5-12 Load versus Deflection (left) and Load versus End Slip (right) for D-1 Panel

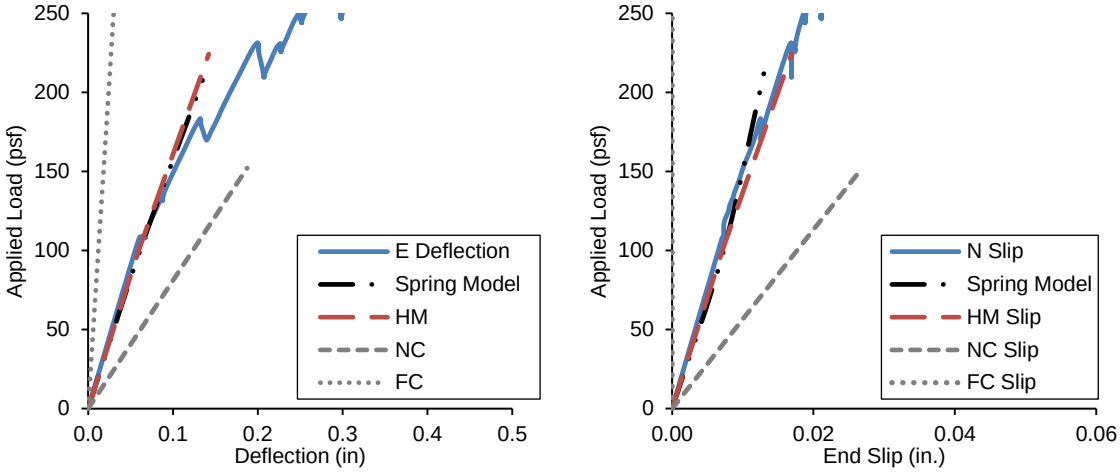

Figure 5-13 Load versus Deflection (left) and Load versus End Slip (right) for D-2 Panel

Table 5-2 presents a comparison of the measured cracking load and deflection at cracking for each full-scale test in this study to the Beam-Spring Model and Elastic Hand Method, respectively. Both methods are very accurate except for the D-2 and BC-2 specimens. The reason for this is unclear and may be due to measurement error. Table 5-3 and Table 5-4 contain the measured-to-predicted ratios for the Beam-Spring Model and the Elastic Hand Method, respectively. As is shown in these tables, on average, the predictions are very good at 0.95 and 0.97 for the Beam-Spring and 0.94 and 0.98 for the Elastic Hand Method for cracking and deflection at cracking, respectively. These accuracies are similar to those of other analysis methods for structures like reinforced and prestressed concrete beams as well as steel members (Nowak and Collins 2000). If the BC-2 and D-2 panels are not included, the measured-to-predicted ratios are nearly 1.0.

Table 5-2 Summary of measured and predicted cracking and deflections

Panel	Measured		Elastic Hand Method		Beam-Spring Model	
	Cracking Load *(psf)*	**Deflection** *(in)*	**Cracking Load** *(psf)*	**Deflection** *(in)*	**Cracking Load** *(psf)*	**Deflection** *(in)*
A-2	155	0.34	156	0.36	156	0.39
A-4	202	0.44	194	0.33	192	0.352
B-1	-	-	150	0.17	152	0.198
B-2	-	-	150	0.17	152	0.198
BC-1	180	0.12	195	0.16	198	0.155
BC-2	164	0.15	195	0.16	197	0.157
D-1	221	0.14	222	0.15	209	0.144
D-2	184	0.13	222	0.15	208	0.138

Table 5-3 Beam-Spring Model Measured-to-Predicted Ratios

Panel	Cracking Load	Deflection
A-2	0.99	0.87
A-4	1.05	1.25
B-1	-	-
B-2	-	-
BC-1	0.91	0.79
BC-2	0.83	0.96
D-1	1.06	1.00
D-2	0.88	0.96
Average	**0.95**	**0.97**

Table 5-4 Elastic Hand Method Measured-to-Predicted Ratios

Panel	Cracking Load	Deflection
A-2	0.99	0.96
A-4	1.04	1.33
B-1	-	-
B-2	-	-
BC-1	0.92	0.77
BC-2	0.84	0.95
D-1	1.00	0.97
D-2	0.83	0.89
Average	**0.94**	**0.98**

5.5 Comparison between Elastic Hand Method and Beam-Spring Model

One of the critical assumption of the Elastic Hand Method is the slip distribution along the length of the member. As noticed by previous research, the slip is not truly a triangular distribution, like the distribution of vertical shear in a simply supported beam with a distributed load (Olsen and Maguire 2016). The distribution seems to look more like a parabola or "hourglass" shape. Figure 5-14 compares the connector force distribution for two different panels using the Elastic Hand Method and Beam-Spring Model, where the distributions do not match, although they are very close. Table 5-5 shows that predictions made with the Elastic Hand Method were similar to those of the Beam-Spring Model (all ratios between 0.93 and 1.15) indicating there is very little difference in the predictions and indicates the linear slip assumption is good enough for design, especially for cracking.

Because engineers are currently used to the concept of percent composite action, Table 5-6 and Table 5-7 show the composite action prediction for cracking moment and deflection, respectively, for the Elastic Hand Method and Beam-Spring model. There is very good agreement again except for the BC-2 and D-2 panels.

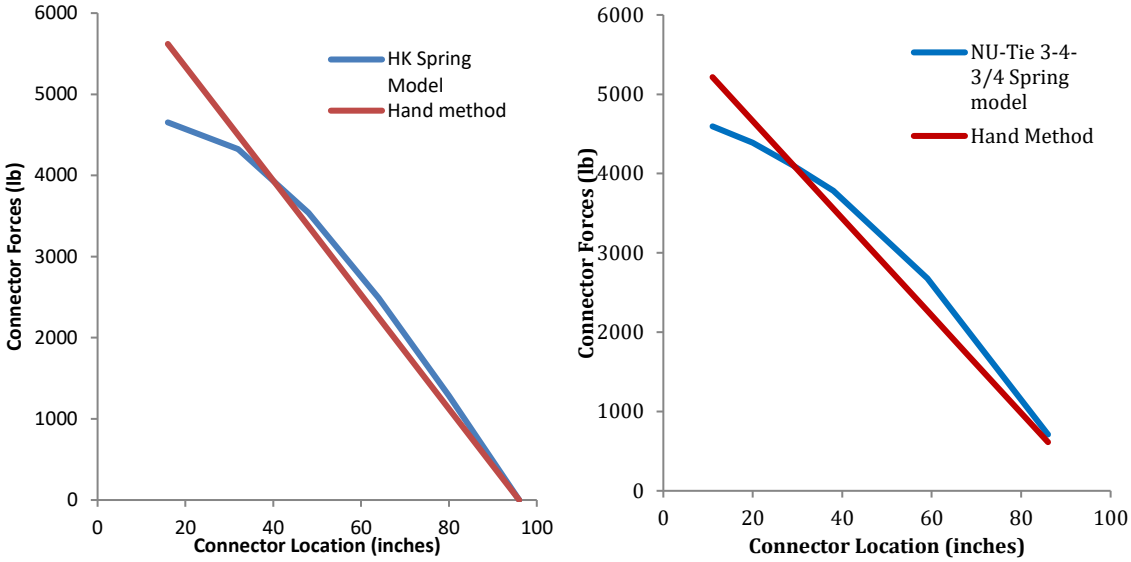

Figure 5-14 Connector forces diagram using the Elastic Hand Method and the Beam-Spring Model

Table 5-5 Caption Ratio of the Beam-Spring Prediction to the Elastic Hand Method Prediction

Panel	**Cracking Load** *(psf)*	**Deflection** *(in.)*
343-2	1.00	1.10
343-4	0.99	1.07
HK 1	0.94	0.97
HK 2	0.94	0.93
T A1	1.02	0.98
T A2	1.01	1.00
T B1	1.01	1.15
T B2	1.01	1.15

Table 5-6 Measured Composite Action for cracking moment

Specimen	**M_{crFC}** *(lb*ft)*	**M_{crNC}** *(lb*ft)*	**Measured Composite Action** *(%)*	**Elastic Hand Method Composite Action** *(%)*	**Beam-Spring model Composite Action** *(%)*
A-2	66,583	12,804	12	12.3	12.2
A-4	66,583	12,804	24	21.8	21.2
B-1	41,481	11,067	-	2.3	2.9
B-2	41,866	11,184	-	1.9	2.5
BC-1	41,481	11,067	11	15.3	13.5
BC-2	41,866	11,184	6	14.8	12.5
D-1	41,481	11,067	23	23.2	18.0
D-2	41,866	11,184	11	22.6	17.0

Table 5-7 Measured Composite Action for deflection

Specimen	**I_{FC}**	**I_{NC}**	**Measured Composite Action**	**Elastic Hand Method Composite Action**	**Beam-Spring Model Composite Action**
	(in^4)	*(in^4)*	*(%)*	*(%)*	*(%)*
A-2	3744	216	5.1	4.0	3.7
A-4	3744	216	5.4	7.7	7.5
B-1	3912	384	-	-	-
B-2	3912	384	-	-	-
BC-1	3912	384	11.1	6.2	5.4
BC-2	3912	384	1.0	7.4	6.9
D-1	3912	384	12.7	10.0	10.2
D-2	3912	384	7.5	12.4	10.9

The accuracy of the developed methods could be hindered by the ability of the research team to accurately identify the cracking load from the experiment. Advanced methods like crack gages (Petigrew et al. 2016) or digital imaging techniques (Dorafshan et al

2016, Dorafshan et al 2017, Dorafshan and Maguire 2017) could have been used, but budgetary and time constraints precluded this.

5.6 Elastic Hand Method Design Procedure

The following procedure outlines the design approach for service loads using the Elastic Hand Method (see Appendix B for a Design Example). This procedure is for sandwich panels with equal wythe thicknesses; however, it can also be used for sandwich panels with unequal wythe thicknesses if appropriate modifications are made.

1. Calculate the material and section properties assuming the sandwich wall panel acts non-compositely.
2. Assume the number and spacing of connectors, and the slip at the end connector line. Calculate the forces in each connector and connector line using Equations (5-6) and (5-7), repeated here for convenience.

$$F_i = \delta(i)\, N_i * K_E \qquad (5\text{-}16)$$

$$F_{sum} = \sum F_i \qquad (5\text{-}17)$$

3. Calculate the cracking moment for a mild reinforced non-composite wythe using Equation (5-18).

$$M_{wy_2} = \frac{M_{service} - F_{sum} * Z}{2} \qquad (5\text{-}18)$$

4. Calculate the equivalent load using Equation (5-9), repeated here for convenience.

$$w_{we2} = \frac{8 * M_{wy_2}}{Span^2} \tag{5-9}$$

5. Using the equivalent load, calculate the axial and rotational displacement assuming the equivalent load distribution using equations (5-10) through (5-12), again repeated here for convenience.

$$\theta = \frac{w_{we2} * Span^3}{24 * E * I_{NC2}} \tag{5-10}$$

$$\Delta_{Rot} = \theta * Z \tag{5-11}$$

$$\Delta_{Axial} = \left[\left(\frac{1}{b * E * t_{conc_1}}\right) + \left(\frac{1}{b * E * t_{conc_2}}\right)\right] * \sum_{i=1}^{n} F_i * \left(\frac{L}{2} - x_i\right) \tag{5-12}$$

6. Calculate a new value of δ_{end} using Equation (5-13). Check if δ_{end} is less than the Elastic Slip limit. If it is not, iterate steps 2-6 until this limit state is satisfied.

$$\delta_{end} = \Delta_{Rot} - \Delta_{Axial} \tag{5-13}$$

7. Check tension stress to verify it is less than modulus of rupture of the concrete with Equation (5-19).

$$f = \frac{M_{wy_2} * t_{conc_2}}{2 * I_{NC2}} + \frac{F_{sum}}{b * t_{conc2}} \leq f_r \qquad (5\text{-}19)$$

8. Calculate the midspan deflection. For a uniform distributed load, use Equation (5-20).

$$\Delta = \frac{5 * w_{we2} * Span^4}{384 * E_c * I_{NC2}} \qquad (5\text{-}20)$$

5.7 Conclusions

In this section, two methods to predict elastic deformations and cracking were developed. First, the Beam-Spring model is a simple, general, matrix analysis framework that allows for accurate prediction of sandwich panel behavior. The proposed Elastic Hand Method was also developed which uses some simplifications and enforces equilibrium and slip kinematics. This method is general enough to predict cracking and deflections in most panels, but requires some iteration. Both models are limited to elastic behavior, although if inelasticity were introduced to the Beam-Spring model (non-linear springs and beam elements), ultimate deflections and ultimate strength could likely be determined, though this may not be necessary (see next chapter).

The Beam-Spring Model presented here is a promising option for elastic analysis of precast concrete sandwich panel walls using composite shear connector systems, including those with unsymmetrical wythes, axial forces and irregular connector patterns, including P-δ and P-Δ effects.

The Elastic Hand Method presented here relies on iteration, which is inconvenient, but easily programmed into excel or anther design aiding program. The iteration could be eliminated, but is difficult due to the summations of force required, and

this would limit the method's versatility and may require additional simplifying assumptions. The Elastic Hand Method is only evaluated on equal wythe panels from this program, but could be extended to unsymmetrical wythes, axial forces, panels with openings and alternate connector patterns.

Both methods were compared to the elastic portions of the full-scale tests from previous sections. Table 5-8 below simply consolidates Table 5-3 and Table 5-4 from the chapter as a summary of the accuracy of the cracking and deflection predictions for the panels tested in this study by displaying the Measured-to-Predicted ratios for each method. Additional validation on more varied panels should be performed, but the results are very promising.

The following conclusions can be made from the result in this chapter:

- A versatile, general matrix-based procedure, termed the Beam-Spring Model, can be used to predict elastic deflections and cracking very accurately, with a 0.97 and 0.96 test-to-prediction ratio for cracking load and deflections, respectively.
- Using first principles and a series of assumptions, a hand based method can be used to predict elastic deflections and cracking very accurately, with a 0.94 and 0.98 test-to-prediction ratio for cracking load and deflections, respectively.

Table 5-8 Measured-to-Predicted ratio

Panel	Elastic Hand Method		Beam-Spring Model	
	Cracking Load	**Deflection**	**Cracking Load**	**Deflection**
A-2	0.99	0.96	0.99	0.87
A-4	1.04	1.33	1.05	1.25
B-1	-	-	-	-
B-2	-	-	-	-
BC-1	0.92	0.77	0.95	0.71
BC-2	0.84	0.95	0.88	0.97
D-1	1.00	0.97	1.06	1.00
D-2	0.83	0.89	0.88	0.96
Average	**0.94**	**0.98**	**0.97**	**0.96**

CHAPTER 6

PREDICTING STRENGTH BEHAVIOR

6.1 Introduction

There are a handful of recently introduced methods proposed to predict the ultimate moment capacity of a concrete sandwich wall panel (Tomlinson 2015; Hassan and Rizkalla 2010; Naito et al. 2012). In addition to being few in number, they are difficult to use for engineers in practice, requiring complicated moment curvature analyses, furthermore, they rely on empirical data and interpolation rather than a general approach, or a combination of these things. There is a significant need to develop an easy-to-use method based on first principles and good design assumptions that is easily fit into an engineer's design routine. To simplify the design process of concrete sandwich wall panels so that a greater number of engineers can safely design them, this chapter presents a new method, the Partially-Composite Strength Prediction Method, to predict the nominal moment capacity of concrete sandwich wall panels that is easy to implement and shown to be accurate. The results of the method are compared to those in the full-scale testing chapter.

6.2 Calculating Percent Composite Action

Design engineers are familiar with the calculations of non-composite and fully-composite sandwich wall panels. The following sections reiterate this for completeness of the below discussion, as well as introduce a formal definition of percent composite action

for ultimate moment. The latter is necessary because there is no standard definition within the industry, although the most popular one is adopted for this discussion.

6.2.1 Non-Composite Ultimate Moment

The ultimate moment for an ideally non-composite panel is the sum of the ultimate moments of the individual wythes, as shown in Figure 6-1. When reinforced with mild steel, the following calculations (based on strain compatibility) can be used to calculate the ultimate moment, with minor variation for a prestressed panel:

$$a_1 = \frac{A_{s1} f_{s1}}{0.85 f_c' b} \tag{6-1}$$

$$a_2 = \frac{A_{s2} f_{s2}}{0.85 f_c' b} \tag{6-2}$$

$$M_{NC} = A_{s1} f_{s1} \left(d_1 - \frac{a_1}{2}\right) + A_{s2} f_{s2} (d_2 - \frac{a_2}{2}) \tag{6-3}$$

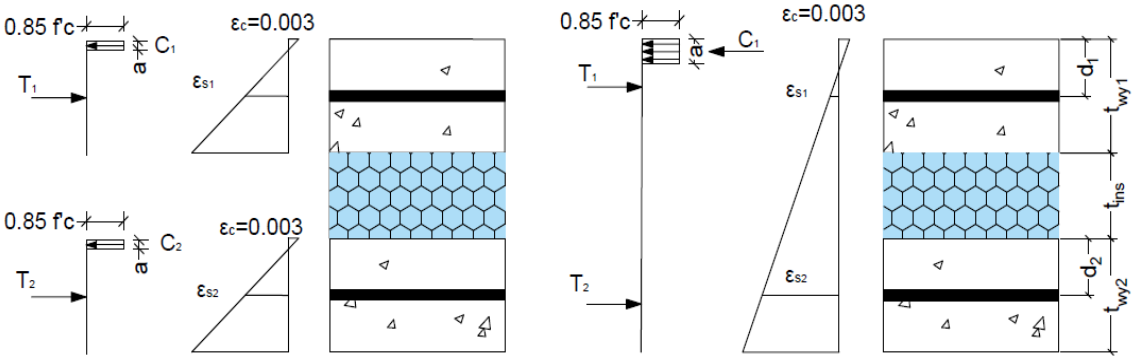

Figure 6-1 Strain and load profile for the non-composite SWP (left) and fully-composite SWP (right)

6.2.2 Fully-Composite Ultimate Moment

To calculate the fully-composite moment, one assumes that the entire panel acts as one beam, without strain discontinuity. Using strain compatibility, the following procedure can be used for mild-steel reinforced panels (with minor variation for prestressed panels):

$$a = \frac{A_{s1} f_{s1} + A_{s2} f_{s2}}{0.85 f_c' b} \tag{6-4}$$

$$M_{FC} = A_{s1} f_{s1} \left(d_1 - \frac{a}{2} \right) + A_{s2} f_{s2} \left(d_2 + t_{wy_1} + t_{ins} - \frac{a}{2} \right) \tag{6-5}$$

6.2.3 Definition of Partial Percent Composite Action for Ultimate Moment

Utilizing the theoretical fully-composite moment, theoretical non-composite moment, and the actual measured moment from the test results or a prediction method, the degree of composite action, K_{Mn}, can be determined using Eq. (6-6).

$$K_{Mn} = \frac{M_{n,test} - M_{n,NC}}{M_{n,FC} - M_{n,NC}} \tag{6-6}$$

Where Mn_{test} = experimental maximum moment of the sandwich panel

Mn_{NC} = theoretical maximum moment of the non-composite sandwich panel

Mn_{FC} = theoretical maximum moment of the fully-composite sandwich panel

Figure 6-2 graphically demonstrates the relationship between moment and degree of composite action in Eq. (6-6).

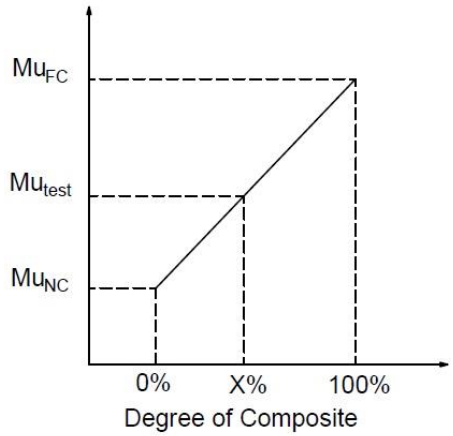

Figure 6-2 Visual demonstration of degree of composite action

6.3 Partially-Composite Strength Prediction Method

6.3.1 Overview and Discussion

The proposed Partially-Composite Strength Prediction Method procedure is based entirely upon first principles (i.e. equilibrium, strain compatibility), a "good enough" assumption about the slip profile along the length of the member, and shear deformation data of the connectors (which many connector companies already collect for ICC-ES certification, and which has been collected by several researchers). As such, this method is robust enough that it may be applied to situations outside of the simply supported panels presented in this report, although this would require validation. Furthermore, the reliance upon familiar first principles makes the procedure easily adopted by precast engineers and is a direct solution as long as recommendations are followed. For the

purposes of validating the method, the approximate stress strain curve of the materials should be used (e.g., Hognestad's Concrete Material Model [Wight and MacGregor 2005], strain hardening of the steel) in lieu of common design assumptions; however, when used for design, standard assumptions (e.g., Whitney's stress block [Whitney, 1937], elastic-perfectly plastic rebar) can (and should) be used.

For the sake of illustrating the Partially-Composite Strength Prediction Method procedure, wythe 1 (or the "top wythe") is considered the fully-composite compression side of the member and wythe 2 (or the "bottom wythe") is considered the fully-composite tension side of the member, as shown in Figure 6-1. The forces in a partially composite member are presented in Figure 6-3 which include the force of the connectors at the point of interest (F_{sum}) assumed to act at the center of each wythe. To maintain static equilibrium within a given wythe, the compression and tension forces in each wythe must transfer the difference between them to the other wythe; i.e.:

$$\sum F_{axial,1} = T_1 - C_1 - F_{sum} = 0 \qquad (6\text{-}7)$$

$$\sum F_{axial,2} = T_2 - C_2 + F_{sum} = 0 \qquad (6\text{-}8)$$

Where F_{sum} = is the sum of the connector forces from one end of the panel to the cross-section of interest

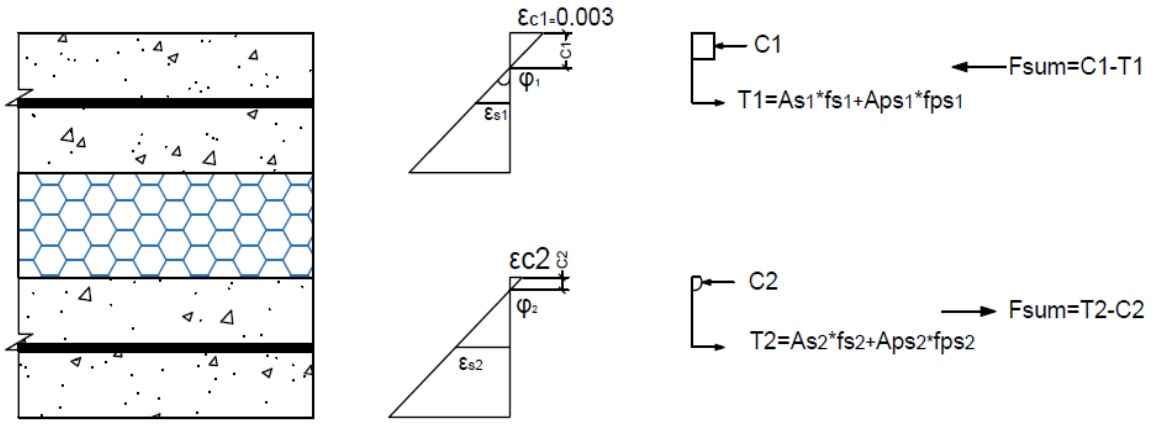

Figure 6-3 Strain and load profile of concrete sandwich wall panel

The shear force provided by the connectors can be estimated using the data from the push off test depending on the number of connectors, the connector spacing, and a linear assumption about the slip distribution as shown in Figure 6-4.

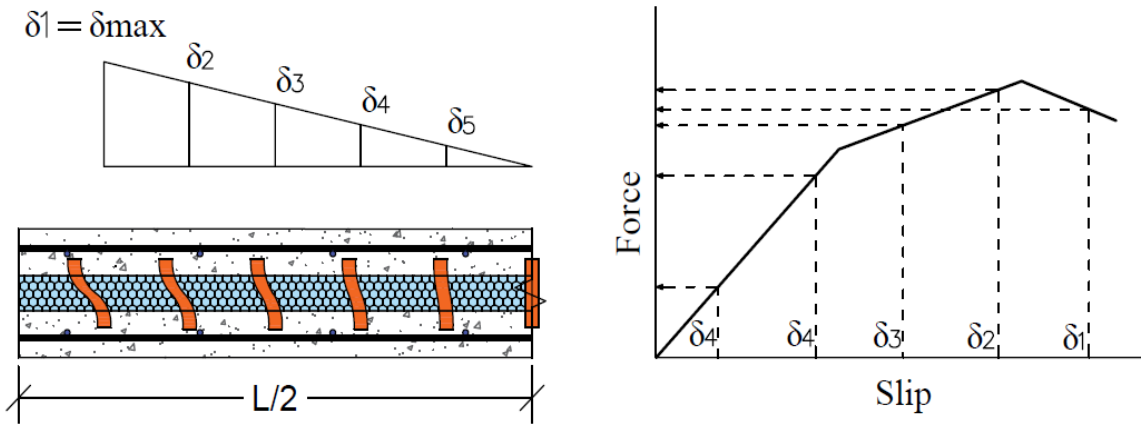

Figure 6-4 Slip distributed along the panel length

After the forces in each connector are determined, they can be summed for any given point along the length of the beam and applied to the beam cross-section as shown

in Figure 6-3. With these simplifying assumptions, determining the moment capacity of a sandwich panel with an arbitrary distribution of shear connectors is no more difficult than determining the capacity of two separate beams with axial loads (F_{sum}, in this case). Similarly, it is known that the two wythes will have equal deflection and equal curvature:

$$\varphi_1 = \varphi_2 \qquad (6\text{-}9)$$

Where φ_1 = is the curvature of the wythe 1

φ_2 = is the curvature of the wythe 2

This method can be extended to all cross-sections along the panel and points on the load deflection curve, but the purpose of this chapter of the report is to determine the ultimate moment strength in a straightforward manner. The condition for failure is determined as either when the connectors fail or when the concrete on wythe 1 crushes (i.e., ε_{c1} = 0.003). It is assumed that designers would prefer to prevent the sudden failure of the connectors to ensure a ductile failure. Therefore, it is recommended to set a reasonable value for the force or slip in the connectors at the end of the panel connectors during design. Once the forces are resolved on the cross-section, one can use the following equation to calculate the nominal moment that can be carried by the cross-section:

$$M = M_1 + M_2 + F_{sum} * \left(\frac{t_{wy1} + t_{wy2}}{2} + t_{ins}\right) \qquad (6\text{-}10)$$

Where M_1 = is the moment in the top wythe created by C_1 and T_1:

M_2 = the moment in the bottom wythe created by C_2 and T_2:

The following sections outline the procedure for analysis of existing concrete sandwich wall panels, as well as a detailed design procedure.

6.3.2 Partially-Composite Strength Prediction Method Procedure

The following steps are proposed to predict the nominal moment capacity for a sandwich wall panel. The steps do not necessarily need to occur in this order, but the authors found this order convenient when analyzing a panel that was already created. A detailed design process is presented in the following section.

1. Find the forces at each connector using the load-slip curve and assuming a linear distribution of slip (see Figure 6-4). The slip can be iterated until it maximizes the connector force, which will be the condition at ultimate, taking into account the post maximum strength of the connectors if desired. This can also be determined by using an influence line.

Design Note: As stated above, for design it may be important to prevent connector failure prior to panel failure by limiting slip or force carried by the most heavily loaded connectors. This can be conservatively done by assuming that the connectors at the end of the panel are at their maximum force (F_u). Connector behavior and mechanical

property variation (e.g., ultimate strength, proportional limit, elastic limit, deformation at ultimate and shear deformation at rupture) are not always understood due to the private and proprietary nature of this part of the industry. Limiting connector forces at different limit states is an important consideration for PCI committees.

The slip at every connector location can be estimated heuristically (by assuming a linear slip profile based on the plot shown in Figure 6-4 or Figure 6-5 and Figure 6-6, which can then be used to create a robust spreadsheet), or by using the following equation (which is based on similar triangles):

$$\delta(i) = \delta_{Ult} * \frac{\frac{L}{2} - x_{con}, i}{\frac{L}{2} - x_{con,1}} \qquad (6\text{-}11)$$

Where $\delta(i)$ = the slip of the wythes at connector i

δ_{Ult} = Maximum slip of the end row of connectors at the ultimate moment

L = length of the panel

$x_{con,i}$ = location of the connector from the end of the panel

i = connector line number from the end of the panel to the point of interest/analysis

Find the force, F_i, at each connector by using the appropriate load-slip curve.

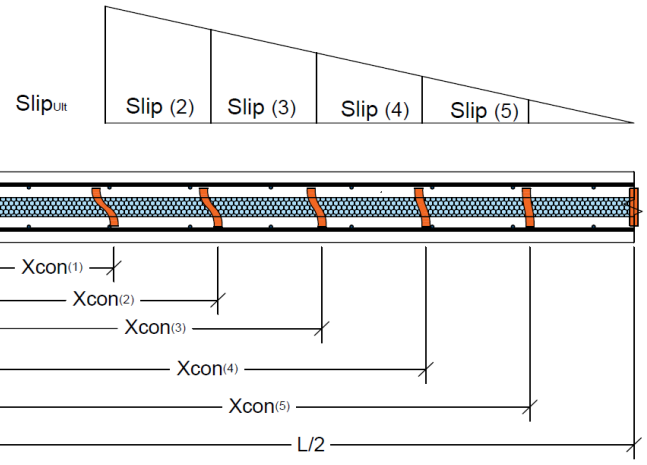

Figure 6-5 Slip diagram

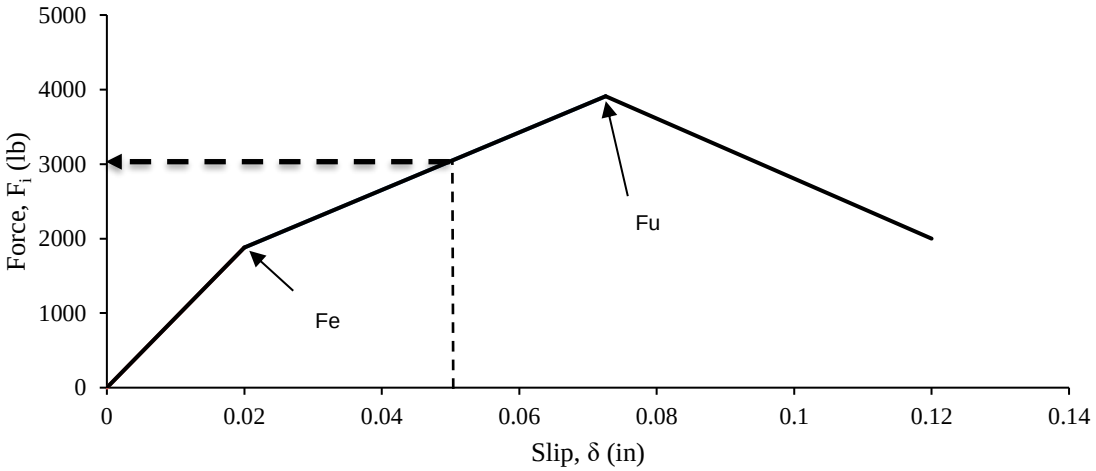

Figure 6-6 Typical load-slip curve

2. Find the total force provided by the connectors

$$F_{sum} = N * \sum F_i \leq A_s f_s + A_{ps} f_{ps} \qquad (6\text{-}12)$$

Where N = number of connectors per row

F_i = the force at connector i

The maximum connector force that can be transferred between wythes is limited to the smaller of the maximum force generated by connectors at the location of interest or maximum tensile force carried by the steel in the bottom wythe, hence the right-hand side of the inequality in Equation (6-12). In other words, adding additional connectors will not increase the strength of the panel over the fully-composite moment, although it is likely to influence deflections.

3. Find C_1 and T_1 for the top wythe as if it were an independent beam with an axial force F_{sum} (see Figure 6-8).

   This process is exactly the same as any other reinforced/prestressed beam:

   a. Assume the top fiber concrete strain is 0.003
   b. Assume a value of the depth of the compression force in the concrete, c_1.
   c. Calculate the curvature, φ_1. Assuming small angles, φ_1 may be calculated as

$$\varphi_1 = \frac{\varepsilon_c}{c_1} \qquad (6\text{-}13)$$

   d. Calculate the compressive force in the top wythe. The compressive force in the concrete will utilize Hognestad's equation to estimate the concrete compressive strength. Hognestad's equation is not required for an accurate prediction of the top wythe, but it will become necessary for the bottom wythe if the panel is partially composite because Whitney's stress block is

only valid when the maximum concrete strain is 0.003. The Hognestad formula is shown in Equation (6-14):

$$f_c = f_c' \left[\frac{2 * \varepsilon_c}{\varepsilon_o} - \left(\frac{\varepsilon_c}{\varepsilon_o} \right)^2 \right] \qquad \textit{(6-14)}$$

Where f_c = stress in the concrete

f_c' = concrete compressive strength

ε_c = strain in the concrete

ε_o = 0.002.

Substituting Hognestad's equation, the concrete compressive force can be calculated as

$$C_1 = b * \int_0^{c_1} f_c \, dy$$

$$= b * \int_0^{c_1} f_c' \left[\frac{2 * \varepsilon_c}{\varepsilon_o} - \left(\frac{\varepsilon_c}{\varepsilon_o} \right)^2 \right] dy$$

$$C_1 = b * \int_0^{c_1} f_c' \left[2 * \frac{\varphi_1 * c_1}{\varepsilon_o} - \left(\frac{\varphi_1 * c_1}{\varepsilon_o} \right)^2 \right] dy$$

$$C_1 = b * \left| f_c' \left[\frac{\varphi_1 * {c_1}^2}{\varepsilon_o} - \left(\frac{{\varphi_1}^2 * {c_1}^3}{3 * {\varepsilon_o}^2} \right) \right] \right|_0^{c1}$$

$$C_1 = b * f_c' \left[\frac{\varphi_1 * {c_1}^2}{\varepsilon_o} - \left(\frac{{\varphi_1}^2 * {c_1}^3}{3 * {\varepsilon_o}^2} \right) \right]$$

$$C_1 = b * f'c * \frac{\varphi_1 * c_1^2}{\varepsilon_o} * \left(1 - \frac{\varphi_1 * c_1}{3\varepsilon_o}\right) \qquad (6\text{-}15)$$

Where C_1 = the compressive force in the concrete in wythe 1

b = width of the panel

$$x_{c1} = \frac{\int_0^{c_1} f_c' \left[\frac{2 * \varepsilon_c}{\varepsilon_o} - \left(\frac{\varepsilon_c}{\varepsilon_o}\right)^2\right] * c_1 * \ dc_1}{\int_0^{c_1} f_c' \left[\frac{2 * \varepsilon_c}{\varepsilon_o} - \left(\frac{\varepsilon_c}{\varepsilon_o}\right)^2\right] \ dc_1}$$

$$x_{c1} = \frac{\int_0^{c_1} f_c' \left[2 * \frac{\varphi_1 * {c_1}^2}{\varepsilon_o} - \frac{{\varphi_1}^2 * {c_1}^3}{{\varepsilon_o}^2}\right] dc_1}{\int_0^{c_1} f_c' \left[2 * \frac{\varphi_1 * c_1}{\varepsilon_o} - \frac{{\varphi_1}^2 * {c_1}^2}{{\varepsilon_o}^2}\right] dc_1}$$

$$x_{c1} = \frac{\left[\frac{2}{3} * \frac{\varphi_1 * {c_1}^3}{\varepsilon_o} - \frac{1}{4} * \frac{{\varphi_1}^2 * {c_1}^4}{{\varepsilon_o}^2}\right]}{\left[\frac{\varphi_1 * {c_1}^2}{\varepsilon_o} - \frac{1}{3} * \frac{{\varphi_1}^2 * {c_1}^3}{{\varepsilon_o}^2}\right]}$$

$$x_{c1} = c_1 - \frac{c_1 * (8 * \varepsilon_o - 3 * \varphi_1 * c_1)}{12 * \varepsilon_o - 4 * \varphi_1 * c_1} \qquad (6\text{-}16)$$

Where x_{c1} = the centroid of compressive force in the concrete from extreme compressive fiber

Hognestad's concrete stress strain relationship is plotted along with the resultant force location in Figure 6-7.

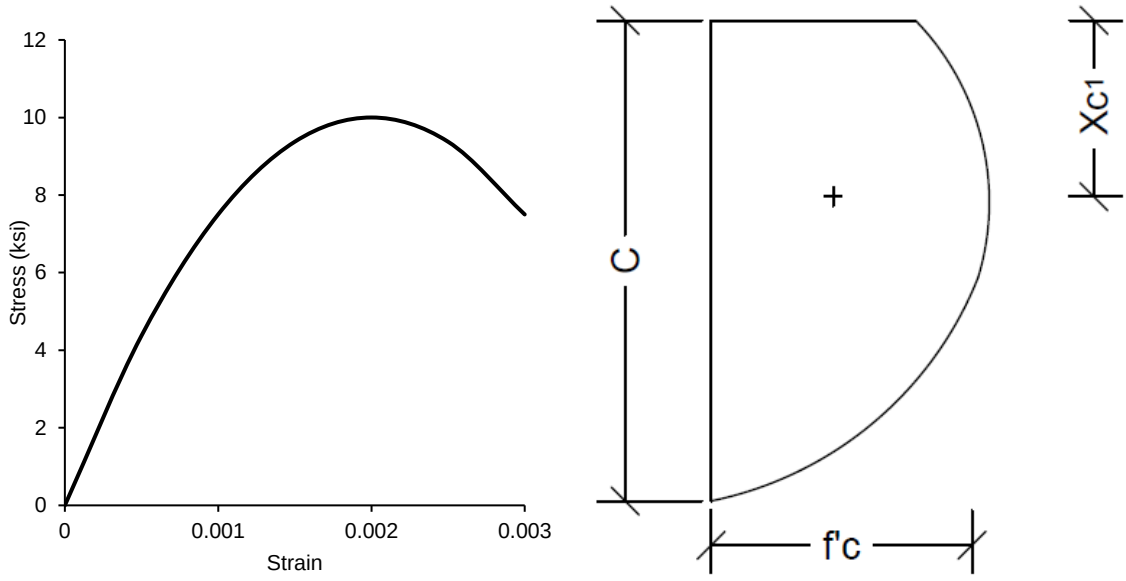

Figure 6-7 Stress vs strain of Hognestad (left) and stress profile (right)

Design Note: To facilitate design it is recommended to use Whitney's stress block. The Hognestad model is only used to analyze partially composite panels in this report and is still an approximation. It is recommended that when designing, the designer designs for a fully-composite panel, preventing compression in the bottom wythe and eliminating the need for and hassle of this more complex material model.

e. Calculate the strain and then stress in the steel. Strain can be determined using similar triangles (see Figure 6-8):

$$\varepsilon_s = \varepsilon_c \frac{d_1 - c_1}{c_1} \qquad (6\text{-}17)$$

Where d_1 = depth to the centroid of the steel measured from the top of wythe 1.

c_1 = depth to neutral axis of wythe 1 measured from the top of wythe 1.

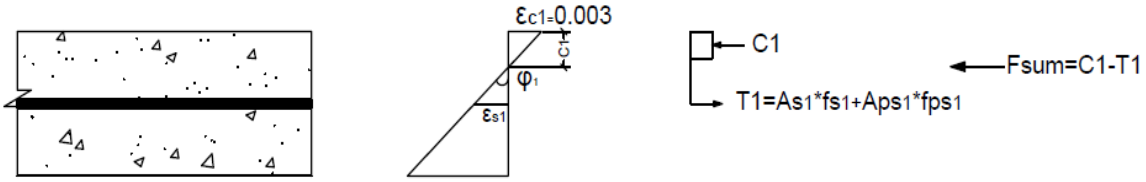

Figure 6-8 Strain and load profile for the top wythe

The stress is then calculated using an appropriate steel model:

Mild Steel for Design: Elastic Perfectly Plastic

$$f_s = \begin{cases} E_s * \varepsilon_s & if\ \varepsilon_s < \varepsilon_y \\ f_y & if\ \varepsilon_s \geq \varepsilon_y \end{cases} \qquad (6\text{-}18)$$

Where f_s = stress in the mild steel

E_s = modulus of elasticity of the steel

ε_s = strain in the mild steel

ε_y = strain of the mild steel at yielding

f_y = mild steel yield stress

For Prestressing Steel: The power formula (Devalapura and Tadros, 1992):

$$f_{ps} = \varepsilon_{ps} * \left\{ 887 + \frac{27600}{\left[1 + \left(112.4 * \varepsilon_{ps}\right)^{7.36}\right]^{7.36^{-1}}} \right\} \qquad (6\text{-}19)$$

$$< 270$$

Where f_{ps} = stress in the prestressing steel

Actual stress versus strain profile for the reinforcement, e.g. see Figure 6-9.

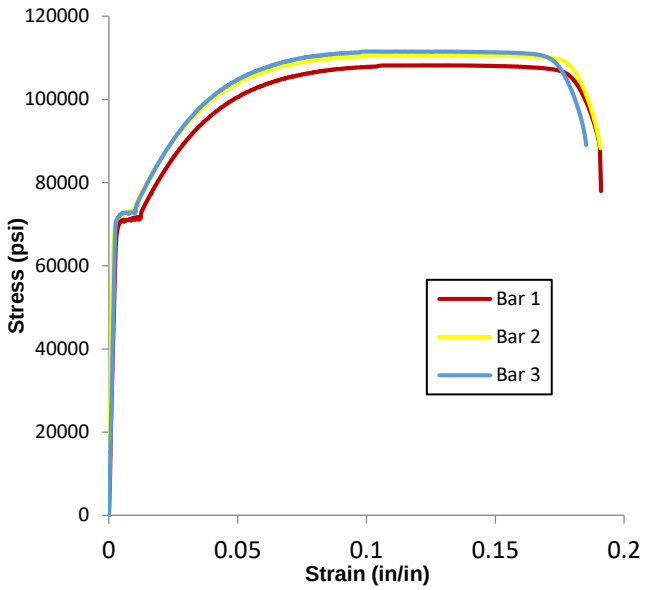

Figure 6-9 Stress vs. Strain for rebar

f. Calculate the tension force in the top wythe. This will just include the tension in the steel:

$$T_1 = f_{s1}A_{s1} + f_{ps1}A_{ps1} \qquad (6\text{-}20)$$

g. Determine if c_1 satisfies the force equilibrium for wythe 1. If not, repeat step 3 and iterate until force equilibrium is satisfied.

$$\sum F_x \rightarrow 0 = T_1 - C_1 - F_{sum} \qquad (6\text{-}21)$$

4. Find C_2 and T_2 for the second wythe as if it is a separate beam with F_{sum} acting as an axial force.
   a. Assume both wythes will deflect equally and maintain $\varphi_2 = \varphi_1$. This is a standard assumption for all composite or non-composite structures, steel, concrete or otherwise (Bai and Davidson 2015; Hassan and Rizkalla 2010; Newmark et al. 1951).
   b. Assume a value of c_2; however, in contrast to the previous example, the top fiber will *not* be 0.003 unless the panel is a non-composite design.
   c. Calculate the compressive force in the bottom wythe, C_2. The compressive force in the concrete will again utilize Hognestad's equation to estimate the concrete compressive strength, but it is critical here because Whitney's stress block is only valid when the top fiber is at 0.003 strain and in the case of partial composite action, this will not be true. Substituting Hognestad's equation, the concrete compressive force can be calculated as before, with appropriate variables changed to reflect wythe 2, as:

$$C_2 = b * f'c * \frac{\varphi_2 * c_2^2}{\varepsilon_o} * \left(1 - \frac{\varphi_2 * c_2}{3\varepsilon_o}\right) \qquad (6\text{-}22)$$

Design note: To facilitate design it is recommended to use Whitney's stress block. The Hognestad model is only used to analyze partially composite panels in this report and is still an approximation. It is recommended that when designing, the designer designs for a fully-composite panel, preventing compression in the bottom wythe and eliminating the need to calculate C_2.

d. Calculate the strain and stress in the steel. Assuming small angles, the strain can be determined using the relationship in Equation (6-13) and (6-17) above and demonstrated in Figure 6-10 below as

$$\varepsilon_s = (d_2 - c_2) * \varphi_2 \qquad (6\text{-}23)$$

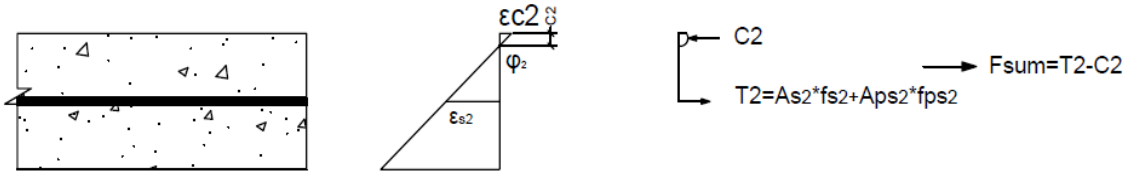

Figure 6-10 Strain and load profile for the bottom wythe

The stress can then be calculated using Equations (6-18) and (6-19) in Step 3e above.

e. Calculate the tension force in the bottom wythe:

$$T_2 = f_{s2}A_{s2} + f_{ps2}A_{ps2} \qquad (6\text{-}24)$$

f. Determine if c_2 satisfies the force equilibrium for Wythe 2. If not, repeat step 4 and iterate until force equilibrium is satisfied.

$$\sum F_x \rightarrow 0 = T_1 - C_1 + F_{sum} \qquad (6\text{-}25)$$

By enforcing equilibrium of each wythe using Equation (6-21) of step 3g and Equation (6-25) from step 4f, force equilibrium for the whole panel is now satisfied.

5. Find the ultimate moment of the concrete sandwich wall panel by taking the moments carried by the different parts of the panel presented in Figure 6-3:

$$M = M_1 + M_2 + F_{sum} * \left(\frac{t_{wy1} + t_{wy2}}{2} + t_{ins}\right) \qquad (6\text{-}26)$$

Where M_1 = the moment in wythe 1 created by C1 and T1

M_2 = the moment in wythe 2 created by C_2 and T_2

M_1 and M_2 are most easily found by summing the moments about the steel locations:

$$M_1 = C_1 * (d_1 - X_{c1}) \qquad (6\text{-}27)$$

$$M_2 = C_2 * (d_2 - X_{c2}) \quad (6\text{-}28)$$

Alternatively, the moment can be taken for all concrete and steel forces over the entire panel cross-section at a convenient location.

6.3.3 Validation of the Partially-Composite Strength Prediction Method

The Partially-Composite Strength Prediction Method presented in the previous section is compared below to the full-scale panel tests for its validation. Table 6-1 shows the experimental ultimate moment compared to predictions made by Partially-Composite Strength Prediction Method. The percent difference was, on average, about 8 percent less than the experimental ultimate moment results. This is a very common error metric, which is comparable to that of most other predictions for other members like normal reinforced concrete in bending or shear (Nowak and Collins 2000). Appendix A contains the detailed calculations for the panels from this study.

Table 6-1 Validation of Partially-Composite Strength Prediction Method

Panel	**Observed Ultimate Moment**		**Partially-Composite Strength Prediction Moment**	**Percent Difference**
	Specimen 1	**Specimen 2**		
	(k-ft)	*(k-ft)*	*(k-ft)*	*(%)*
Nu-Tie 343-2	43.36	-	39.5	8.9
Nu-Tie 343-4	60.86	-	55.37	9.0
HK	45.23	42.5	39.9	9.0
T A	45.1	41.3	41.1	4.9
T B	29.82	25.6	25.36	8.5
Average				**8.0**

6.3.4 Recommendations for Design

To make the Partially-Composite Strength Prediction Method easier to follow during the design stage, several recommendations are suggested to facilitate the strength calculation at failure:

a) Consider the panel as a fully-composite panel and find the required area of steel, which can be set equal to F_{sum} to select the total number of shear connectors. If satisfied, this assumption implies that the second wythe compression force (C_2) will be zero. Anything less than fully-composite requires the use of Hognestad's concrete material model (or another model of the engineer's choice) or another simplifying assumption. While Hognestad's material model is not complicated and the required equations derived and presented are above, it does add enough complication that a designer unfamiliar with it may not be comfortable.

b) Find the ultimate moment of the panel using the methods presented above. Several simplifications can be made to bring the method more in line with current reinforced concrete and prestressed concrete design:

    a. The Whitney stress block can be used as long as there is no compression force in the wythe 2.
    b. Elastic Plastic Mild Steel
    c. Power Formula or PCI formula for prestressing steel
    d. Limit end connector slip to the slip at maximum force (F_u) per the shear testing results

c) Find the number of connectors and spacing that provide the required F_{sum} for the cross-section. Although uniform spacing of connectors is recommended based on discussions with connector manufacturers and their in-house testing, alternate spacing layouts have been noted to be beneficial (Olsen and Maguire 2016).

Some of these design assumptions are not appreciably different than those used by connector manufacturers, but are formalized here and fit within the design parameters discussed in this chapter. See Appendix C for Design Examples using the Partially-Composite Strength Prediction Method.

6.4 Conclusions

There is a significant need to develop an easy-to-use method based on first principles and good design assumptions that is easily fit into an engineer's design routine. This chapter presented a new method, the Partially-Composite Strength Prediction Method, to predict the nominal moment capacity of concrete sandwich wall panels that is easy to implement and shown to be accurate. The results of the method are compared to those in the full-scale testing chapter and use the results generated in the shear-testing chapter. The following conclusions can be made about the findings in this chapter:

- A design method based on familiar first principles and a series of assumptions was developed
- The developed Partially-Composite Strength Prediction Method was shown to be accurate to within 8% on average for the panels produced and tested in a preceding chapter. These panels represented very different

configurations and were reinforced with different connectors and connector patterns, further demonstrating robustness.

- The developed method relies only on connector load-slip information extracted from the push off tests.
- The developed, recommended, design procedure suggests designing for 100% composite action to facilitate design using standard assumptions, like Whitney's Stress block, and limiting connector end slip at ultimate to F_u.

CHAPTER 7

CONCLUSIONS

7.1. Full Scale Testing

Eight full-scale concrete sandwich panels were tested to failure at the Utah State University Structures Lab. The purpose of the testing was to evaluate the percent composite action for the connector configurations and compare the results to those reported by composite connector manufacturers. The following conclusions can be made from the experimental program:

- The type and intensity of shear connectors significantly affect the degree of composite action achieved in a concrete sandwich wall panel. Doubling the number of shear connectors in the Connector A (Nu-Tie connector) panels resulted in a large gain in percent composite action. (Note that the A-2 panel was more lightly reinforced than would be detailed for an actual building)
- The manufacturer-reported degree of composite action can be considered conservative for the panel configurations and connectors and connector patterns tested in this paper.
- Most of the panels exhibited ductile behavior even the panels that were used brittle connectors like HK. Ductile behavior was observed for the full scale test due to concrete cracking and steel yield which reduced the total slip of connectors.

7.2. Elastic Prediction Methods

In this section, two methods to predict elastic deformations and cracking were developed. First, the Beam Spring model is a simple, general, matrix analysis framework that allows for accurate prediction of sandwich panel behavior. The proposed hand method was also developed which uses some simplifications and enforces equilibrium and slip kinematics. This method is general enough to predict cracking and deflections in most panels, but requires some iteration. Both models are limited to elastic behavior, although if inelasticity were introduced to the beam spring model (non-linear springs and beam elements), ultimate deflections and ultimate strength could be determined, though this may not be necessary for design.

The Beam Spring Model presented herein is a promising option for elastic analysis of precast concrete sandwich panel walls using composite shear connector systems, including those with unsymmetrical wythes, axial forces and irregular connector patterns, including P-δ and P-Δ effects.

The hand method presented herein relies on iteration, which is inconvenient, but easily programmed into excel or anther design aiding program. The iteration could be eliminated, but is difficult due to the summations of force required and this would limit the method's versatility and may require additional simplifying assumptions. The hand method is only evaluated on equal wythe panels from this program, but could be extended to unsymmetrical wythes, axial forces, panels with openings and alternate connector patterns. The following conclusions can be made about the elastic prediction methods:

- A versatile, general matrix-based procedure, termed the Beam Spring Model, can be used to predict elastic deflections and cracking very accurately, with a 0.97 and 0.96 test-to-prediction ratio for cracking load and deflections, respectively.
- Using first principles and a series of assumptions, a hand based method can be used to predict elastic deflections and cracking very accurately, with a 0.94 and 0.98 test-to-prediction ratio for cracking load and deflections, respectively.
- The connectors may be inelastic range while the sandwich panel did not crack yet.
- Achieved high composite action at service load is difficult. Longer panel has higher composite action compare to short panel.

7.3. Nominal Strength Method

There is a significant need to develop an easy-to-use method based on first principles and good design assumptions that is easily fit into an engineer's design routine. This chapter presented a new method to predict the nominal moment capacity of concrete sandwich wall panels that is easy to implement and shown to be accurate. The results of the method are compared to those in the full-scale testing chapter and use the results generated in the shear-testing chapter. The following conclusions can be made about the findings in this chapter:

- A design method based on familiar first principles and a series of assumptions was developed.

- The developed partially-composite nominal moment design procedure was shown to be accurate to within 8% on average for the panels tested. These panels represented very different configurations and were reinforced with different connectors and connector patterns, further demonstrating robustness.
- The developed method relies only on connector load-slip information extracted from the push off tests.
- The procedure developed herein suggests designing for 100% composite action to facilitate using standard assumptions, like Whitney's Stress block, and limiting connector end slip at ultimate to F_u.

7.4. Future Research

1. Develop simplified method to predict the behavior of the sandwich panel using the principle of the hand methods.
2. Developed the hand methods to account for the axial load and including second order effect due to thermal, P-δ, and P-Δ effects.
3. Even the simplified methods have a good agreement with experiment data, it should be verified.
4. Test Full scale Sandwich panel under shear cyclic load to investigate the effect of connector on the shear capacity.
5. Verify that hand methods work for Full scale sandwich panel with opining.

REFERENCES

Al-Rubaye, S., Sorensen, T., Dorafshan, S., Maguire, M., (2018) "Matrix Model Accuracy of Partially Composite Concrete Sandwich Panels." PCI/NBC. Denver, CO., in press.

Al-Rubaye, S., Sorenson, T., and Maguire, M., (2017) "Investigating Composite Action at Ultimate for Commercial Sandwich Panel Composite Connectors." PCI/NBC. Cleveland, OH.

Al-Rubaye, S., Olsen, J., Sorensen, T., Maguire, M., (2018) "Evaluating Elastic Behavior for Partially Composite Precast Concrete Sandwich Wall Panels." *PCI Journal*., in press.

American Concrete Institute (ACI) Committee 318. (2014). *Building Code Requirements for Structural Concrete. ACI 318-14.* Farmington Hills, MI.

ASTM Standard A370-14 (2014) "Standard Test Methods and Definitions for Mechanical Testing of Steel Products." ASTM International. West Conshohocken, PA. 2014. DOI: 10.1520/A0370-14. www.astm.org.

ASTM Standard C39 (2015) "Standard Test Method for Compressive Strength of Cylindrical Concrete Specimens." ASTM International. West Conshohocken, PA. 2015. DOI: 10.1520/C0039_C0039M-15A. www.astm.org.

Bai, F., and Davidson, J. S. (2015). "Analysis of Partially Composite Foam Insulated Concrete Sandwich Structures." *Journal of Engineering Structures*, 91, 197-209.

Bunn, W. G. (2011). "CFRP Grid/Rigid Foam Shear Transfer Mechanism for Precast, Prestressed Concrete Sandwich Wall Panels." Thesis, presented to North Carolina State

University at Raleigh, NC in partial fulfillment of requirements for the degree of Master of Science.

Bush, T. D., and Wu, Z. (1998). “Flexural Analysis of Prestressed Concrete Sandwich Panels with Truss Connectors.” *PCI Journal*, 43(5), 76–86.

Chang, M., Maguire, M., and Sun, Y. (2017). “Framework for Mitigating Human Bias in Selection of Explanatory Variables for Bridge Deterioration Modeling.” *Journal of Infrastructure Systems*, 23(3), 04017002.

Devalapura, R. K and Tadros, M. K. (1992). “Stress-Strain Modeling of 270 ksi Low-Relaxation Prestressing Strands.” *PCI Journal*, 37(2), 100-106.

Dorafshan, S., & Maguire, M. (2017). Autonomous Detection of Concrete Cracks on Bridge Decks and Fatigue Cracks on Steel Members. In *Digital Imaging 2017*, 33-44.

Dorafshan, S., Maguire, M., Hoffer, N. V., and Coopmans, C. (2017). “Challenges in bridge inspection using small unmanned aerial systems: Results and lessons learned.” *2017 International Conference on Unmanned Aircraft Systems (ICUAS)*.

Dorafshan, Sattar; Maguire, Marc; and Qi, Xiaojun, (2016). "Automatic Surface Crack Detection in Concrete Structures Using OTSU Thresholding and Morphological Operations". *Civil and Environmental Engineering Faculty Publications.* Paper 1234.

Drysdale, R. G., Hamid, A. A., and Baker, L. R. (1994). *Masonry Structures: Behavior and Design*. Prentice Hall, Englewood Cliffs, NJ.

Einea, A., Salmon, D. C., Fogarasi, G. J., Culp, T. D., and Tadros, M. K. (1991). State-of-of-the-Art of Precast Concrete Sandwich Panels. *PCI Journal*, 36(6), 78-98.

Einea, A., Salmon, D. C., Tadros, M. K., and Culp, T. D. (1994). A New Structurally and Thermally Efficient Precast Sandwich Panel System. *PCI Journal*, 39(4), 90-101.

Frankl, B. A., Lucier, G. W., Hassan, T. K., and Rizkalla, S. H. (2011). Behavior of Precast, Prestressed Concrete Sandwich Wall panels Reinforced with CFRP Shear Grid. *PCI Journal*, 56(2), 42-54.

Hassan, T. K., and Rizkalla, S. H. (2010). "Analysis and Design Guidelines of Precast, Prestressed Concrete, Composite Load-Bearing Sandwich Wall Panels Reinforced with CFRP Grid." *PCI Journal*, 55(2), 147-162.

Holmberg, A., and Plem, E. (1965). *Behaviour of load-bearing sandwich-type structures*. Nat. Swed. Cncl. Bldg. Res.

ICC-ES Acceptance Criteria AC320 (2015) "Acceptance Criteria for Fiber-Reinforced Polymer Composite or Unreinforced Polymer Connectors Anchored in Concrete." International Code Council (ICC) Evaluation Service, LLC. Washington, DC. 2015. www.icc-es.org.

Jacobs, D. R. (1987). "Elemental Study of Glass-Fiber-Composite Connectors used in Concrete Sandwich Wall Construction". M. Sc. Iowa State University, Ames, Iowa.

Kent, D. C., and Park, R. (1971). "Flexural Members with Confined Concrete." *Journal of the Structural Division*, 97(7), 1969-1990.

Lee, B. J., and Pessiki, S. (2004). Analytical Investigation of Thermal Performance of Precast Concrete Three-Wythe Sandwich Wall Panels. *PCI Journal*, 49(4), 88-101.

Losch, E. D., Hynes, P. W., Andrews Jr., R., Browning, R., Cardone, P., Devalapura, R., . . . Yan, L. (2011) State of the Art of Precast/Prestressed Concrete Sandwich Wall Panels (2nd Ed). *PCI Journal*, 56(2), 131-176.

Maguire, M., (2009) "Impact of 0.7-inch Diameter Prestressing Strands in Bridge Girders" Thesis, presented to University of Nebraska-Lincoln at Lincoln, NE in partial fulfillment of requirements for the degree of Master of Science.

Maguire, M., Chang, M., Collins, W. N., and Sun, Y. (2017). "Stress Increase of Unbonded Tendons in Continuous Posttensioned Members." *Journal of Bridge Engineering*, 22(2), 04016115.

Maguire, M., Collins, W. N., Halbe, K. R., and Roberts-Wollmann, C. L. (2015). "Multi-Span Members with Unbonded Tendons: Ultimate Strength Behavior." *ACI Structural Journal*, 113(2)

Maguire, M., Moen, C. D., Roberts-Wollmann, C., and Cousins, T. (2015). "Field Verification of Simplified Analysis Procedures for Segmental Concrete Bridges." *Journal of Structural Engineering*, 141(1).

Morcous, G., Hatami, A., Maguire, M., Hanna, K., and Tadros, M. (2012). "Mechanical and Bond Properties of 18- mm- (0.7-in.-) Diameter Prestressing Strands." *Journal of Materials in Civil Engineering*, 24(6), 735-744. DOI: 10.1061/(ASCE)MT.1943-5533.0000424, 735-744.

Morcous, G., Henin, E., Lafferty, M., and Tadros, M. K. (2011). "Design and testing of tornado-resistant precast/prestressed concrete sandwich panels with GFRP ties." *Proc., PCI 57th Annual Convention,* Precast/Prestressed Concrete Institute, Chicago.

Morcous, G., Henin, E., Lafferty, M., and Tadros, M., (2011) “Design and Testing Of Tornado-Resistant Precast/Prestressed Concrete Sandwich Panels With GFRP Ties.” PCI/NBC. Salt Lake City, UT.,

Bean, B., Maguire, M., and Sun, Y. (2017). “Predicting Utah Ground Snow Loads with PRISM.” *Journal of Structural Engineering*, 143(9), 04017126.

Morcous, G., Maguire, M., and Tadros, M. K. (2011). “Welded-wire reinforcement versus random steel fibers in precast, prestressed concrete bridge girders.” *PCI Journal*, 56(2), 113–129.

Naito, C. J., Hoemann, J. M., Shull, J. S., Saucier, A., Salim, H. A., Bewick, B. T., and Hammons, M. I. (2011). Precast/Prestressed Concrete Experiments Performance on Non-Load Bearing Sandwich Wall Panels. *Air Force Research Laboratory Rep. AFRL-RX-TY-TR-2011-0021*. Tyndall Air Force Base, Panama City, FL.

Naito, C. J., Hoemann, J., Beacraft, M., and Bewick, B. (2012) “Performance and Characterization of Shear Ties for Use in Insulated Precast Concrete Sandwich Wall Panels.” *Journal of Structural Engineering*, 138(1), 52- 61.

Newmark, N. M., Siess, C. P., Viest, I. M. (1951). “Tests and Analysis of Composite Beams with Incomplete Interaction.” *Proceedings of the Society of Experimental Stress Analysis*, 9 (1), 75–92.

Nowak, A. S. and Collins, K. R. (2000) *Reliability of Structures*. McGraw-Hill, Boston, MA. Print.

Olsen, J., Maguire, M., (2016) “Shear Testing of Precast Concrete Sandwich Wall Panel Composite Shear Connectors.” PCI/NBC. Nashville, TN.

Pantelides, C. P., Surapaneni, R., Reaveley, L. D. (2008) Structural Performance of Hybrid GFRP/Steel Concrete Sandwich Panels. *Journal of Composites for Construction*. 12(5), 570-576.

Pessiki, S., and Mlynarczyk, A. (2003). Experimental Evaluation of the Composite Behavior of Precast Concrete Sandwich Wall Panels. *PCI Journal*, 48(2), 54-71.

Rizkalla, S. H., Hassan, T. K., and Lucier, G. (2009). FRP Shear Transfer Mechanism for Precast, Prestressed Concrete Sandwich Load-Bearing Panels. *American Concrete Institute Fall 2009 Convention: Thomas T.C. Hsu Symposium*. 265, pp. 603-625. New Orleans: American Concrete Institute.

Salmon, D. C., and Einea, A. (1995). Partially Composite Sandwich Panel Deflections. *Journal of Structural Engineering*, 121, 778-783.

Seeber, K. E., Andrews, R. J., Baty, J. R., Campbell, P. S., Dobbs, J. E., Force, G., . . . Wescott, H. E. (1997).

State-of-the-Art of Precast/Prestressed Sandwich Wall Panels. *PCI Journal*, 42(2), 92-134.

Teixeira, N., Tomlinson, D. G., and Fam, A. (2016). "Precast Concrete Sandwich Wall Panels with Bolted Angle Connections Tested in Flexure Under Simulated Wind Pressure and Suction." *PCI Journal*, 61(4), 65–83.

Tomlinson, D. G. (2015). "Behaviour of Partially Composite Precast Concrete Sandwich Panels under Flexural and Axial Loads." Thesis, presented to Queen's University at Kingston, Ontario, Canada in partial fulfillment of requirements for the degree of Doctor of Philosophy.

Whitney, C. S. (1937). “Design of Reinforced Concrete Members Under Flexure or Combined Flexure and Direct Compression.” *ACI Journal Proceedings*, 33(3), 483–498.

Wight, J. K., and MacGregor, J. G. (2005). *Reinforced Concrete Mechanics and Design*. Pearson Education, Inc., Upper Saddle River, NJ. Print.

Woltman, G., Tomlinson, D., and Fam, A. (2013). Investigation of Various GFRP Shear Connectors for Insulated Precast Concrete Sandwich Wall Panels. *Journal of Composites of Construction*, 3(17), 711-721. DOI:10.1061/(ASCE)CC.1943-5614.0000373

APPENDICES

APPENDIX A.

Elastic Hand Method Analysis Examples

This appendix contains examples and predictions for predicting cracking moment of the full-scale panels (which utilized HK Composite, Nu-Tie, and Thermomass connectors) using the Elastic Hand Method proposed in this report. Table A-1 Load, Deflection, and Slip predictions for panels using Table A-1 summarizes the results of this section. The calculations of the values in Table A-1 follow thereafter. These examples illustrate how the Elastic Hand Method predicts the deflection and cracking of a given panel. Note that the Elastic Hand Procedure is iterative.

Table A-1 Load, Deflection, and Slip predictions for panels using

Panel	**Load Considered**	**Load** *(psf)*	**Deflection** *(in)*	**Slip** *(in)*
A-2	Self-Weight	75	0.154	0.0184
	Four-Point	81.3	0.202	0.0239
	Total Applied	156.3	0.356	0.0423
A-4	Self-Weight	75.00	0.1130	0.0130
	Four-Point	119.52	0.2173	0.0247
	Total Applied	194.52	0.3303	0.0377
B-1 and B-2	Self-Weight	100	0.1074	0.0142
	Four-Point	49.4	0.0648	0.0085
	Total Applied	149.9	0.1722	0.0227
BC-1 and BC-2	Self-Weight	100	0.073	0.0103
	Four-Point	95.77	0.0845	0.0090
	Total Applied	195.77	0.1575	0.0193
D-1 and D-2	Self-Weight	100.00	0.0600	0.0071
	Four-Point	122.62	0.0888	0.0105
	Total Applied	222.62	0.1488	0.0176

A-2 Panel (Nu-Tie connectors) Analysis Example (Prestressed)

Panel Properties

$L = 16\ ft$ $Span = 15\ ft$

$t_{wy1} = 3\ in$ $t_{wy2} = 3\ in$

$t_{ins} = 4\ in$ $b = 4\ ft$

$f_c' = 10.43\ ksi$ $A_{ps} = 0.255\ in^2$ (three prestressing strands)

$x_i = \begin{bmatrix} 24 \\ 72 \end{bmatrix} in$ $N = 2$

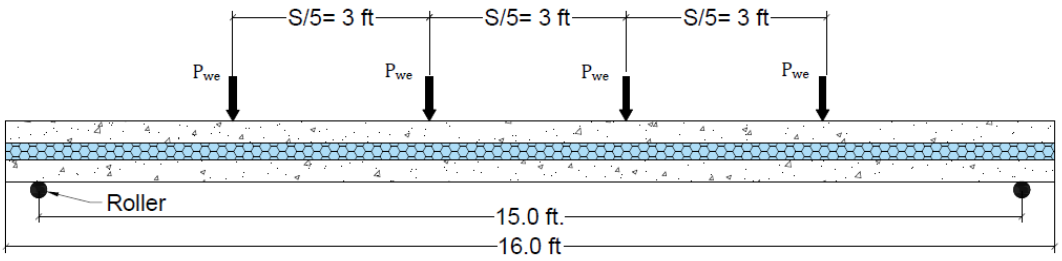

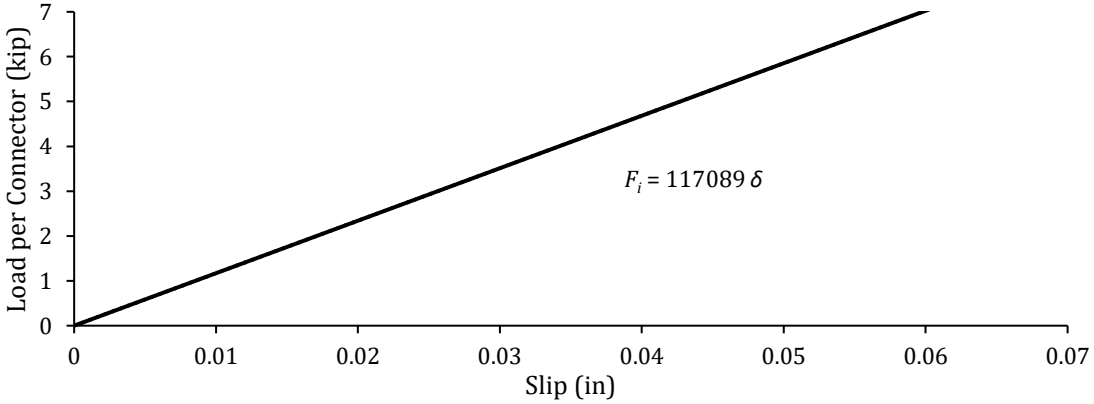

Figure A-1 Load vs Slip of Connector A (Nu-Tie connector)

Solution

1. Calculate the material and section properties of a non-composite sandwich panel.

$$x_{P1} = \frac{Span}{5} = 3\ ft \qquad x_{P2} = 2 * x_{P1} = 6\ ft$$

$$E_c = 6191.46\ ksi$$

$$f_r = \frac{7.5\ ksi}{1000} * \sqrt{10430\ psi} + \frac{170\ ksi * 0.085\ in^2 * 3}{48\ in * 3\ in} = 1.067\ ksi$$

$$I_{NC1} = \frac{b}{12} * \left(t_{wy_1}^3\right) = \frac{4\ ft * 12\frac{in}{ft}}{12} * (3\ in)^3 = 108\ in^4$$

$$I_{NC2} = \frac{b}{12} * \left(t_{wy_2}^3\right) = \frac{4\ ft * 12\frac{in}{ft}}{12} * (3\ in)^3 = 108\ in^4$$

$$Z = \frac{t_{wy_1} + t_{wy_2}}{2} + t_{insul} = \frac{3\ in + 3\ in}{2} + 4\ in = 7\ in$$

2. Assume an end slip, which is the slip at the end connector line (see Figure 5-2). Calculate the slip in the other connectors using similar triangles or Eq. (5-5).

   Assuming δ_{max} = 0.0423 in

$$\delta(i) = \delta_{max} * \frac{\left(\frac{L}{2} - x_i\right)}{\left(\frac{L}{2} - x_1\right)} = \begin{bmatrix} 0.0423 \\ 0.0141 \end{bmatrix} in$$

3. Calculate the shear forces in each connector using Figure A.

$$F_i = 2 * \begin{bmatrix} 4955.7 \\ 1652 \end{bmatrix} lb$$

$$F_{sum} = \sum F_i = 13220\ lb$$

4. Calculate the cracking moment:

$$M_{wy_2} = 2 * I_{NC2} * \left(\frac{f_r}{t_{wy_2}} - \frac{F_{sum}}{b * t_{wy_2}^2}\right)$$

$$= 2 * 108\ in^4 * \left(\frac{1.067\ ksi}{3\ in} - \frac{13.22\ kip}{48\ in * (3\ in)^2}\right) = 5.851\ kip * ft$$

5. Calculate the equivalent load that wythe 2 can carry using equations (5-9).

$$w_{we2} = \frac{8 * M_{wy_2}}{Span^2} = \frac{8 * 5.851\ \ kip * ft}{(15\ ft)^2} = \ 0.208 \frac{kip}{ft}$$

$$P_{we2} = \frac{M_{wy_2}}{(x_{P1} + x_{P2})} = \frac{5.851\ kip * ft}{(3\ ft + 6\ ft)} = \ 0.65\ kips$$

6. Using the equivalent load from the previous step, calculate axial and rotational displacement at the end connector using Eq

$$\theta_{w_{we2}} = \frac{w_{we2} * Span^3}{24 * E * I_{NC2}} = \frac{0.208 \frac{kip}{ft} * (15\ ft)^3 * 144\ in^2/ft^2}{24 * 6191.46\ ksi * 108\ in^4}$$

$$= \ 0.00630$$

$$\theta_{P_{we2}} = P_{we2} \left\{ \frac{x_{P1}[(Span^2 - x_{P1}^2) + (Span - x_{P1})(2Span - x_{P1})]}{6 * Span * E_c * I_{NC2}} \right.$$

$$\left. + \frac{x_{P2}[(Span^2 - x_{P2}^2) + (Span - x_{P2})(2Span - x_{P2})]}{6 * Span * E_c * I_{NC2}} \right\}$$

$$\theta_{P_{we2}} = 0.65 \left\{ \frac{3[(15^2 - 3^2) + (15 - 3)(30 - 3)]}{6 * 15 * 6191.46 * 108} \right.$$

$$\left. + \frac{6[(15^2 - 6^2) + (15 - 6)(30 - 6)]}{6 * 15 * 6191.46 * 108} \right\}$$

$$= 0.00630$$

$$\Delta_{Rot} = \theta * Z = 0.00630 * 7\ in = 0.04410\ in$$

$$\Delta_{Axial} = 2 * \sum_{i=1}^{n} F(i) * \left(\frac{\frac{L}{2} - x_i}{b * E_c * t_{wy_1}} \right) = 0.00178 \text{ in}$$

7. Using Equation (5-11) and (5-12), calculate the slip at the end connector and compare to assumed value.

$$\delta_{max} = \Delta_{Rot} - \Delta_{Axial} = 0.0441\ in - 0.00178 \text{ in} = 0.04232\ in$$

$$\delta_{max} = Assumed\ \delta_{max} \qquad \therefore \qquad OK$$

8. Calculate the cracking moment using Equation (5-14).

$$M_{cr} = M_{wy_2} * 2 + F_{sum} * Z$$

$$= 2 * 5.851\ kip * ft + 13.22\ kip * 7\ in = \mathbf{19.4137\ kip * ft}$$

$$\Delta_{w_{we2}} = \frac{5 * w_{we2} * Span^4}{384 * E_c * I_{NC2}} = \frac{5 * 0.208 \frac{kip}{ft} * (15\ ft)^4 * \left(12 \frac{in}{ft}\right)^3}{384 * 6191.46\ ksi * 108\ in^4}$$

$$= 0.3544\ in$$

$$\Delta_{P_{we2}} = \left(\frac{P_{we2}}{24 * E_c * I_{NC2}} \right) \{ x_{\mathrm{P1}} * (3 * Span^2 - 4 * x_{\mathrm{P1}}^2) + x_{\mathrm{P2}}$$

$$* (3 * Span^2 - 4 * x_{\mathrm{P2}}^2) \}$$

$$\Delta_{P_{we2}} = \left(\frac{0.559}{24 * 6191.46 * 108} \right) \{ 3 * (3 * 15^2 - 4 * 3^2) + 6$$

$$* (3 * 15^2 - 4 * 6^2) \} * 12^3$$

$$= 0.357\ in$$

The actual load on the sandwich wall panel included the four-point applied load as well as self-weight.

Table A-2 Total Load, Equivalent Load Deflection, and Slip

Load Distribution	**Total Load, p_{Total}**	**Equivalent Load Deflection, Δ_e** *(in)*	**Slip** *(in)*
Uniform Distributed Load	$\frac{M_{applied} * 8}{Span^2 * b} = \frac{19.4 * 8}{15^2 * 4} = 172.55\ psf$	0.3544	0.04232
Four-Point Loads	$\frac{4M_{applied}}{(x_{P1} + x_{P2}) * Span * b} = \frac{4 * 19.4}{9 * 15 * 4} = 143.79\ psf$	0.357	0.04232

$$p_{self} = 150\ pcf * (6\ in) = 75\ psf$$
$$w_{self} = p_{self} * b = 75\ psf * 4\ ft = 300\ plf$$
$$M_{self} = \frac{\left(w_{self} * Span^2\right)}{8} = \frac{300\ plf * (15ft)^2}{8} = 8.4375\ kip * ft$$
$$M_{FourPt} = M_{cr} - M_{self} = 19.4137\ kip * ft - 8.4375\ kip * ft = 10.976\ kip * ft$$
$$P_{FourPt} = 4 * \left(\frac{10.976\ kip * ft}{36\ in + 72\ in}\right) = 4.878\ kip$$
$$p_{FourPt} = \frac{4878\ lbs}{15\ ft * 4\ ft} = 81.3\ psf$$
$$\boldsymbol{p_{TotalApplied} = p_{self} + p_{FourPt} = 75\ psf + 81.3\ psf = 156.3\ psf}$$

Similar effects can be calculated for deflection also, as well as slip. Since self-weight is a distributed load, the uniform distributed load values will be used from Table A-2.

$$\Delta_{self} = \frac{p_{self}}{p_{Total}} * \Delta_e = \frac{75\ psf}{172.55\ psf} * 0.3544\ in = 0.154\ in$$
$$\Delta_{FourPt} = \frac{p_{FourPt}}{p_{Total}} * \Delta_e = \frac{81.3\ psf}{143.79\ psf} * 0.357\ in = 0.202\ in$$
$$\boldsymbol{\Delta_{Total} = 0.154\ in + 0.202\ in = 0.356\ in}$$

$$\delta_{self} = \frac{p_{self}}{p_{Total}} * \delta_{max} = \frac{75\ psf}{172.55\ psf} * 0.04232\ in = 0.0184\ in$$

$$\delta_{FourPt} = \frac{p_{FourPt}}{p_{Total}} * \Delta_{max} = \frac{81.3\ psf}{143.79\ psf} * 0.04232\ in = 0.0239\ in$$

$$\boldsymbol{\delta_{Total} = \delta_{self} + \delta_{FourPt} = 0.0184\ in + 0.0239\ in = 0.0423\ in}$$

A-4 Panel (Nu-Tie connectors) Analysis Example (Prestressed)

Panel Properties

$L = 16\ ft$ $Span = 15\ ft$

$t_{wy1} = 3\ in$ $t_{wy2} = 3\ in$

$t_{ins} = 4\ in$ $b = 4\ ft$

$f_c' = 10.43\ ksi$ $A_{ps} = 0.255\ in^2$ (three prestressing strands)

$x_i = \begin{bmatrix} 24 \\ 72 \end{bmatrix} in$ $N = 4$

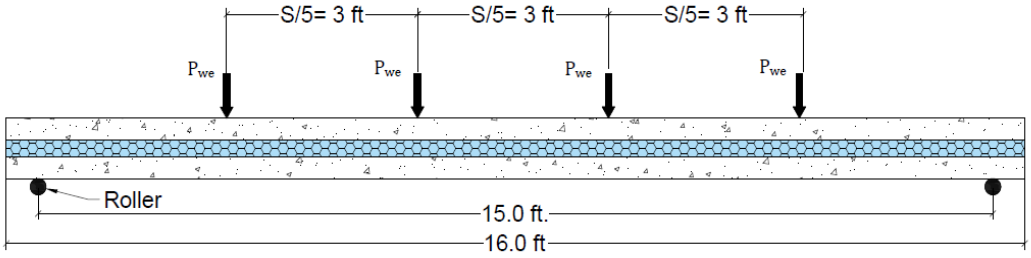

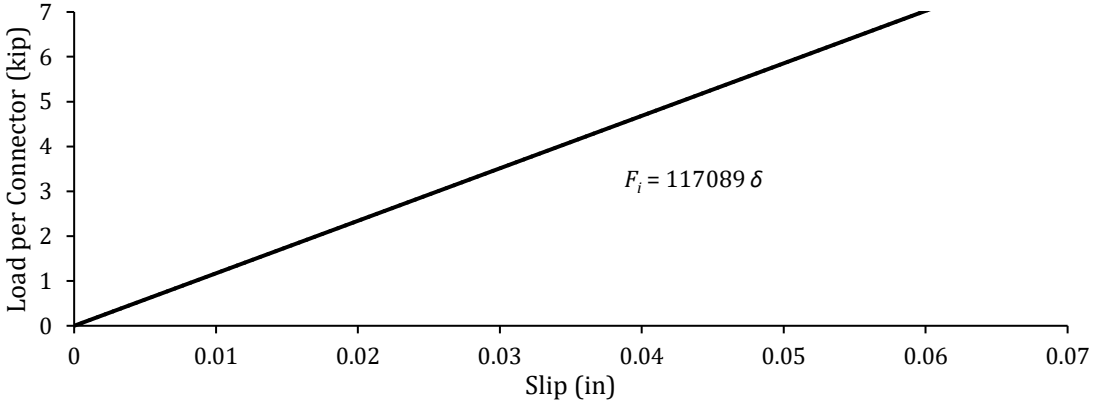

Figure A-2 Load vs Slip of Connector A (Nu-Tie connector)

Solution

1. Calculate the material and section properties of a non-composite sandwich panel.

$$x_{P1} = \frac{Span}{5} = 3\ ft \qquad x_{P2} = 2 * x_{P1} = 6\ ft$$

$$E_c = 6191.46\ ksi$$

$$f_r = \frac{7.5\ ksi}{1000} * \sqrt{10430\ psi} + \frac{170\ ksi * 0.085\ in^2 * 3}{48\ in * 3\ in} = 1.067\ ksi$$

$$I_{NC1} = \frac{b}{12} * \left(t_{wy_1}^3\right) = \frac{4\ ft * 12\frac{in}{ft}}{12} * (3\ in)^3 = 108\ in^4$$

$$I_{NC2} = \frac{b}{12} * \left(t_{wy_2}^3\right) = \frac{4\ ft * 12\frac{in}{ft}}{12} * (3\ in)^3 = 108\ in^4$$

$$Z = \frac{t_{wy_1} + t_{wy_2}}{2} + t_{insul} = \frac{3\ in + 3\ in}{2} + 4\ in = 7\ in$$

2. Assume an end slip, which is the slip at the end connector line (see Figure 5-2). Calculate the slip in the other connectors using similar triangles or Eq. (5-5).

Assuming δ_{max} = 0.0377 in

$$\delta(i) = \delta_{max} * \frac{\left(\frac{L}{2} - x_i\right)}{\left(\frac{L}{2} - x_1\right)} = \begin{bmatrix} 0.0377 \\ 0.0126 \end{bmatrix} in$$

3. Calculate the shear forces in each connector using Figure A-2.Figure A-2 Load vs Slip of Connector A (Nu-Tie connector)

$$F_i = \begin{bmatrix} 4413.4 \\ 1471.1 \end{bmatrix} lb$$

$$F_{sum} = 4 * \sum F_i = 23540\ lb$$

4. Calculate the cracking moment:

$$M_{wy_2} = 2 * I_{NC2} * \left(\frac{f_r}{t_{wy_2}} - \frac{F_{sum}}{b * t_{wy_2}^2}\right)$$

$$= 2 * 108\ in^4 * \left(\frac{1.067\ ksi}{3\ in} - \frac{23.54\ kip}{48\ in * (3\ in)^2}\right) = 5.421\ kip * ft$$

5. Calculate the equivalent load that wythe 2 can carry using equations (5-9).

$$w_{we2} = \frac{8 * M_{wy_2}}{Span^2} = \frac{8 * 5.421\ \ kip * ft}{(15\ ft)^2} = \ 0.1927 \frac{kip}{ft}$$

$$P_{we2} = \frac{M_{wy_2}}{(x_{P1} + x_{P2})} = \frac{5.421\ kip * ft}{(3\ ft + 6\ ft)} = \ 0.602\ kips$$

6. Using the equivalent load from the previous step, calculate axial and rotational displacement at the end connector using Eq

$$\theta_{w_{we2}} = \frac{w_{we2} * Span^3}{24 * E * I_{NC2}} = \frac{0.1927 \frac{kip}{ft} * (15\ ft)^3 * 144\ in^2/ft^2}{24 * 6191.46\ ksi * 108\ in^4}$$

$$= \ 0.005837$$

$$\theta_{P_{we2}} = P_{we2} \left\{ \frac{x_{P1}[(Span^2 - x_{P1}^2) + (Span - x_{P1})(2 * Span - x_{P1})]}{6 * Span * E_c * I_{NC2}} \right.$$

$$\left. + \frac{x_{P2}[(Span^2 - x_{P2}^2) + (Span - x_{P2})(2 * Span - x_{P2})]}{6 * Span * E_c * I_{NC2}} \right\}$$

$$\theta_{P_{we2}} = 0.602 \left\{ \frac{3[(15^2 - 3^2) + (15 - 3)(30 - 3)]}{6 * 15 * 6191.46 * 108} \right.$$

$$\left. + \frac{6[(15^2 - 6^2) + (15 - 6)(30 - 6)]}{6 * 15 * 6191.46 * 108} \right\}$$

$$= 0.005837$$

$$\Delta_{Rot} = \theta * Z = 0.005837 * 7\ in = 0.04086\ in$$

$$\Delta_{Axial} = 2 * \sum_{i=1}^{n} F(i) * \left(\frac{\frac{L}{2} - x_i}{b * E_c * t_{wy_1}} \right) = 0.003168 \text{ in}$$

7. Using Equation (5-11) and (5-12), calculate the slip at the end connector and compare to assumed value.

$$\delta_{max} = \Delta_{Rot} - \Delta_{Axial} = 0.04086\ in - 0.003168 \text{ in} = 0.0377\ in$$

$$\delta_{max} = Assumed\ \delta_{max} \qquad \therefore \qquad OK$$

8. Calculate the cracking moment using Equation (5-14).

$$M_{cr} = M_{wy_2} * 2 + F_{sum} * Z$$

$$= 2 * 5.421\ kip * ft + 23.54\ kip * 7\ in = \mathbf{24.573\ kip * ft}$$

$$\Delta_{w_{we2}} = \frac{5 * w_{we2} * Span^4}{384 * E_c * I_{NC2}} = \frac{5 * 0.1927 \frac{kip}{ft} * (15\ ft)^4 * \left(12 \frac{in}{ft}\right)^3}{384 * 6191.46\ ksi * 108\ in^4}$$

$$= 0.3283\ in$$

$$\Delta_{P_{we2}} = \left(\frac{P_{we2}}{24 * E_c * I_{NC2}} \right) \{ x_{\mathrm{P1}} * (3 * Span^2 - 4 * x_{\mathrm{P1}}^2) + x_{\mathrm{P2}} * (3 * Span^2 - 4 * x_{\mathrm{P2}}^2) \}$$

$$\Delta_{P_{we2}} = \left(\frac{0.602}{24 * 6191.46 * 108} \right) \{ 3 * (3 * 15^2 - 4 * 3^2) + 6 * (3 * 15^2 - 4 * 6^2) \} * 12^3$$

$$= 0.331\ in$$

The actual load on the sandwich wall panel included the four-point applied load as well as self-weight.

$$p_{self} = 150\ pcf * (6\ in) = 75\ psf$$
$$w_{self} = p_{self} * b = 75\ psf * 4\ ft = 300\ plf$$

$$M_{self} = \frac{\left(w_{self} * Span^2\right)}{8} = \frac{300\ plf * (15ft)^2}{8} = 8.4375\ kip * ft$$

$$M_{FourPt} = M_{cr} - M_{self} = 24.573\ kip * ft - 8.4375\ kip * ft = 16.1355\ kip * ft$$

$$P_{FourPt} = 4 * \left(\frac{16.1355\ kip * ft}{36\ in + 72\ in}\right) = 7.171\ kip$$

$$p_{FourPt} = \frac{7171\ lbs}{15\ ft * 4\ ft} = 119.52\ psf$$

$$\boldsymbol{p_{TotalApplied} = p_{self} + p_{FourPt} = 75\ psf + 119.52\ psf = 194.52\ psf}$$

Table A-3 Total Load, Equivalent Load Deflection, and Slip

Load Distribution	**Total Load, p_{Total}**	**Deflection from Equivalent Load, Δ_e** *(in)*	**Slip** *(in)*
Uniform Distributed Load	$\frac{M_{applied} * 8}{Span^2 * b} = \frac{24.57 * 8}{15^2 * 4} = 218.43\ psf$	0.3283	0.0377
Four-Point Loads	$\frac{4M_{applied}}{(x_{P1} + x_{P2}) * Span * b} = \frac{4 * 24.57}{9 * 15 * 4} = 182\ psf$	0.3310	0.0377

Similar effects can be calculated for deflection also, as well as slip. Since self-weight is a distributed load, the uniform distributed load values will be used from Table A-3.

$$\Delta_{self} = \frac{p_{self}}{p_{Total}} * \Delta_e = \frac{75\ psf}{218.43\ psf} * 0.3283\ in = 0.113\ in$$

$$\Delta_{FourPt} = \frac{p_{FourPt}}{p_{Total}} * \Delta_e = \frac{119.52\ psf}{182\ psf} * 0.3310\ in = 0.2173\ in$$

$$\boldsymbol{\Delta_{Total} = 0.113\ in + 0.2173\ in = 0.3303\ in}$$

$$\delta_{self} = \frac{p_{self}}{p_{Total}} * \delta_{max} = \frac{75\ psf}{218.43\ psf} * 0.0377\ in = 0.013\ in$$

$$\delta_{FourPt} = \frac{p_{FourPt}}{p_{Total}} * \Delta_{max} = \frac{119.52\ psf}{182\ psf} * 0.0377\ in = 0.02476\ in$$

$$\boldsymbol{\delta_{Total} = \delta_{self} + \delta_{FourPt} = 0.0130\ in + 0.02476\ in = 0.0377\ in}$$

B Panel (only Thermomass CC connectors) Analysis Example (Mild Reinforcement)

Panel Properties

$L = 16\ ft$ $Span = 14\ ft$

$t_{wy1} = 4\ in$ $t_{wy2} = 4\ in$

$t_{ins} = 3\ in$ $b = 3\ ft$

$f_c' = 9.23\ ksi$

$x_i = \begin{bmatrix} 30 \\ 82 \end{bmatrix} in$ $N = 3$

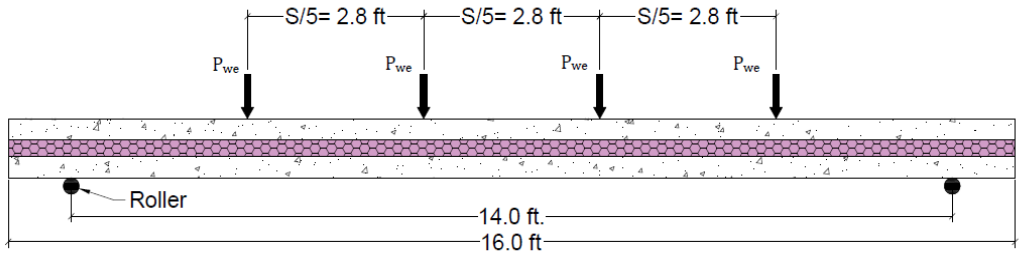

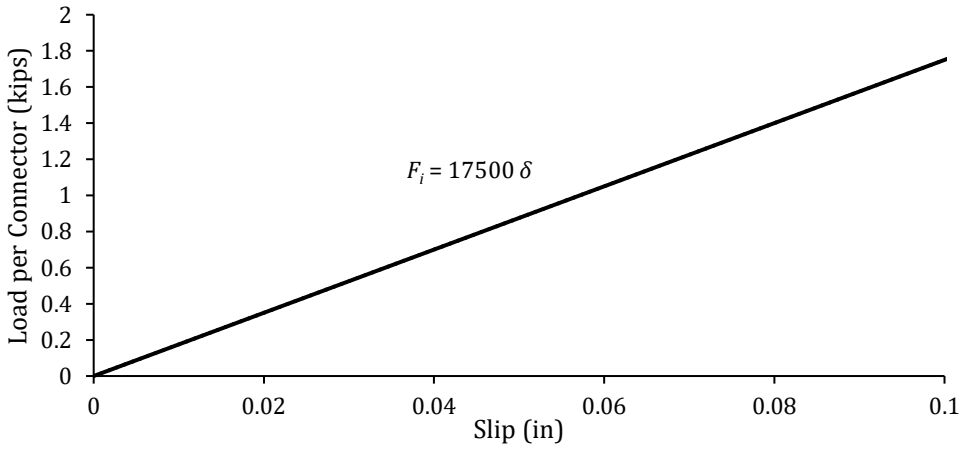

Figure A-3 Load vs slip of Connector B (Thermomass CC connector)

Solution

1. Calculate the material and section properties of a non-composite sandwich panel. The modulus of rupture of the concrete (f_r) was measured in this case, so the actual value is included here.

$$x_{P1} = \frac{Span}{5} = 2.8\ ft \qquad x_{P2} = 2 * x_{P1} = 5.6\ ft$$

$$E_c = 5824.4\ ksi$$

$$f_r = 0.691\ ksi$$

$$I_{NC1} = \frac{b}{12} * \left(t_{wy_1}^3\right) = \frac{3\ ft * 12\frac{in}{ft}}{12} * (4\ in)^3 = 192\ in^4$$

$$I_{NC2} = \frac{b}{12} * \left(t_{wy_2}^3\right) = \frac{3\ ft * 12\frac{in}{ft}}{12} * (4\ in)^3 = 192\ in^4$$

$$Z = \frac{t_{wy_1} + t_{wy_2}}{2} + t_{insul} = \frac{4\ in + 4\ in}{2} + 3\ in = 7\ in$$

2. Assume an end slip, which is the slip at the end connector line (see Figure 5-2). Calculate the slip in the other connectors using similar triangles or Eq. (5-5).

   Assuming δ_{max} = 0.0227 in

$$\delta(i) = \delta_{max} * \frac{\left(\frac{L}{2} - x_i\right)}{\left(\frac{L}{2} - x_1\right)} = \begin{bmatrix}0.0227\\0.0048\end{bmatrix} in$$

3. Calculate the shear forces in each connector using Figure A-3.

$$F_i = 3 * \begin{bmatrix}405.5\\86\end{bmatrix} lb$$

$$F_{sum} = \sum F_i = 1475\ lb$$

4. Calculate the cracking moment:

$$M_{wy_2} = 2 * I_{NC2} * \left(\frac{f_r}{t_{wy_2}} - \frac{F_{sum}}{b * t_{wy_2}^2}\right)$$

$$= 2 * 192\ in^4 * \left(\frac{0.691\ ksi}{4\ in} - \frac{1.475\ kip}{36\ in * (4\ in)^2}\right) = 5.446\ kip * ft$$

5. Calculate the equivalent load that wythe 2 can carry using equations (5-9).

$$w_{we2} = \frac{8 * M_{wy_2}}{Span^2} = \frac{8 * 5.446\ \ kip * ft}{(14\ ft)^2} = \ 0.2223 \frac{kip}{ft}$$

$$P_{we2} = \frac{M_{wy_2}}{(x_{P1} + x_{P2})} = \frac{5.446\ kip * ft}{(2.8\ ft + 5.6\ ft)} = \ 0.648\ kip$$

6. Using the equivalent load from the previous step, calculate axial and rotational displacement at the end connector using Eq

$$\theta_{w_{we2}} = \frac{w_{we2} * Span^3}{24 * E_c * I_{NC2}} = \frac{0.2223 \frac{kip}{ft} * (14\ ft)^3 * 144}{24 * 5824.4\ ksi * 192\ in^4} = \ 0.003273$$

$$\theta_{P_{we2}} = P_{we2} \left\{ \frac{x_{P1}[(Span^2 - x_{P1}^2) + (Span - x_{P1})(2Span - x_{P1})]}{6 * Span * E_c * I_{NC2}} \right.$$

$$\left. + \frac{x_{P2}[(Span^2 - x_{P2}^2) + (Span - x_{P2})(2Span - x_{P2})]}{6 * Span * E_c * I_{NC2}} \right\}$$

$$\theta_{P_{we2}} = 0.648 \left\{ \frac{2.8[(14^2 - 2.8^2) + (14 - 2.8)(28 - 2.8)]}{6 * 14 * 5824.4 * 192} \right.$$

$$\left. + \frac{5.6[(14^2 - 5.6^2) + (14 - 5.6)(28 - 5.6)]}{6 * 14 * 5824.4 * 192} \right\} = 0.00327$$

$$\Delta_{Rot} = \theta * Z = 0.003273 * 7\ in = 0.02291\ in$$

$$\Delta_{Axial} = 2 * \sum_{i=1}^{n} F(i) * \left(\frac{\frac{L}{2} - x_i}{b * E_c * t_{wy_1}}\right) = 0.0002 \text{ in}$$

7. Using Eq. (5-11) and (5-12), calculate the slip at the end connector and compare to assumed value.

$$\delta_{max} = \Delta_{Rot} - \Delta_{Axial} = 0.02291\ in - 0.0002\ \text{in} = 0.02271\ in$$

$$\delta_{max} = Assumed\ \delta_{max} \qquad \therefore \qquad OK$$

8. Calculate the cracking moment using Equation (5-14).

$$M_{cr} = M_{wy_2} * 2 + F_{sum} * Z$$

$$= 2 * 5.446\ kip * ft + 1475\ lb * 7\ in = \mathbf{11.752\ kip * ft}$$

$$\Delta_{w_{we2}} = \frac{5 * w_{we2} * Span^4}{384 * E_c * I_{NC2}} = \frac{5 * 0.2223 \frac{kip}{ft} * (14\ ft)^4 * \left(12 \frac{in}{ft}\right)^3}{384 * 5824.4\ ksi * 192\ in^4}$$

$$= 0.1718\ in$$

$$\Delta_{P_{we2}} = \left(\frac{P_{we2}}{24 * E_c * I_{NC2}}\right)\{x_{\mathrm{P1}} * (3 * Span^2 - 4 * x_{\mathrm{P1}}^2) + x_{\mathrm{P2}}$$

$$* (3 * Span^2 - 4 * x_{\mathrm{P2}}^2)\}$$

$$\Delta_{P_{we2}} = \left(\frac{0.648}{24 * 5824.4 * 192}\right)\{2.8 * (3 * 14^2 - 4 * 2.8^2) + 5.6$$

$$* (3 * 14^2 - 4 * 5.6^2)\} * 12^3$$

$$= 0.1732\ in$$

The actual load on the sandwich wall panel included the four-point applied load as well as self-weight.

$$p_{self} = 150\ pcf * (8\ in) = 100\ psf$$

$$w_{self} = p_{self} * b = 100\ psf * 3\ ft = 300\ plf$$

$$M_{self} = \frac{\left(w_{self} * Span^2\right)}{8} = \frac{300\ plf * (14ft)^2}{8} = 7.35\ kip * ft$$

$$M_{FourPt} = M_{cr} - M_{self} = 11.752\ kip * ft - 7.35\ kip * ft = 4.402\ kip * ft$$

$$P_{FourPt} = 4 * \left(\frac{4.402\ kip * ft}{33.6\ in + 67.2\ in}\right) = 2.096\ kip$$

$$p_{FourPt} = \frac{2096\ lbs}{14\ ft * 3\ ft} = 49.9\ psf$$

$$\boldsymbol{p_{TotalApplied} = p_{self} + p_{FourPt} = 100\ psf + 49.9\ psf = 149.9\ psf}$$

Table A-4 Total Load, Equivalent Load Deflection, and Slip

Load Distribution	**Total Load, p_{Total}**	**Deflection from Equivalent Load, Δ_e** *(in)*	**Slip** *(in)*
Uniform Distributed Load	$\frac{M_{applied} * 8}{Span^2 * b} = \frac{11.75 * 8}{14^2 * 3} = 160\ psf$	0.1718	0.02271
Four-Point Loads	$\frac{4M_{applied}}{(x_{P1} + x_{P2})b * Span} = \frac{4 * 11.75}{8.4 * 3 * 14} = 133.2\ psf$	0.1732	0.02271

Similar effects can be calculated for deflection also, as well as slip. Since self-weight is a distributed load, the uniform distributed load values will be used from Table A-4.

$$\Delta_{self} = \frac{p_{self}}{p_{Total}} * \Delta_e = \frac{100\ psf}{160\ psf} * 0.1718\ in = 0.1074\ in$$

$$\Delta_{FourPt} = \frac{p_{FourPt}}{p_{Total}} * \Delta_e = \frac{49.9\ psf}{133.24\ psf} * 0.1732\ in = 0.0648\ in$$

$$\boldsymbol{\Delta_{Total} = 0.1074\ in + 0.0648\ in = 0.1722\ in}$$

$$\delta_{self} = \frac{p_{self}}{p_{Total}} * \delta_{max} = \frac{100\ psf}{160\ psf} * 0.0227\ in = 0.0142\ in$$

$$\delta_{FourPt} = \frac{p_{FourPt}}{p_{Total}} * \Delta_{max} = \frac{49.9\ psf}{133.24\ psf} * 0.0227\ in = 0.0085\ in$$

$$\boldsymbol{\delta_{Total} = \delta_{self} + \delta_{FourPt} = 0.0142\ in + 0.0085\ in = 0.0227\ in}$$

BC Panel (Thermomass CC and X connectors) Analysis Example (Mild Reinforcement)

Panel Properties

$L = 16\ ft$ $Span = 14\ ft$

$t_{wy1} = 4\ in$ $t_{wy2} = 4\ in$

$t_{ins} = 3\ in$ $b = 3\ ft$

$f_c' = 9.23\ ksi$ $A_s = 0.44\ in^2$

$$x_{CCi} = \begin{bmatrix} 16 \\ 32 \\ 48 \\ 64 \\ 80 \end{bmatrix} in \qquad N_{CC} = 3$$

$x_{Xi} = [24] in$ $N_X = 3$

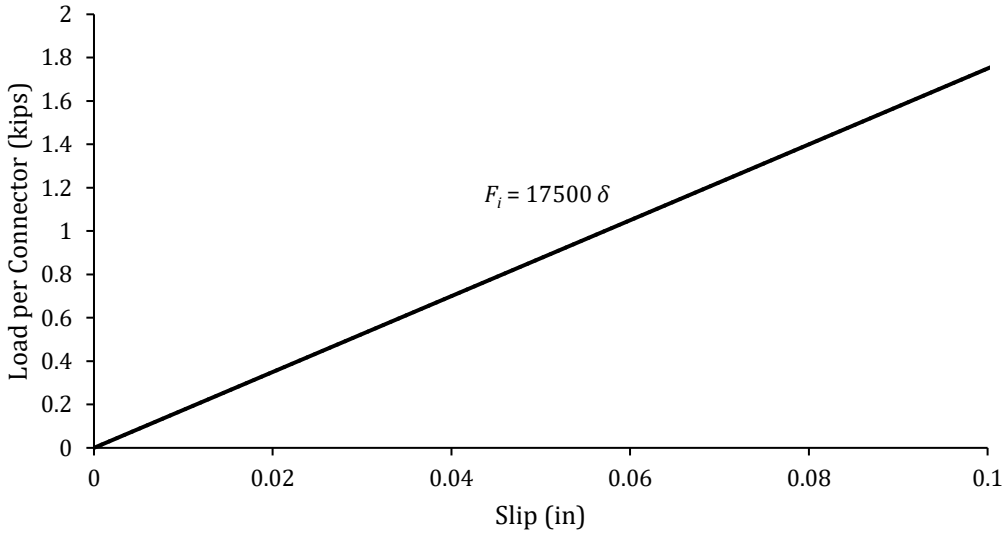

Figure A-4 Load vs slip of Connector B (Thermomass CC connector)

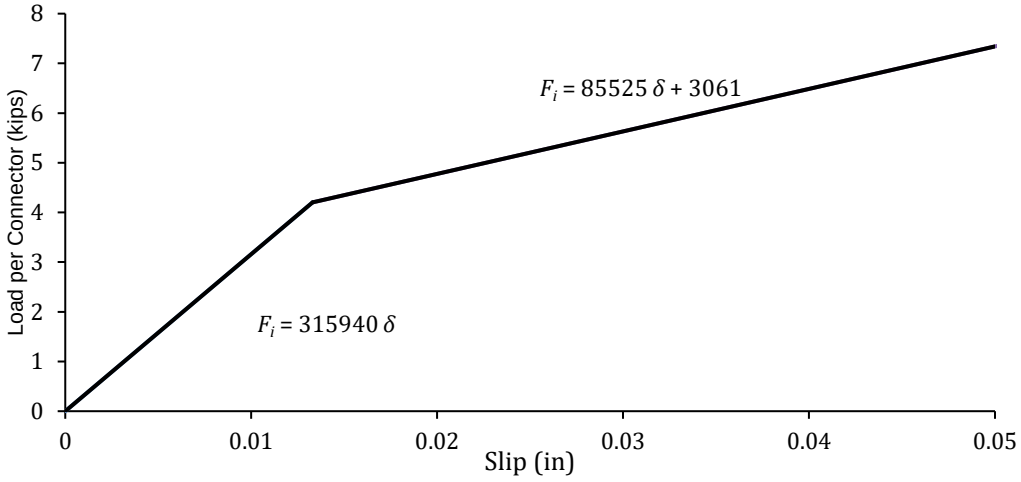

Figure A-5 Load vs slip of Connector C (Thermomass X connector)

Solution

1. Calculate the material and section properties of a non-composite sandwich panel. The modulus of rupture of the concrete (f_r) was measured in this case, so the actual value is included here.

$$x_{P1} = \frac{Span}{5} = 2.8\ ft \qquad x_{P2} = 2 * x_{P1} = 5.6\ ft$$

$$E_c = 5824.4\ ksi$$

$$f_r = 0.691\ ksi$$

$$I_{NC1} = \frac{b}{12} * \left(t_{wy_1}^3\right) = \frac{3\ ft * 12\frac{in}{ft}}{12} * (4\ in)^3 = 192\ in^4$$

$$I_{NC2} = \frac{b}{12} * \left(t_{wy_2}^3\right) = \frac{3\ ft * 12\frac{in}{ft}}{12} * (4\ in)^3 = 192\ in^4$$

$$Z = \frac{t_{wy_1} + t_{wy_2}}{2} + t_{insul} = \frac{4\ in + 4\ in}{2} + 3\ in = 7\ in$$

2. Assume an end slip, which is the slip at the end connector line (see Figure 5-2). Calculate the slip in the other connectors using similar triangles or Eq. (5-5).

   Assuming δ_{max} = 0.01929 in

$$x_i = \begin{bmatrix} 16 \\ 24 \\ 32 \\ 48 \\ 64 \\ 80 \end{bmatrix} in \qquad \delta(i) = \delta_{max} * \frac{\left(\frac{L}{2} - x_i\right)}{\left(\frac{L}{2} - x_1\right)} = \begin{bmatrix} 0.01929 \\ 0.01736 \\ 0.01543 \\ 0.01157 \\ 0.00772 \\ 0.00386 \end{bmatrix} in$$

3. Calculate the shear forces in each connector using Figure A-4 and Figure A-5.

$$F_i = \begin{bmatrix} 3 * 344.4 \\ 2 * 3472 \\ 3 * 275.5 \\ 3 * 206.7 \\ 3 * 137.8 \\ 3 * 68.9 \end{bmatrix} lb$$

$$F_{sum} = \sum F_i = 10040\ lb$$

4. Calculate the cracking moment:

$$M_{wy_2} = 2 * I_{NC2} * \left(\frac{f_r}{t_{wy_2}} - \frac{F_{sum}}{b * t_{wy_2}^2}\right)$$

$$= 2 * 192\ in^4 * \left(\frac{0.691\ ksi}{4\ in} - \frac{10.04\ kip}{36\ in * (4\ in)^2}\right) = 4.97\ kip * ft$$

5. Calculate the equivalent load that wythe 2 can carry using equations (5-9).

$$w_{we2} = \frac{8 * M_{wy_2}}{Span^2} = \frac{8 * 4.97\ \ kip * ft}{(14\ ft)^2} = \ 0.203 \frac{kip}{ft}$$

$$P_{we2} = \frac{M_{wy_2}}{(x_{P1} + x_{P2})} = \frac{4.97\ kip * ft}{(2.8\ ft + 5.6\ ft)} = \ 0.5917\ kip$$

6. Using the equivalent load from the previous step, calculate axial and rotational displacement at the end connector using Eq

$$\theta_{w_{we2}} = \frac{w_{we2} * Span^3}{24 * E * I_{NC2}} = \frac{0.203\frac{kip}{ft} * (14\,ft)^3 * 144}{24 * 5824.4\,ksi * 192\,in^4} = 0.00299$$

$$\theta_{P_{we2}} = P_{we2}\left\{\frac{x_{P1}[(Span^2 - x_{P1}^2) + (Span - x_{P1})(2Span - x_{P1})]}{6 * Span * E_c * I_{NC2}} + \frac{x_{P2}[(Span^2 - x_{P2}^2) + (Span - x_{P2})(2Span - x_{P2})]}{6 * Span * E_c * I_{NC2}}\right\}$$

$$\theta_{P_{we2}} = 0.5917\left\{\frac{2.8[(14^2 - 2.8^2) + (14 - 2.8)(28 - 2.8)]}{6 * 14 * 5824.4 * 192} + \frac{5.6[(14^2 - 5.6^2) + (14 - 5.6)(28 - 5.6)]}{6 * 14 * 5824.4 * 192}\right\} = 0.00299$$

$$\Delta_{Rot} = \theta * Z = 0.00299 * 7\,in = 0.0209\,in$$

$$\Delta_{Axial} = 2 * \sum_{i=1}^{n} F(i) * \left(\frac{\frac{L}{2} - x_i}{b * E_c * t_{wy_1}}\right) = 0.001618 \text{ in}$$

7. Using Equation (5-11) and (5-12), calculate the slip at the end connector and compare to assumed value.

$$\delta_{max} = \Delta_{Rot} - \Delta_{Axial} = 0.0209\,in - 0.001618 \text{ in} = 0.01928\,in$$

$$\delta_{max} = Assumed\ \delta_{max} \qquad \therefore \qquad OK$$

8. Calculate the cracking moment using Equation (5-14).

$$M_{cr} = M_{wy_2} * 2 + F_{sum} * Z$$

$$= 2 * 4.97\,kip * ft + 10040\,lb * 7\,in = \mathbf{15.797\ kip * ft}$$

$$\Delta_{w_{we2}} = \frac{5 * w_{we2} * Span^4}{384 * E_c * I_{NC2}} = \frac{5 * 0.203\frac{kip}{ft} * (14\ ft)^4 * \left(12\frac{in}{ft}\right)^3}{384 * 5824.4\ ksi * 192\ in^4}$$

$$= 0.157\ in$$

$$\Delta_{P_{we2}} = \left(\frac{P_{we2}}{24 * E_c * I_{NC2}}\right)\{x_{\mathrm{P1}} * (3 * Span^2 - 4 * x_{\mathrm{P1}}^2) + x_{\mathrm{P2}}$$

$$* (3 * Span^2 - 4 * x_{\mathrm{P2}}^2)\}$$

$$\Delta_{P_{we2}} = \left(\frac{0.559}{24 * 5824.4 * 192}\right)\{2.8 * (3 * 14^2 - 4 * 2.8^2) + 5.6$$

$$* (3 * 14^2 - 4 * 5.6^2)\} * 12^3$$

$$= 0.158\ in$$

Table A-5 Total Load, Equivalent Load Deflection, and Slip

Load Distribution	**Total Load, p_{Total}**	**Deflection from Equivalent Load, Δ_e** *(in)*	**Slip** *(in)*
Uniform Distributed Load	$\frac{M_{applied} * 8}{Span^2 * b} = \frac{15.8 * 8}{14^2 * 3} = 214.95\ psf$	0.1570	0.01929
Four-Point Loads	$\frac{4M_{applied}}{(x_{P1} + x_{P2})b * Span} = \frac{4 * 15.8}{8.4 * 3 * 14} = 179.1\ psf$	0.1581	0.01929

The actual load on the sandwich wall panel included the four-point applied load as well as self-weight.

$$p_{self} = 150\ pcf * (8\ in) = 100\ psf$$

$$w_{self} = p_{self} * b = 100\ psf * 3\ ft = 300\ plf$$

$$M_{self} = \frac{\left(w_{self} * Span^2\right)}{8} = \frac{300\ plf * (14ft)^2}{8} = 7.35\ kip * ft$$

$$M_{FourPt} = M_{cr} - M_{self} = 15.797\ kip * ft - 7.35\ kip * ft = 8.447\ kip * ft$$

$$P_{FourPt} = 4 * \left(\frac{8.447\ kip * ft}{33.6\ in + 67.2\ in}\right) = 4.02\ kip$$

$$p_{FourPt} = \frac{4020\ lbs}{14\ ft * 3\ ft} = 95.77\ psf$$

$$\boldsymbol{p_{TotalApplied} = p_{self} + p_{FourPt} = 100\ psf + 95.77\ psf = 195.77\ psf}$$

Similar effects can be calculated for deflection also, as well as slip. Since self-weight is a distributed load, the uniform distributed load values will be used from Table A-5.

$$\Delta_{self} = \frac{p_{self}}{p_{Total}} * \Delta_e = \frac{100\ psf}{214.95\ psf} * 0.157\ in = 0.0730\ in$$

$$\Delta_{FourPt} = \frac{p_{FourPt}}{p_{Total}} * \Delta_e = \frac{95.77\ psf}{179.13\ psf} * 0.158\ in = 0.0845\ in$$

$$\boldsymbol{\Delta_{Total} = 0.0730\ in + 0.0845\ in = 0.1575\ in}$$

$$\delta_{self} = \frac{p_{self}}{p_{Total}} * \delta_{max} = \frac{100\ psf}{214.95\ psf} * 0.01929\ in = 0.00897\ in$$

$$\delta_{FourPt} = \frac{p_{FourPt}}{p_{Total}} * \Delta_{max} = \frac{95.77\ psf}{179.13\ psf} * 0.01929\ in = 0.0103\ in$$

$$\boldsymbol{\delta_{Total} = \delta_{self} + \delta_{FourPt} = 0.00897\ in + 0.0103\ in = 0.01928\ in}$$

D Panel (HK Composite connectors) Panel Analysis Example (Mild Reinforcement)

Panel Properties

$L = 16\ ft$ $Span = 14\ ft$

$t_{wy1} = 4\ in$ $t_{wy2} = 4\ in$

$t_{ins} = 3\ in$ $b = 3\ ft$

$f_c' = 9.23\ ksi$

$x_i = \begin{bmatrix} 16 \\ 32 \\ 48 \\ 64 \\ 80 \end{bmatrix} in$ $N = 3$

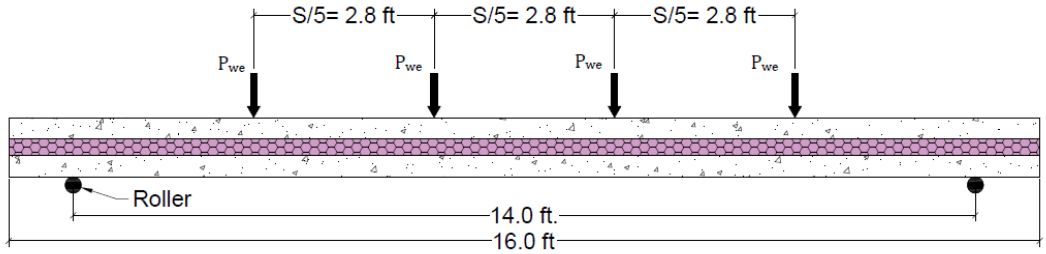

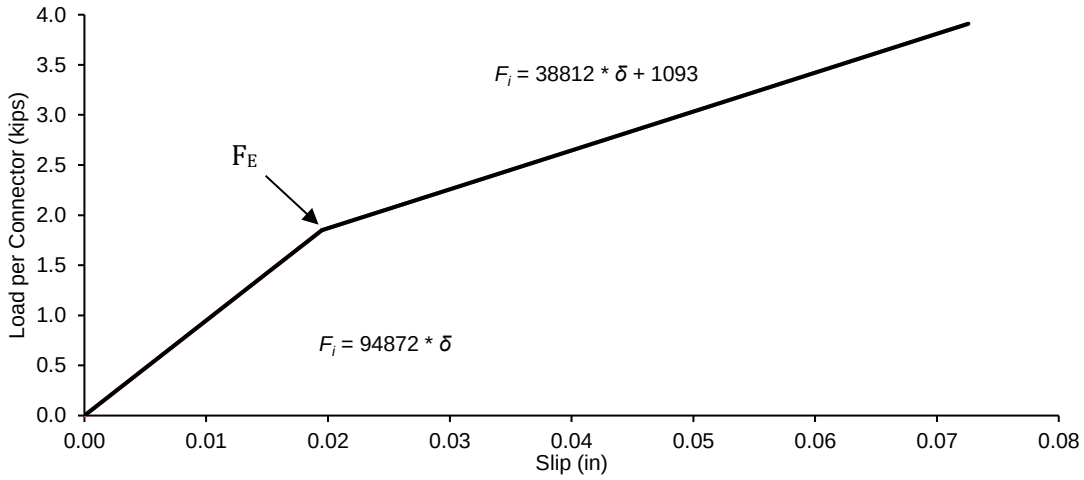

Figure A-6 Load vs slip of HK connector

Solution

1. Calculate the material and section properties of a non-composite sandwich panel. The modulus of rupture of the concrete (f_r) was measured in this case, so the actual value is included here.

$$x_{P1} = \frac{Span}{5} = 2.8\ ft \qquad x_{P2} = 2 * x_{P1} = 5.6\ ft$$

$$E_c = 5824.4\ ksi$$

$$f_r = 0.691\ ksi$$

$$I_{NC1} = \frac{b}{12} * \left(t_{wy_1}^3\right) = \frac{3\ ft * 12\frac{in}{ft}}{12} * (4\ in)^3 = 192\ in^4$$

$$I_{NC2} = \frac{b}{12} * \left(t_{wy_2}^3\right) = \frac{3\ ft * 12\frac{in}{ft}}{12} * (4\ in)^3 = 192\ in^4$$

$$Z = \frac{t_{wy_1} + t_{wy_2}}{2} + t_{insul} = \frac{4\ in + 4\ in}{2} + 3\ in = 7\ in$$

2. Assume an end slip, which is the slip at the end connector line (see Figure 5-2). Calculate the slip in the other connectors using similar triangles or Eq. (5-5).

   Assuming δ_{max} = 0.01763 in

$$\delta(i) = \delta_{max} * \frac{\left(\frac{L}{2} - x_i\right)}{\left(\frac{L}{2} - x_1\right)} = \begin{bmatrix} 0.01763 \\ 0.01410 \\ 0.01058 \\ 0.00705 \\ 0.00353 \end{bmatrix} in$$

3. Calculate the shear forces in each connector using Figure A-6.

$$F_i = \begin{bmatrix} 1673 \\ 1338 \\ 1004 \\ 669 \\ 335 \end{bmatrix} lb$$

$$F_{sum} = 3\sum F_i = 15053\ lb$$

4. Calculate the cracking moment:

$$M_{wy_2} = 2 * I_{NC2} * \left(\frac{f_r}{t_{conc_2}} - \frac{F_{sum}}{b * t_{wy_2}^2}\right)$$

$$= 384\ in^4 * \left(\frac{0.691\ ksi}{4\ in} - \frac{15.053\ kip}{36\ in * (4\ in)^2}\right) = 4.692\ kip * ft$$

5. Calculate the equivalent load that wythe 2 can carry using equations (5-9).

$$w_{we2} = \frac{8 * M_{wy_2}}{Span^2} = \frac{8 * 4.692\ kip * ft}{(14\ ft)^2} = 0.1917\frac{kip}{ft}$$

$$P_{we2} = \frac{M_{wy_2}}{(x_{P1} + x_{P2})} = \frac{4.692\ kip * ft}{(2.8\ ft + 5.6\ ft)} = 0.559\ kip$$

6. Using the equivalent load from the previous step, calculate axial and rotational displacement at the end connector using Eq

$$\theta_{w_{we2}} = \frac{w_{we2} * Span^3}{24 * E * I_{NC2}} = \frac{0.1915\frac{kip}{ft} * (14\ ft)^3 * 144}{24 * 5824.4\ ksi * 192\ in^4} = 0.00282$$

$$\theta_{P_{we2}} = P_{we2}\left\{\frac{x_{P1}[(Span^2 - x_{P1}^2) + (Span - x_{P1})(2Span - x_{P1})]}{6 * Span * E_c * I_{NC2}}\right.$$

$$\left. + \frac{x_{P2}[(Span^2 - x_{P2}^2) + (Span - x_{P2})(2Span - x_{P2})]}{6 * Span * E_c * I_{NC2}}\right\}$$

$$\theta_{P_{we2}} = 0.559\left\{\frac{2.8[(14^2 - 2.8^2) + (14 - 2.8)(28 - 2.8)]}{6 * 14 * 5824.4 * 192}\right.$$

$$\left. + \frac{5.6[(14^2 - 5.6^2) + (14 - 5.6)(28 - 5.6)]}{6 * 14 * 5824.4 * 192}\right\} = 0.00282$$

$$\Delta_{Rot} = \theta * Z = 0.00282 * 7\ in = 0.01974\ in$$

$$\Delta_{Axial} = 2 * \sum_{i=1}^{n} F(i) * \left(\frac{\frac{L}{2} - x_i}{b * E_c * t_{wy_1}} \right) = 0.002106 \text{ in}$$

7. Using Equation (5-11) and (5-12), calculate the slip at the end connector and compare to assumed value.

$$\delta_{max} = \Delta_{Rot} - \Delta_{Axial} = 0.01974\ in - 0.00211 \text{ in} = 0.01763\ in$$

$$\delta_{max} = Assumed\ \delta_{max} \qquad \therefore \qquad OK$$

8. Calculate the cracking moment using Equation (5-14).

$$M_{cr} = M_{wy_2} * 2 + F_{sum} * Z$$

$$= 2 * 4.692\ kip * ft + 15053\ lb * 7\ in = \mathbf{18.165\ kip * ft}$$

$$\Delta_{w_{we2}} = \frac{5 * w_{we2} * Span^4}{384 * E_c * I_{NC2}} = \frac{5 * 0.1917 \frac{kip}{ft} * (14\ ft)^4 * \left(12 \frac{in}{ft}\right)^3}{384 * 5824.4\ ksi * 192\ in^4}$$

$$= 0.148\ in$$

$$\Delta_{P_{we2}} = \left(\frac{P_{we2}}{24 * E_c * I_{NC2}}\right) \{x_{\mathrm{P1}} * (3 * Span^2 - 4 * x_{\mathrm{P1}}^2) + x_{\mathrm{P2}}$$

$$* (3 * Span^2 - 4 * x_{\mathrm{P2}}^2)\}$$

$$\Delta_{P_{we2}} = \left(\frac{0.559}{24 * 5824.4 * 192}\right) \{2.8 * (3 * 14^2 - 4 * 2.8^2) + 5.6$$

$$* (3 * 14^2 - 4 * 5.6^2)\} * 12^3$$

$$= 0.1493\ in$$

The actual load on the sandwich wall panel included the four-point applied load as well as self-weight.

$$p_{self} = 150\ pcf * (8\ in) = 100\ psf$$

$$w_{self} = p_{self} * b = 100\ psf * 3\ ft = 300\ plf$$

$$M_{self} = \frac{\left(w_{self} * Span^2\right)}{8} = \frac{300\ plf * (14ft)^2}{8} = 7.35\ kip * ft$$

$$M_{FourPt} = M_{cr} - M_{self} = 18.165\ kip*ft - 7.35\ kip*ft = 10.815\ kip*ft$$

$$P_{FourPt} = 4 * \left(\frac{10.815\ kip*ft}{33.6\ in + 67.2\ in}\right) = 5.15\ kip$$

$$p_{FourPt} = \frac{5150\ lbs}{14\ ft * 3\ ft} = 122.62\ psf$$

$$\boldsymbol{p_{TotalApplied} = p_{self} + p_{FourPt} = 100\ psf + 122.62\ psf = 222.62\ psf}$$

Similar effects can be calculated for deflection also, as well as slip. Since self-weight is a distributed load, the uniform distributed load values will be used from Table A-6.

$$\Delta_{self} = \frac{p_{self}}{p_{Total}} * \Delta_e = \frac{100\ psf}{247.13\ psf} * 0.148\ in = 0.06\ in$$

$$\Delta_{FourPt} = \frac{p_{FourPt}}{p_{Total}} * \Delta_e = \frac{122.62\ psf}{205.95\ psf} * 0.1492\ in = 0.0888\ in$$

$$\boldsymbol{\Delta_{Total} = 0.06\ in + 0.0888\ in = 0.1488\ in}$$

$$\delta_{self} = \frac{p_{self}}{p_{Total}} * \delta_{max} = \frac{100\ psf}{247.13\ psf} * 0.01763\ in = 0.00713\ in$$

$$\delta_{FourPt} = \frac{p_{FourPt}}{p_{Total}} * \Delta_{max} = \frac{122.62\ psf}{205.95\ psf} * 0.01763\ in = 0.0105\ in$$

$$\boldsymbol{\delta_{Total} = \delta_{self} + \delta_{FourPt} = 0.00713\ in + 0.0105\ in = 0.01763\ in}$$

Table A-6 Total Load, Equivalent Load Deflection, and Slip

Load Distribution	**Total Load, p_{Total}**	**Deflection from Equivalent Load, Δ_e** *(in)*	**Slip** *(in)*
Uniform Distributed Load	$\frac{M_{applied} * 8}{Span^2 * b} = \frac{18.16 * 8}{14^2 * 3} = 247.1\ psf$	0.1480	0.01763
Four-Point Loads	$\frac{4M_{applied}}{(x_{P1} + x_{P2})b * Span} = \frac{4 * 18.16}{8.4 * 3 * 14} = 205.95\ psf$	0.1492	0.01763

APPENDIX B.

Elastic Hand Method Design Examples

This appendix serves to clarify the Beam-Spring and Elastic Hand Method prediction methodology described in Chapter 5. The example included herein illustrates the design method to predict the deflection and cracking of a given panel. Note that the Elastic Hand Procedure is iterative.

Panel Properties

$L = 37\ ft$ $Span = 35\ ft$

$t_{wy1} = 3\ in$ $t_{wy2} = 3\ in$

$t_{ins} = 3\ in$ $b = 8\ ft$

$f_c' = 6.0\ ksi$ $f_y = 60\ ksi$

$Wind\ Load = W_L = 30\ psf$ Insulation Type: XPS

$K_E = 94.8\ kips/in$

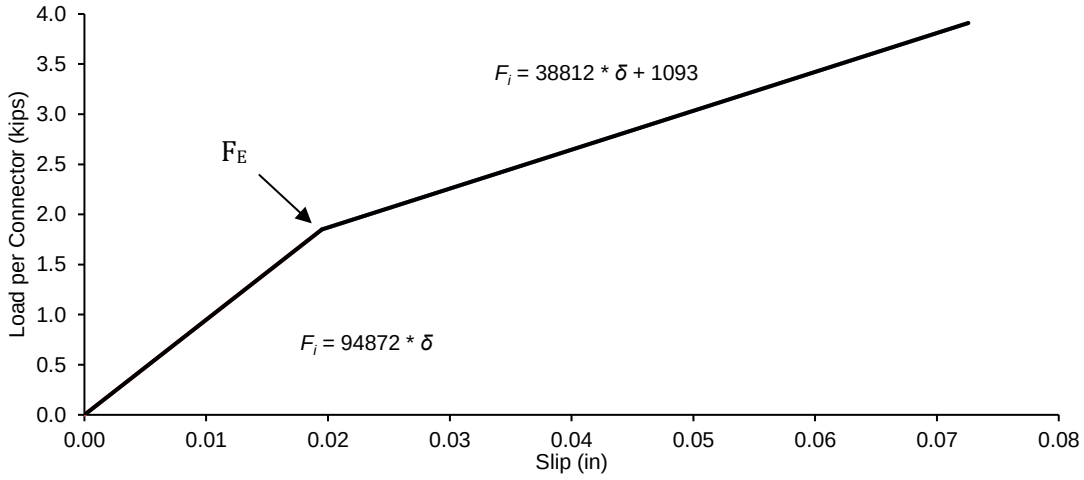

Figure B-1 Load vs slip of HK connector

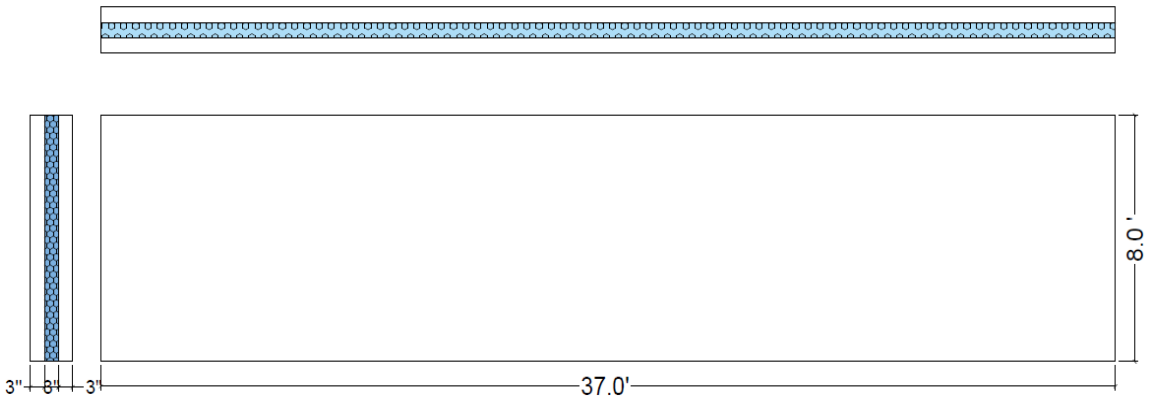

Figure B-2 Design example sandwich panel dimensions

Elastic Hand Method

Solution

1. Calculate the material and section properties of a non-composite sandwich panel.

$$E_c = 4696\ ksi$$

$$f_r = 7.5 * \sqrt{f'c} = 7.5 * \sqrt{6000} = 0.581\ ksi$$

$$I_{NC2} = \frac{b}{12} * \left(t_{wy_2}^3\right) = \frac{8 * 12}{12} * (3^3) = 216\ in^4$$

$$Z = \frac{t_{wy_1} + t_{wy_2}}{2} + t_{insul} = 3\ in + 3\ in = 6\ in$$

$$M_{service} = 1.0 * \frac{W_L * L * Span^2}{8} = \frac{30\ psf * 8\ ft * (35\ ft)^2}{8}$$

$$= 36.75\ kip.ft$$

2. Assume four connectors in a row (***N* = 4**) with 24 in. longitudinal spacing. This spacing means there will be 9 connector rows in half of the span (***n* = 9**).

Now assume the slip at the end connector line and then calculate the shear forces in the connectors. A good initial assumption is to assume the ultimate elastic slip of the connectors.

Assume $\delta_{end} = 0.02\ in$

$$x_i = \begin{bmatrix} 12 \\ 36 \\ 60 \\ 84 \\ 108 \\ 132 \\ 156 \\ 180 \\ 204 \end{bmatrix} in \qquad \therefore \qquad \delta(i) = \delta_{end} * \frac{\left(\frac{L}{2} - x_i\right)}{\left(\frac{L}{2} - x_1\right)} = \begin{bmatrix} 0.02 \\ 0.0177 \\ 0.0154 \\ 0.0131 \\ 0.0109 \\ 0.0086 \\ 0.0063 \\ 0.0040 \\ 0.0017 \end{bmatrix} in$$

Calculate the forces in each connector and connector line using Equations (5-6) and (5-7) or use Figure 5-2 and Figure B-1to find the forces that correspond to connector slip

$$F_i = \delta(i) N_i * K_E = \begin{bmatrix} 0.02 \\ 0.0177 \\ 0.0154 \\ 0.0131 \\ 0.0109 \\ 0.0086 \\ 0.0063 \\ 0.0040 \\ 0.0017 \end{bmatrix} in * 4 * 94.8 \frac{kips}{in} = \begin{bmatrix} 7584 \\ 6717 \\ 5851 \\ 4984 \\ 4117 \\ 3250 \\ 2384 \\ 1517 \\ 650 \end{bmatrix} lb$$

$$F_{sum} = \sum F_i = 37{,}053.3\ lb$$

3. Calculate the cracking moment for a mild reinforced non-composite wythe using Equation (5-8).

$$M_{wy_2} = \frac{M_{service} - F_{sum} * Z}{2} = \frac{36.75\ kip * ft - 37.05\ kip * 6\ in * \frac{1\ ft}{12\ in}}{2}$$

$$= 9.112\ kip * ft$$

4. Calculate the equivalent load using Equations (5-9).

$$w_{we2} = \frac{8 * M_{wy_2}}{Span^2} = \frac{8 * 9.112\ kip * ft}{(35\ ft)^2} = 0.0595 \frac{kip}{ft}$$

5. Using the equivalent load, calculate the axial and rotational displacement assuming the equivalent load distribution by using Equations (5-10) through (5-12).

$$\theta = \frac{w_{we2} * Span^3}{24 * E * I_{NC2}} = \frac{0.0595\ \frac{kip}{ft} * (35\ ft)^3}{24 * 4696\ ksi * 216\ in^2} = 0.0151$$

$$\Delta_{Rot} = \theta * Z = 0.0151 * 6\ in = 0.0905 in$$

$$\Delta_{Axial} = 2 * \sum_{i=1}^{n} F(i) * \left(\frac{\frac{L}{2} - x_i}{b * E * t_{wy_2}} \right)$$

$$= \frac{2}{b * E * t_{wy_2}} * \sum_{i=1}^{n} F(i) * \left(\frac{L}{2} - x_i \right)$$

$$= \frac{2}{8\ ft * 4696\ ksi * 3\ in} * \sum_{i=1}^{n} \begin{bmatrix} 7584 \\ 6717 \\ 5851 \\ 4984 \\ 4117 \\ 3250 \\ 2384 \\ 1517 \\ 650 \end{bmatrix} lb * \left(\frac{444\ in}{2} - \begin{bmatrix} 12 \\ 36 \\ 60 \\ 84 \\ 108 \\ 132 \\ 156 \\ 180 \\ 204 \end{bmatrix} in \right)$$

$$= 0.00809\ in$$

6. Calculate a new δ_{end} using equation (5-13).

$$\delta_{end} = \Delta_{Rot} - \Delta_{Axial} = 0.0906\ in - 0.00809\ in = 0.0825\ in$$

Check to see if $\delta_{end} < \delta_E$

$$\delta_{end} = 0.0825\ in > \delta_E = 0.02\ in$$

This **violates the linear elastic assumption**, therefore more connectors are required. Repeat steps 2 through 6 and iterate until this limit is satisfied.

2. This time assume six connectors in a row (***N* = 6**) with 16 in. longitudinal spacing. This spacing means there will result in 13 connector rows in half of the span (***n* = 13**).

   Again assume a slip at the end connector line and then calculate the shear forces in the connectors.

   Assume $\delta_{end} = 0.01568\ in$

$$x_i = \begin{bmatrix} 16 \\ 32 \\ 48 \\ 64 \\ 80 \\ 96 \\ 112 \\ 128 \\ 144 \\ 160 \\ 176 \\ 192 \\ 208 \end{bmatrix} in \qquad \therefore \qquad \delta(i) = \delta_{end} * \frac{\left(\frac{L}{2} - x_i\right)}{\left(\frac{L}{2} - x_1\right)} = \begin{bmatrix} 0.0157 \\ 0.0145 \\ 0.0132 \\ 0.012 \\ 0.0108 \\ 0.0096 \\ 0.0084 \\ 0.0072 \\ 0.0059 \\ 0.0047 \\ 0.0035 \\ 0.0023 \\ 0.0011 \end{bmatrix} in$$

   Calculate the forces in each connector and connector line using Equations (5-6) and (5-7) or use Figure 5-2 and Figure B-1 to find the forces that correspond to connector slip.

$$F_i = (i)N_i * K_E = \begin{bmatrix} 0.0157 \\ 0.0145 \\ 0.0132 \\ 0.012 \\ 0.0108 \\ 0.0096 \\ 0.0084 \\ 0.0072 \\ 0.0059 \\ 0.0047 \\ 0.0035 \\ 0.0023 \\ 0.0011 \end{bmatrix} in * 6 * 94.8\ kips/in = \begin{bmatrix} 8922 \\ 8229 \\ 7536 \\ 6843 \\ 6150 \\ 5457 \\ 4764 \\ 4071 \\ 3378 \\ 2685 \\ 1992 \\ 1299 \\ 606 \end{bmatrix} lb$$

$$F_{sum} = \sum F_i = 61{,}932\ lb$$

3. Calculate the cracking moment for a mild reinforced non-composite wythe using Equation (5-8).

$$M_{wy_2} = \frac{M_{service} - F_{sum} * Z}{2} = \frac{36.75\ kip.ft - 61.932\ kip * 6\ in * \frac{1\ ft}{12\ in}}{2}$$

$$= 2.892\ kip * ft$$

4. Calculate the equivalent load using Equations (5-9).

$$w_{we2} = \frac{8 * M_{wy_2}}{Span^2} = \frac{8 * 2.892\ kip * ft}{(35\ ft)^2} = 0.01889 \frac{kip}{ft}$$

5. Using the equivalent load, calculate axial and rotational displacement assuming equivalent load distribution using equations by using Equations (5-10) through (5-12).

$$\theta = \frac{w_{we2} * Span^3}{24 * E * I_{NC2}} = \frac{0.01889 \frac{kip}{ft} * (35\ ft)^3}{24 * 4696\ ksi * 216\ in^2} = 0.00479$$

$$\Delta_{Rot} = \theta * Z = 0.00479 * 6\ in = 0.02874\ in$$

$$\Delta_{Axial} = 2 * \sum_{i=1}^{n} F(i) * \left(\frac{\frac{L}{2} - x_i}{b * E * t_{wy_2}} \right)$$

$$= \frac{2}{b * E * t_{wy_2}} * \sum_{i=1}^{n} F(i) * \left(\frac{L}{2} - x_i \right)$$

$$= \frac{2}{8\ ft * 4696\ ksi * 3\ in} * \sum_{i=1}^{13} \begin{bmatrix} 8922 \\ 8229 \\ 7536 \\ 6843 \\ 6150 \\ 5457 \\ 4764 \\ 4071 \\ 3378 \\ 2685 \\ 1992 \\ 1299 \\ 606 \end{bmatrix} lb * \left(\frac{444\ in}{2} - \begin{bmatrix} 16 \\ 32 \\ 48 \\ 64 \\ 80 \\ 96 \\ 112 \\ 128 \\ 144 \\ 160 \\ 176 \\ 192 \\ 208 \end{bmatrix} in \right)$$

$$= 0.0130 \text{ in}$$

6. Calculate a new δ_{end} using equation (5-13).

$$\delta_{end} = \Delta_{Rot} - \Delta_{Axial} = 0.0287 - 0.013 = 0.0157\ in$$

$$\delta_{end} = 0.01568 = Assumed\ \delta_{end}$$

Check to see if $\delta_{end} < \delta_E$

$$\delta_{end} = 0.0157\ in < \delta_E = 0.02\ in \quad \therefore \quad OK$$

7. Check tension stress to verify it is less than modulus of rupture of the concrete with Equation (5-19).

$$f = \frac{M_{wy_2} * t_{wy_2}}{2 * I_{NC2}} + \frac{F_{sum}}{b * t_{wy_2}} = \frac{2.892\ kip * ft * 3\ in}{2 * 216\ in^4} + \frac{61.932\ kip}{8ft * 3\ in}$$

$$= 0.456\ ksi$$

$$f < fr \quad \therefore \quad OK$$

Therefore, use six connectors per row with 16 in. longitudinal spacing.

8. Calculate deflection at midspan using Equation (5-20) for a uniform distributed load.

$$\Delta = \frac{5 * w_{we2} * Span^4}{384 * E_c * I_{NC2}} = \frac{5 * 0.01889 \frac{kip}{ft} * (35ft)^4 * (12\ in/ft)^3}{384 * 4696\ ksi * 216\ in^4}$$

$$= 0.628\ in$$

Beam-Spring Model

Creating the beam spring model requires a two-dimensional finite element software and only requires assignment of gross individual wythe properties and connector shear stiffness. Assuming the connector spacing is equal to 16 inches in both directions, each spring will have a shear stiffness of $N * K_E$. Figure B-3shows the Beam-Spring model for this example.

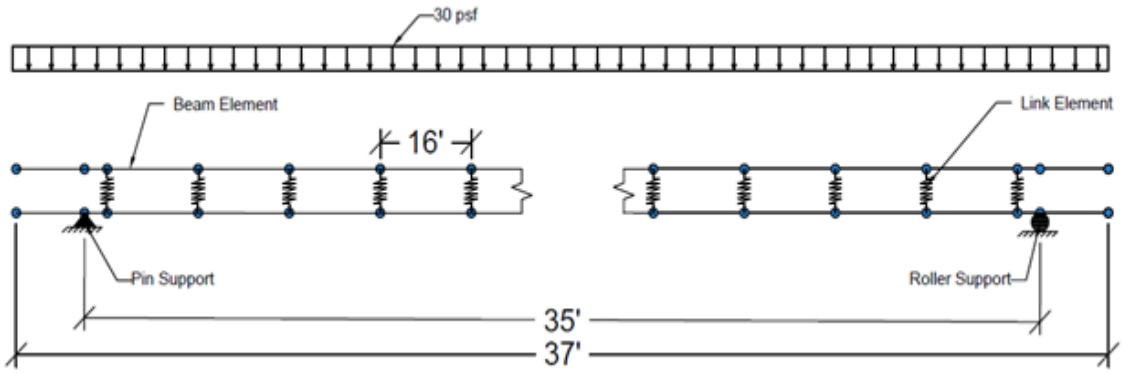

Figure B-3 Beam-Spring Model of design example

Table B-1 Results from the Beam-Spring Model for wythe 2

Moment (kip-ft)	2.72 kip-ft
Tension force (kip)	61.7 kips
Slip (in)	0.014 in
Deflection at mid span (in)	0.58 in

$$f = \frac{P}{A} + \frac{M * c}{I}$$

$$f = \frac{61.7\ kip}{288\ in^2} + \frac{2.67\ kip * ft * \frac{12\ in}{ft} * 1.5\ in}{216} = 441\ psi\ < f_r\ \therefore OK$$

APPENDIX C.

Partially-Composite Strength Prediction Method Design Examples

This Appendix presents the analysis for predicting the ultimate moment using the partially composite moment prediction method presented above for the HK, Nu-Tie, and Thermomass panels tested in this report.

A-2 Panel Analysis Example (Nu-Tie connectors, Prestressed Reinforcement)

Strain Compatibility

Section and Material Properties

$f_{ps} = 270\ ksi$ $\quad A_{ps} = 0.255\ in^2$

$f_c' = 10.43\ ksi$ $\quad b = 48\ in$

$t_{wy1} = 3\ in$ $\quad t_{wy2} = 3\ in$

$t_{ins} = 4\ in$ $\quad L = 192\ in$

$x_{conX} = \begin{bmatrix} 24 \\ 72 \end{bmatrix} in$ $\quad N = 2$

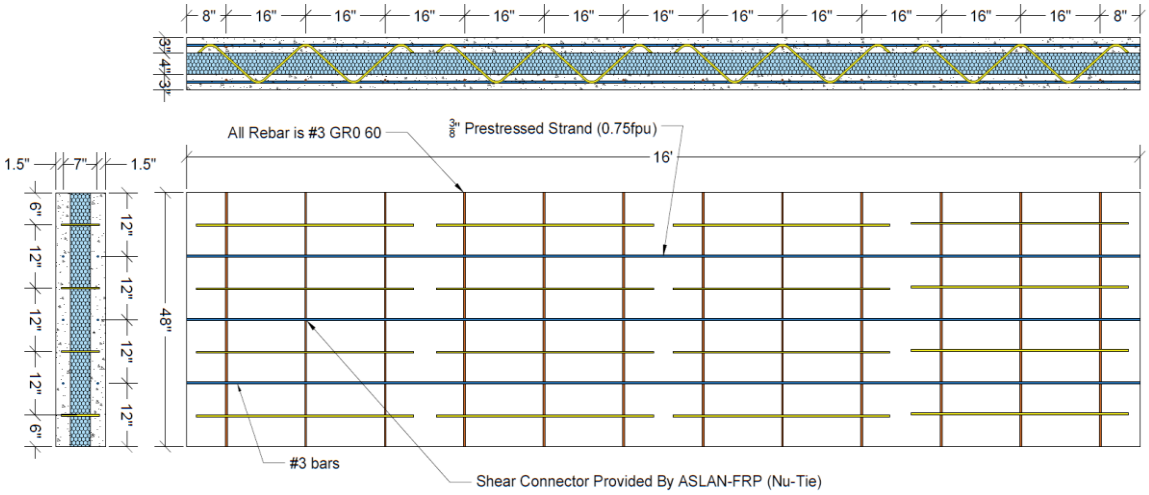

Solution

1. Find the forces in each connector using the load-slip relation. Using an influence line, the ultimate slip (δ_{Ult}) that occurs at the maximum force is determined to be 0.267 in.

$$\delta(i) = \frac{\delta_{Ult}}{\frac{L}{2} - x_1} * \left(\frac{L}{2} - x_i\right)$$

$$\delta(i) = \frac{0.267\ in}{\frac{192}{2} in - 24\ in} * \begin{bmatrix} \frac{192}{2} - 24 \\ \frac{192}{2} - 72 \end{bmatrix} \text{in} = \begin{bmatrix} 0.267 \\ 0.089 \end{bmatrix} in$$

Find F_i at each connector by using Figure C-1.

$$F(i) = \begin{bmatrix} 11.25 \\ 9.26 \end{bmatrix} \text{kips}$$

The full load-slip diagram for the connector is used to obtain the most accurate prediction

2. Find the total sum of the connector forces using Equation (6-12):

$$F_{sum} = N * \sum F_i = 41.0\ kips$$

$$F_{sum} \leq A_{ps} * f_{pu} = 0.255\ in^2 * 270\ ksi = 68.9\ kips \quad \therefore \quad OK$$

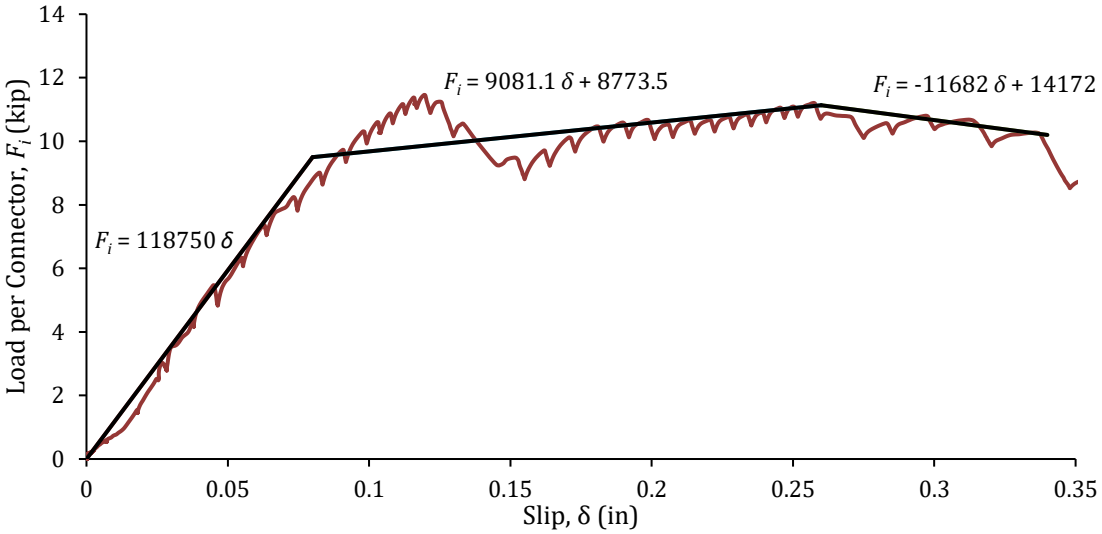

Figure C-1 Load-slip curve for Nu-Tie Panels

3. Find C_1 and T_1 for the first wythe

   a. Assume $\varepsilon_c = 0.003$.

   b. Assume a value of c_1. We will assume $c_1 = 0.287$ in

   c. Calculate curvature using Equation (6-13):

$$\varphi = \frac{0.003}{0.287} = 0.01045$$

   d. Calculate the compressive force in the top wythe using Equation (6-15). This will incorporate Hognestad's Equation (6-14).

$$C_1 = b * f_c' * \frac{\varphi_1 * c_1^2}{\varepsilon_0} * \left(1 - \frac{\varphi_1 * c_1}{3\varepsilon_0}\right)$$

$$C_1 = 48\ in * 10.43\ ksi * \frac{0.01045 * 0.287^2}{0.002} * \left(1 - \frac{0.01045 * 0.287}{0.006}\right)$$

$$= 107.83\ kips$$

e. Calculate the strain and stress in the steel using Equations (6-17) and (6-19).

$$\varepsilon_1 = \frac{f_{pe}}{E_{ps}} = \frac{170}{28500} = 0.00596 \qquad \varepsilon_2 \approx 0$$

$$\varepsilon_{ps} = 0.003 * \frac{1.5 - 0.287}{0.287} + 0.00596 + 0 = 0.01864$$

$$f_{ps} = \varepsilon_{ps} * \left\{ 887 + \frac{27600}{\left[1 + \left(112.4 * \varepsilon_{ps}\right)^{7.36}\right]^{7.36^{-1}}} \right\} = 261.98\ ksi$$

f. Calculate the tension force in wythe 1 with Equation (6-20)

$$T_1 = 261.98\ ksi * 0.255\ in^2 = 66.8\ kips$$

g. Enforce force equilibrium for wythe 1 with Equation (6-21):

$$C_1 - T_1 = 107.83\ kips - 66.8\ kips = 41.0\ kips = F_{sum} \quad \therefore \quad OK$$

4. Find C_2 and T_2 for the second wythe

a. Assume both wythes will deflect equally, therefore assume $\varphi_2 = \varphi_1 = 0.01045$

b. Assume a value of c_2. We will assume $c_2 = 0.11154$ in (neutral axis in the bottom wythe)

c. Calculate the compressive force in the bottom wythe, C_2, using Equation (6-22). The compressive force in the concrete will again utilize Hognestad's equation to estimate the concrete compressive strength, but it is critical here because Whitney's stress block is only valid when the top fiber is at 0.003 strain and in the case of partial composite action, this will not be true.

$$C_2 = b * f_c' * \frac{\varphi_2 * c_2^2}{\varepsilon_0} * \left(1 - \frac{\varphi_2 * c_2}{3\varepsilon_0}\right)$$

$$C_2 = 48\ in * 10.43\ ksi * \frac{0.01045 * 0.11154^2}{0.002}$$

$$* \left(1 - \frac{0.01045 * 0.11154}{0.006}\right) = 26.2\ kips$$

d. Calculate the strain and stress in the steel.

$$\varepsilon_{ps} = (d - c_2) * \varphi_2 + \varepsilon_1$$

$$\varepsilon_{ps} = \big(1.5 - (0.11154)\big) * 0.01045 + 0.00596 = 0.02052$$

$$f_{ps} = \varepsilon_{ps} * \left\{887 + \frac{27600}{\left[1 + \left(112.4 * \varepsilon_{ps}\right)^{7.36}\right]^{7.36^{-1}}}\right\} = 263.68\ ksi$$

e. Calculate the tension force in wythe 2 using Equation (6-24):

$$T_2 = 263.68\ ksi * 0.255\ in^2 = 67.2\ kips$$

f. Enforce force equilibrium for wythe 2 with Equation (6-25):

$$T_2 - C_2 = 67.2\ kips - 26.2\ kips = 41.0\ kips = F_{sum} \quad \therefore \quad OK$$

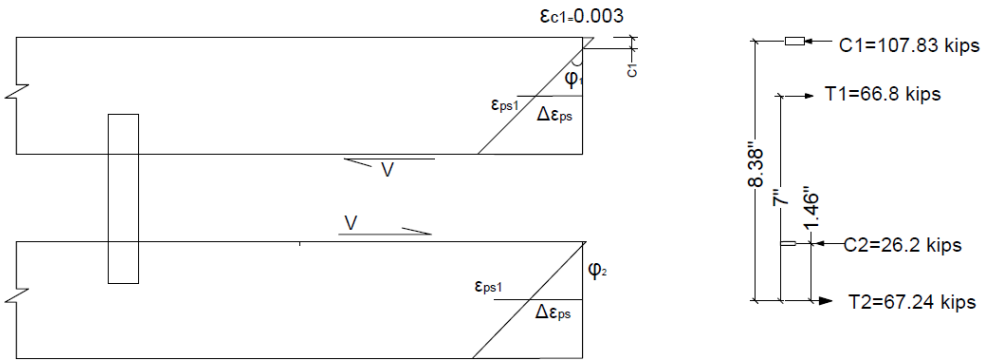

Figure C-2 Nu-Tie 343-2 Panel Design Example

5. Calculate the ultimate moment of the concrete sandwich wall panel using Equation (6-26). In addition, Using Equation (6-16) to calculate the centroid of C_1 and C_2.

$$x_{c1} = c_1 - \frac{c_1 * (8 * \varepsilon_o - 3 * \varphi_1 * c_1)}{12 * \varepsilon_o - 4 * \varphi_1 * c_1}$$

$$= 0.287 - \frac{0.287 * (8 * 0.002 - 3 * 0.01045 * 0.287)}{12 * 0.002 - 4 * 0.01045 * 0.287} = 0.12\ in$$

$$M_1 = C_1 * (d_1 - X_{c1}) = 107.83 * (1.5 - 0.12) = 148.8\ kip.in$$

$$x_{c2} = c_2 - \frac{c_2 * (8 * \varepsilon_o - 3 * \varphi_2 * c_2)}{12 * \varepsilon_o - 4 * \varphi_2 * c_2}$$

$$= 0.1115 - \frac{0.1115 * (8 * 0.002 - 3 * 0.01045 * 0.1115)}{12 * 0.002 - 4 * 0.1115 * 0.01045}$$

$$= 0.0348\ in$$

$$M_2 = C_2 * (d_2 - x_{c2}) = 26.2 * (1.5 - 0.0348) = 38.4\ kip.in$$

$$M = M_1 + M_2 + F_{sum} * \left(\frac{t_{wy1} + t_{wy2}}{2} + t_{ins}\right)$$

$$= 148.8 + 38.4 + 41 * \left(\frac{3+3}{2} + 4\right) = 474.2\ kip * in$$

$$= \mathbf{39.5\ kip * ft}$$

A-4 Panel Analysis Example (Nu-Tie connectors, Prestressed Reinforcement)

Strain Compatibility

Section and Material Properties

$f_{ps} = 270\ ksi$ $\quad A_{ps} = 0.255\ in^2$

$f_c' = 10.43\ ksi$ $\quad b = 48\ in$

$t_{wy1} = 3\ in$ $\quad t_{wy2} = 3\ in$

$t_{ins} = 4\ in$ $\quad L = 192\ in$

$x_i = \begin{bmatrix} 24 \\ 72 \end{bmatrix} in$ $\quad N = 4$

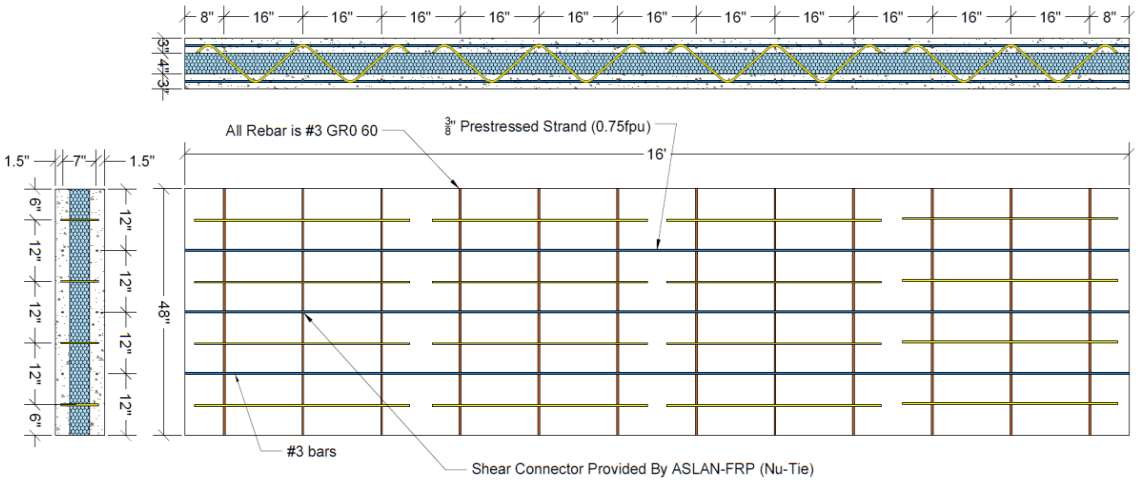

Solution

1. Find the forces in each connector using the load-slip relation. Using an influence line, the ultimate slip (δ_{Ult}) that occurs at the maximum force is 0.267 in., but because of the limit $F_{sum} \leq A_{ps} * f_{pu}$, the ultimate slip will actually occur at a force of F_{sum}, which is δ_{Ult} = 0.187 in. Calculate slip using Equation (6-11):

$$\delta(i) = \frac{\delta_{Ult}}{\frac{L}{2} - x_1} * \left(\frac{L}{2} - x_i\right)$$

$$\delta(i) = \frac{0.187\ in}{\frac{192}{2} in - 24\ in} * \begin{bmatrix} \frac{192}{2} - 24 \\ \frac{192}{2} - 72 \end{bmatrix} \text{in} = \begin{bmatrix} 0.187 \\ 0.0623 \end{bmatrix} in$$

Find F_i at each connector by using Figure C-3.

$$F(i) = \begin{bmatrix} 9.928 \\ 7.3 \end{bmatrix} \text{kips}$$

The full load-slip curve for the connector is used to obtain the most accurate prediction. In a design, the bilinear curve recommended above should be used.

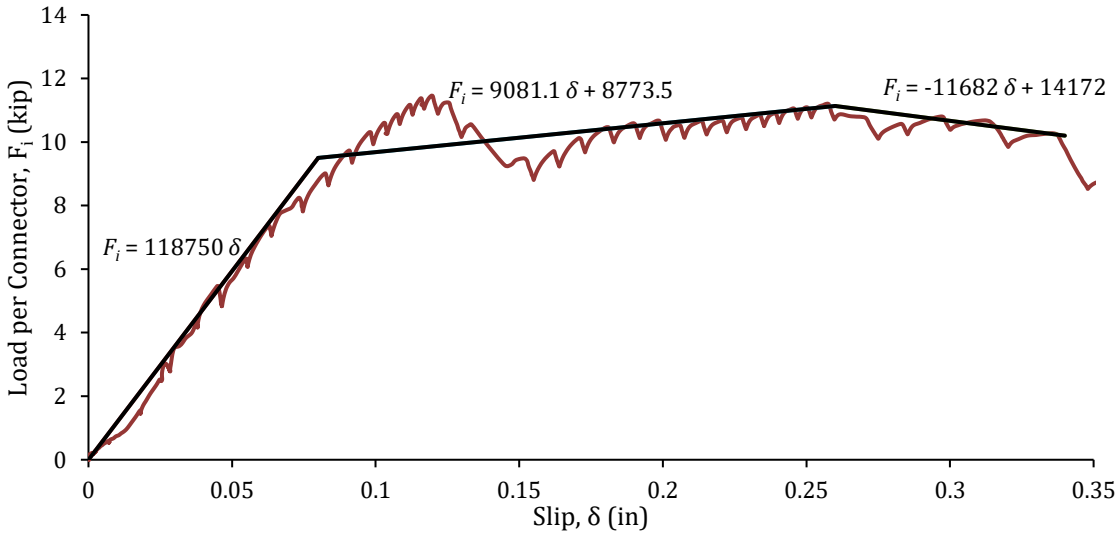

Figure C-3 Load-slip curve for Nu-Tie Panels

2. Find the total sum of the connector forces using Equation (6-12):

$$F_{sum} = N * \sum F_i = 68.9\ kips$$

$$F_{sum} \leq A_{ps} * f_{pu} = 0.255\ in^2 * 270\ ksi = 68.9\ kips \quad \therefore \quad OK$$

3. Find C_1 and T_1 for the first wythe

    a. Assume $\varepsilon_c = 0.003$.

    b. Assume a value of c_1. We will assume $c_1 = 0.359$ in.

    c. Calculate curvature using Equation (6-13):

$$\varphi = \frac{0.003}{0.359} = 0.00835$$

    d. Calculate the compressive force in the top wythe using Equation (6-15). This will incorporate Hognestad's Equation (6-14).

$$C_1 = b * f_c' * \frac{\varphi_1 * c_1^2}{\varepsilon_0} * \left(1 - \frac{\varphi_1 * c_1}{3\varepsilon_0}\right)$$

$$C_1 = 48\ in * 10.43\ ksi * \frac{0.00835 * 0.359^2}{0.002} * \left(1 - \frac{0.00835 * 0.359}{0.006}\right)$$

$$= 134.9\ kips$$

    e. Calculate the strain and stress in the steel using Equations (6-17) and (6-19).

$$\varepsilon_1 = \frac{f_{pe}}{E_{ps}} = \frac{170}{28500} = 0.00596 \qquad \varepsilon_2 \approx 0$$

$$\varepsilon_{ps} = 0.003 * \frac{1.5 - 0.359}{0.359} + 0.00596 + 0 = 0.01554$$

$$f_{ps} = \varepsilon_{ps} * (887 + \frac{27600}{\left(1 + \left(112.4 * \varepsilon_{ps}\right)^{7.36}\right)^{7.36^{-1}}}) = 258.8\ ksi$$

    f. Calculate the tension force in wythe 1 with Equation (6-20)

$$T_1 = 258.8\ ksi * 0.255\ in^2 = 66.0\ kips$$

    g. Enforce force equilibrium for wythe 1 with Equation (6-21):

$$C_1 - T_1 = 134.9\ kips - 66.0\ kips = 68.9\ kips = F_{sum} \quad \therefore \quad OK$$

4. Find C_2 and T_2 for the second wythe

    a. Assume both wythes will deflect equally, therefore assume $\varphi_2 = \varphi_1 = 0.00835$

    b. Assume a value of c_2. We will assume $c_2 = -1.11$ in (neutral axis in the foam)

    c. Calculate the compressive force in the bottom wythe, C_2, using Equation (6-22). The compressive force in the concrete will again utilize Hognestad's equation to estimate the concrete compressive strength, but it is critical here because Whitney's stress block is only valid when the top fiber is at 0.003 strain and in the case of partial composite action, this will not be true.

$$C_2 = b * f_c' * \frac{\varphi_2 * c_2^2}{\varepsilon_0} * \left(1 - \frac{\varphi_2 * c_2}{3\varepsilon_0}\right)$$

$$C_2 = 0\ kips$$

    d. Calculate the strain and stress in the steel.

$$\varepsilon_{ps} = (d - c_2) * \varphi_2 + \varepsilon_1$$

$$\varepsilon_{ps} = \big(1.5 - (-1.112)\big) * 0.00835 + 0.00596 = 0.02783$$

$$f_{ps} = \varepsilon_{ps} * (887 + \frac{27600}{\left(1 + \left(112.4 * \varepsilon_{ps}\right)^{7.36}\right)^{7.36^{-1}}}) = 270\ ksi$$

    e. Calculate the tension force in wythe 2 using Equation (6-24):

$$T_2 = 270\ ksi * 0.255\ in^2 = 68.9\ kips$$

    f. Enforce force equilibrium for wythe 2 with Equation (6-25):

$$T_2 - C_2 = 68.9\ kips - 0\ kips = 68.9\ kips = F_{sum} \quad \therefore \quad OK$$

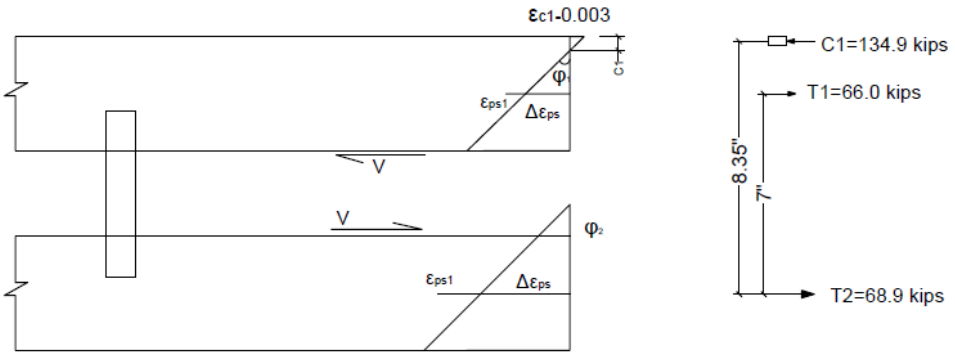

Figure C-4 Nu-Tie 343-2 Panel Design Example

5. Calculate the ultimate moment of the concrete sandwich wall panel using Equation (6-26). In addition, Using Equation (6-16) to calculate the centroid of C_1 and C_2.

$$x_{c1} = c_1 - \frac{c_1 * (8 * \varepsilon_o - 3 * \varphi_1 * c_1)}{12 * \varepsilon_o - 4 * \varphi_1 * c_1}$$

$$= 0.359 - \frac{0.359 * (8 * 0.002 - 3 * 0.00835 * 0.359)}{12 * 0.002 - 4 * 0.00835 * 0.359} = 0.15\ in$$

$$M_1 = C_1 * (d_1 - x_{c1}) = 134.9 * (1.5 - 0.15) = 182.1\ kip * in$$

$$M_2 = C_2 * (d_2 - x_{c2}) = 0$$

$$M = M_1 + M_2 + F_{sum} * \left(\frac{t_{wy1} + t_{wy2}}{2} + t_{ins}\right)$$

$$= 182.1 + 0 + 68.9 * \left(\frac{3+3}{2} + 4\right) = 664.4\ kip * in$$

$$= \mathbf{55.4\ kip * ft}$$

B Panel Analysis Example (Thermomass CC connectors only, Mild Reinforcement)

Section and Material Properties

$f_c' = 9.23\ ksi$ $A_s = 0.44\ in^2$

$b = 36\ in$ $t_{wy1} = 4\ in$

$t_{wy2} = 4\ in$ $t_{ins} = 3\ in$

$L = 192\ in$

$x_i = \begin{bmatrix} 30 \\ 82 \end{bmatrix} in$ $N = 3$

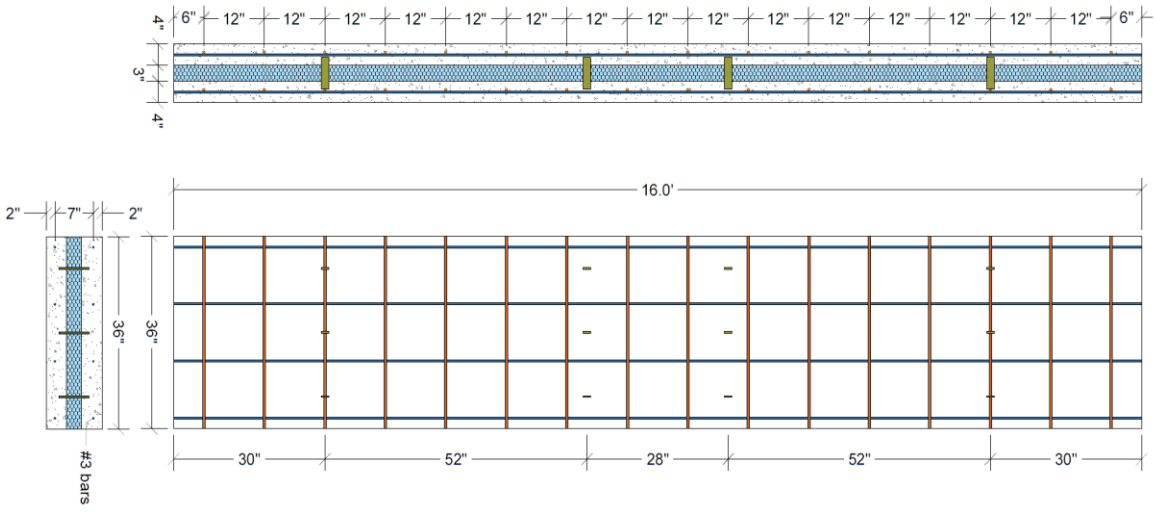

Solution

1. Find the forces in each connector using the load-slip relationship. Using an influence line, the ultimate slip (δ_{Ult}) that occurs at the maximum force is determined to be 0.18 in. In addition, the sum of the forces should be less than or equal to A_s * f_s in the bottom wythe. Calculate slip using Equation (6-11):

$$\delta(i) = \frac{\delta_{Ult}}{\frac{L}{2} - x_1} * \left(\frac{L}{2} - x_i\right)$$

$$\delta(i) = \frac{0.833\ in}{\frac{192}{2} in - 30\ in} * \begin{bmatrix} \frac{192}{2} - 30 \\ \frac{192}{2} - 82 \end{bmatrix} \text{in} = \begin{bmatrix} 0.833 \\ 0.1767 \end{bmatrix} in$$

Find F_i at each connector by using Figure C-5.

$$F(i) = \begin{bmatrix} 4.99 \\ 2.56 \end{bmatrix} \text{kips}$$

Note that the full connector load-slip diagram is used to obtain the most accurate answer.

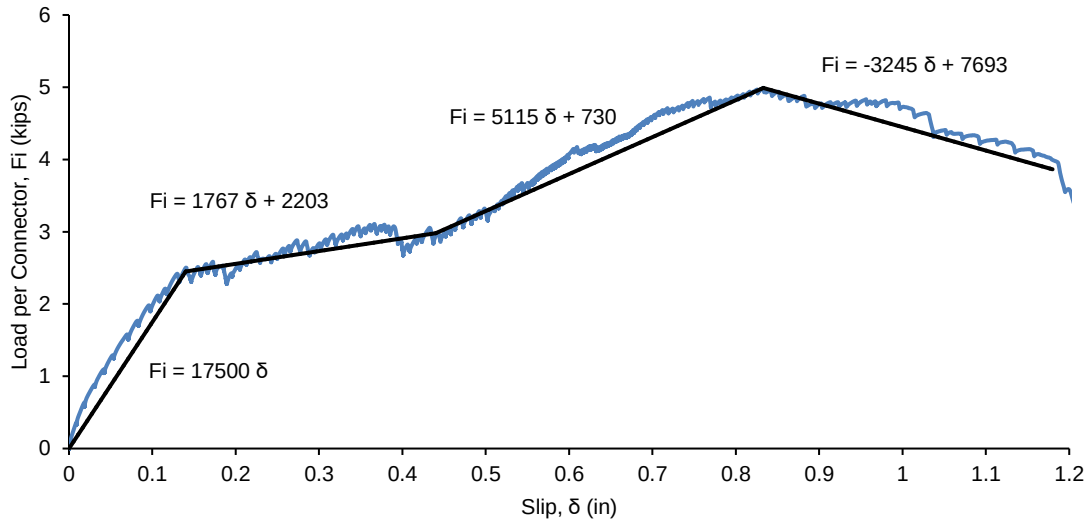

Figure C-5 Load-slip curve for Thermomass B

2. Find the total sum of the connector forces using Equation (6-12):

$$F_{sum} = N * \sum F_i = 22.65\ kips$$

$$F_{sum} \leq A_s * f_u = 0.44\ in^2 * 110\ ksi = 48.4\ kips \quad \therefore \quad OK$$

3. Find C_1 and T_1 for the first wythe

   a. Assume ε_c = 0.003.

   b. Assume a value of c_1. We will assume c_1 = 0.242 in

c. Calculate curvature using Equation (6-13):

$$\varphi = \frac{0.003}{0.242} = 0.01238$$

d. Calculate the compressive force in the top wythe using Equation (6-15). This will incorporate Hognestad's Equation (6-14).

$$C_1 = b * f_c' * \frac{\varphi_1 * c_1^2}{\varepsilon_0} * \left(1 - \frac{\varphi_1 * c_1}{3\varepsilon_0}\right)$$

$$C_1 = 36\ in * 9.23\ ksi * \frac{0.01238 * 0.242^2}{0.002} * \left(1 - \frac{0.01238 * 0.242}{0.006}\right)$$

$$= 60.38\ kips$$

e. Calculate the strain and stress in the steel using Equations (6-17) and the experimental stress-strain curve for the actual steel in the panel (see Chapter 5).

$$\varepsilon_s = 0.003 * \frac{2.0 - 0.242}{0.242} = 0.02176$$

$$f_s = 85.75\ ksi$$

f. Calculate the tension force in wythe 1 with Equation (6-20)

$$T_1 = 85.75\ ksi * 0.44\ in^2 = 37.73\ kips$$

g. Enforce force equilibrium for wythe 1 with Equation (6-21):

$$C_1 - T_1 = 60.38\ kips - 37.73\ kips = 22.65\ kips = F_{sum} \quad \therefore \quad OK$$

4. Find C_2 and T_2 for the second wythe

a. Assume both wythes will deflect equally, therefore assume $\varphi_2 = \varphi_1 = 0.01238$

b. Assume a value of c_2. We will assume $c_2 = 0.0982$ in (neutral axis in the bottom wythe)

c. Calculate the compressive force in the bottom wythe, C_2, using Equation (6-22). The compressive force in the concrete will again utilize Hognestad's equation to estimate the concrete compressive strength, but it is critical here because Whitney's stress block is only valid when the top fiber is at 0.003 strain and in the case of partial composite action, this will not be true.

$$C_2 = b * f_c' * \frac{\varphi_2 * c_2^2}{\varepsilon_0} * \left(1 - \frac{\varphi_2 * c_2}{3\varepsilon_0}\right)$$

$$C_2 = 36\ in * 9.23\ ksi * \frac{0.01238 * 0.0982^2}{0.002} * \left(1 - \frac{0.01238 * 0.0982}{0.006}\right)$$

$$= 15.8\ kips$$

d. Calculate the strain and stress in the steel using experimental curve (Chapter 5).

$$\varepsilon_s = (d - c_2) * \varphi_2$$

$$\varepsilon_s = (2.0 - 0.0982) * 0.01238 = 0.02358$$

$$f_s = 87.42\ ksi$$

e. Calculate the tension force in wythe 2 using Equation (6-24):

$$T_2 = 87.42\ ksi * 0.44\ in^2 = 38.46\ kips$$

f. Enforce force equilibrium for wythe 2 with Equation (6-25):

$$T_2 - C_2 = 38.46\ kips - 15.8\ kips = 22.66\ kips = F_{sum} \quad \therefore \quad OK$$

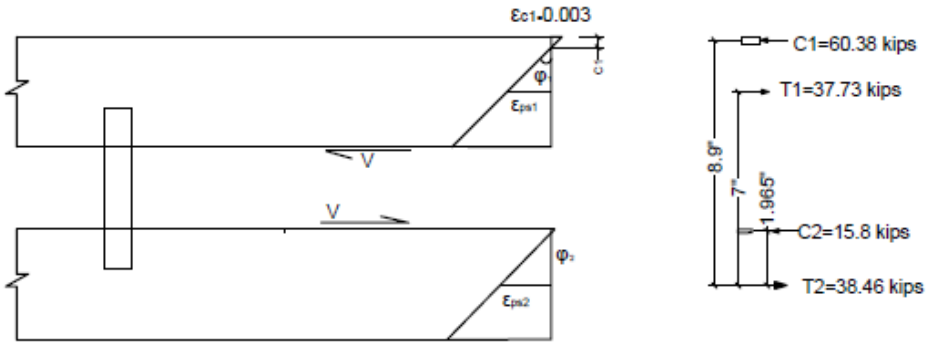

Figure C-6 Thermomass B Panel Design Example

5. Calculate the ultimate moment of the concrete sandwich wall panel using Equation (6-26). In addition, Using Equation (6-16) to calculate the centroid of C_1 and C_2.

$$x_{c1} = c_1 - \frac{c_1 * (8 * \varepsilon_o - 3 * \varphi_1 * c_1)}{12 * \varepsilon_o - 4 * \varphi_1 * c_1}$$

$$= 0.242 - \frac{0.242 * (8 * 0.002 - 3 * 0.01238 * 0.242)}{12 * 0.002 - 4 * 0.01238 * 0.242} = 0.10\ in$$

$$M_1 = C_1 * (d_1 - x_{c1}) = 60.38\ kips * (2.0\ in - 0.1\ in) = 114.7\ kip * in$$

$$x_{c2} = c_2 - \frac{c_2 * (8 * \varepsilon_o - 3 * \varphi_2 * c_2)}{12 * \varepsilon_o - 4 * \varphi_2 * c_2}$$

$$= 0.0982 \text{ in} - \frac{0.0982 * (8 * 0.002 - 3 * 0.01238 * 0.0982)}{12 * 0.002 - 4 * 0.0982 * 0.01238}$$

$$= 0.0348\ in$$

$$M_2 = C_2 * (d_2 - x_{c2}) = 15.8\ kips * (2.0\ in - 0.0348\ in) = 31.05\ kip * in$$

$$M = M_1 + M_2 + F_{sum} * \left(\frac{t_{wy1} + t_{wy2}}{2} + t_{ins}\right)$$

$$= 114.7 + 31.05 + 22.66 * \left(\frac{4+4}{2} + 3\right) = 304.4\ kip * in = \mathbf{25.36\ kip * ft}$$

BC Panel Analysis Example (both Thermomass CC and X connectors, Mild Reinforcement)

Section and Material Properties

$f_c' = 9.23\ ksi$ $A_s = 0.44\ in^2$

$b = 36\ in$ $t_{wy1} = 4\ in$

$t_{wy2} = 4\ in$ $t_{ins} = 3\ in$

$L = 192\ in$

$x_{CCi} = \begin{bmatrix} 16 \\ 32 \\ 48 \\ 64 \\ 80 \end{bmatrix} in$ $N_{CC} = 3$

$x_{Xi} = [24] in$ $N_X = 2$

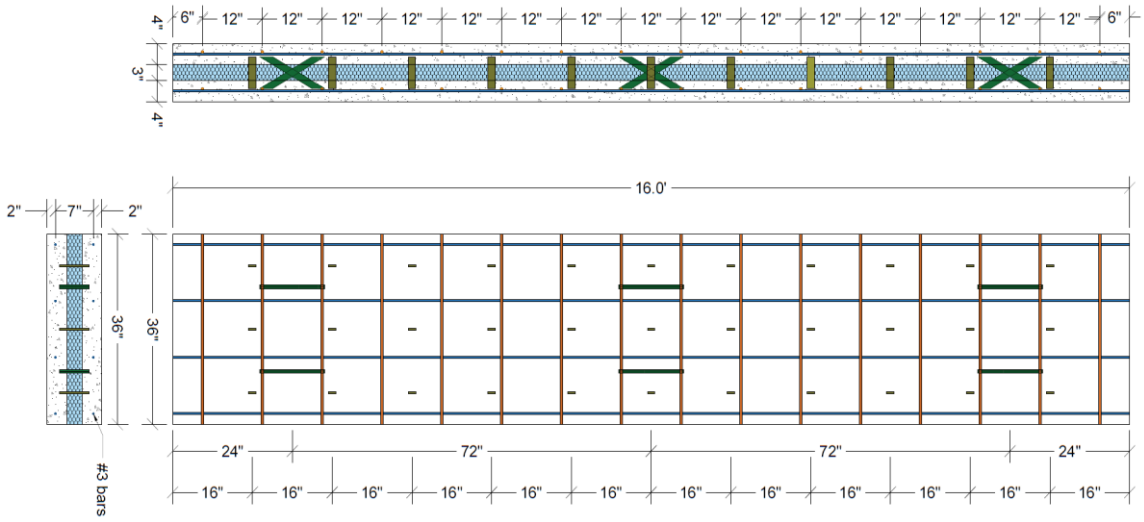

Solution

1. Find the forces in each connector using the load-slip relationship. Using an influence line, the ultimate slip (δ_{Ult}) that occurs at the maximum force is determined to be 0.18 in. Calculate slip using Equation (6-11):

$$\delta(i) = \frac{\delta_{Ult}}{\frac{L}{2} - x_1} * \left(\frac{L}{2} - x_i\right)$$

$$\delta(i) = \frac{0.18\ in}{\frac{192}{2} in - 16\ in} * \begin{bmatrix} \frac{192}{2} - 16 \\ \frac{192}{2} - 24 \\ \frac{192}{2} - 32 \\ \frac{192}{2} - 48 \\ \frac{192}{2} - 64 \\ \frac{192}{2} - 80 \end{bmatrix} \text{in} = \begin{bmatrix} 0.18 \\ 0.162 \\ 0.144 \\ 0.108 \\ 0.072 \\ 0.036 \end{bmatrix} in$$

Find F_i at each connector by using Figure C-7. The entire curve is used to obtain the most accurate prediction. Because there are different N values for each connector (N_{CC} = 3 and N_X = 2), we incorporate that into this step.

$$F(i) = \begin{bmatrix} 3 * 2.567 \\ 2 * 12.17 \\ 3 * 2.5 \\ 3 * 1.93 \\ 3 * 1.28 \\ 3 * 0.643 \end{bmatrix} \text{kips}$$

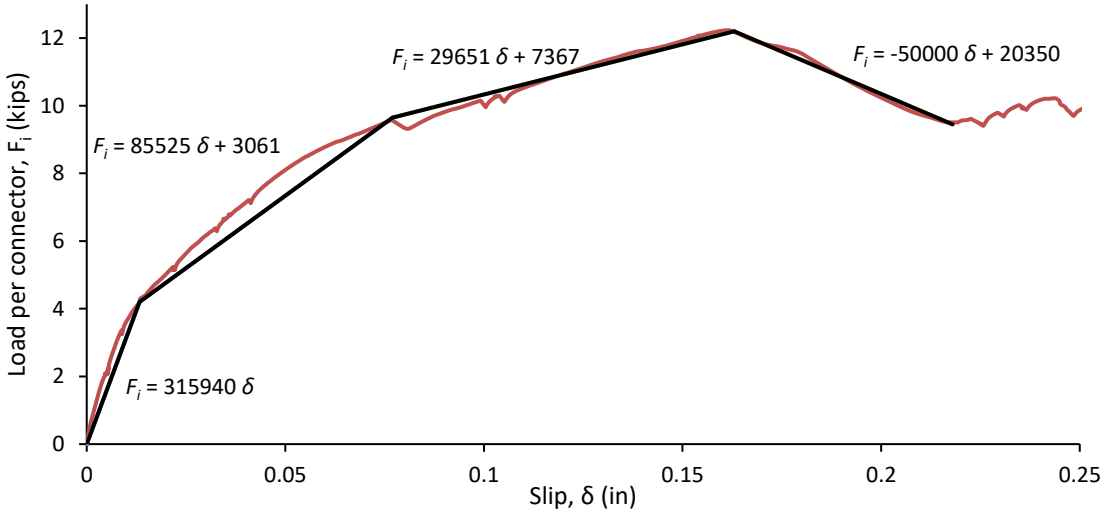

Figure C-7 Load-slip curve for Thermomass A

2. Find the total sum of the connector forces using Equation (6-12). Note that we already accounted for *N* values in the previous step in this example only because there were two different values for N_{CC} and N_X.

$$F_{sum} = \sum F_i = 51.13\ kips$$

$F_{sum} \geq A_s * f_u = 0.44\ in^2 * 110\ ksi = 48.4\ kips \quad \therefore \quad$ Use $F_{sum} = 48.4\ kips$

Ultimate Slip corresponding to $F_{sum} = 48.4\ kips$ is $\delta_{Ult} = 0.162\ in$

3. Find C_1 and T_1 for the first wythe
    a. Assume $\varepsilon_c = 0.003$.
    b. Assume a value of c_2. We will assume $c_1 = 0.33307$ in.
    c. Calculate curvature using Equation (6-13):

$$\varphi = \frac{\varepsilon_c}{c_1} = \frac{0.003}{0.33307} = 0.009007$$

d. Calculate the compressive force in the top wythe using Equation (6-15). This will incorporate Hognestad's Equation (6-14).

$$C_1 = b * f_c' * \frac{\varphi_1 * c_1^2}{\varepsilon_0} * \left(1 - \frac{\varphi_1 * c_1}{3\varepsilon_0}\right)$$

$$C_1 = 36\ in * 9.23\ ksi * \frac{0.009007 * 0.33307^2}{0.002}$$

$$* \left(1 - \frac{0.009007 * 0.33307}{0.006}\right) = 83\ kips$$

e. Calculate the strain and stress in the steel using Equations (6-17). The stress will come from a stress-strain curve for the actual steel in this panel as shown in Figure C-10.

$$\varepsilon_s = 0.003 * \frac{2.0 - 0.33307}{0.33307} = 0.01501$$

$$f_s = 78.65\ ksi$$

f. Calculate the tension force in wythe 1 with Equation (6-20)

$$T_1 = 78.65\ ksi * 0.44\ in^2 = 34.6\ kips$$

g. Enforce force equilibrium for wythe 1 with Equation (6-21):

$$C_1 - T_1 = 83\ kips - 34.6\ kips = 48.4\ kips = F_{sum} \quad \therefore \quad OK$$

4. Find C_2 and T_2 for the second wythe

a. Assume both wythes will deflect equally, therefore assume $\varphi_2 = \varphi_1 = 0.009007$

b. Assume a value of c_2. Assume c_2 = -6.5 (the neutral axis is not in the bottom wythe; no compression force)

c. Calculate the compressive force in the bottom wythe, C_2, using Equation (6-22). The compressive force in the concrete will again utilize Hognestad's equation to estimate the concrete compressive strength, but it is critical here because Whitney's stress block is only valid when the top fiber is at 0.003 strain and in the case of partial composite action, this will not be true.

$$C_2 = b * f_c' * \frac{\varphi_2 * c_2^2}{\varepsilon_0} * \left(1 - \frac{\varphi_2 * c_2}{3\varepsilon_0}\right)$$

$$C_2 = 0\ kips$$

d. Calculate the strain and stress in the steel. This step is only necessary to calculate the tension force in wythe 2, and since we discovered in step 2 that the steel yields, this step is unnecessary and we move to step 4e.

e. Calculate the tension force in wythe 2. Because the Steel has yielded:

$$T_2 = 48.4\ kips$$

f. Enforce force equilibrium for Wythe 2 with Equation (6-25):

$$T_2 - C_2 = 48.4\ kips - 0\ kips = 48.4\ kips = F_{sum} \quad \therefore \quad OK$$

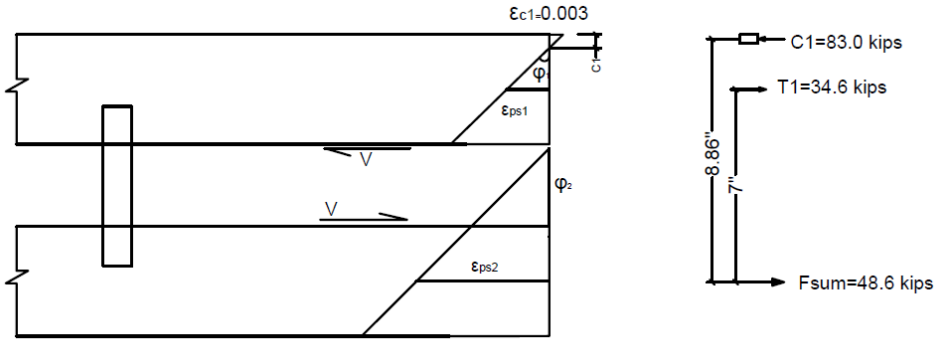

Figure C-8 Thermomass A Panel Design Example

5. Calculate the ultimate moment of the concrete sandwich wall panel using Equation (6-26). In addition, Using Equation (6-16) to calculate the centroid of C_1

$$x_{c1} = c_1 - \frac{c_1 * (8 * \varepsilon_o - 3 * \varphi_1 * c_1)}{12 * \varepsilon_o - 4 * \varphi_1 * c_1}$$

$$= 0.333 - \frac{0.333 * (8 * 0.002 - 3 * 0.009 * 0.333)}{12 * 0.002 - 4 * 0.009 * 0.333} = 0.139\ in$$

$$M_1 = C_1 * (d_1 - x_{c1}) = 83 * (2.0 - 0.139) = 154.5\ kip * in$$

$$M_2 = C_2 * (d_2 - x_{c2}) = 0$$

$$M = M_1 + M_2 + F_{sum} * \left(\frac{t_{wy1} + t_{wy2}}{2} + t_{ins}\right)$$

$$= 154.5 + 0 + 48.4 * \left(\frac{4 + 4}{2} + 3\right) = 493.3\ kip * in$$

$$= \mathbf{41.1\ \ kip * ft}$$

D Panel Analysis Example (HK Composite connectors, Mild Reinforcement)

Section and Material Properties

$f_c' = 9.23\ ksi$ $A_s = 0.44\ in^2$

$b = 36\ in$ $t_{wy1} = 4\ in$

$t_{wy2} = 4\ in$ $t_{ins} = 3\ in$

$L = 192\ in$

$x_i = \begin{bmatrix} 16 \\ 32 \\ 48 \\ 64 \\ 80 \end{bmatrix} in$ $N = 3$

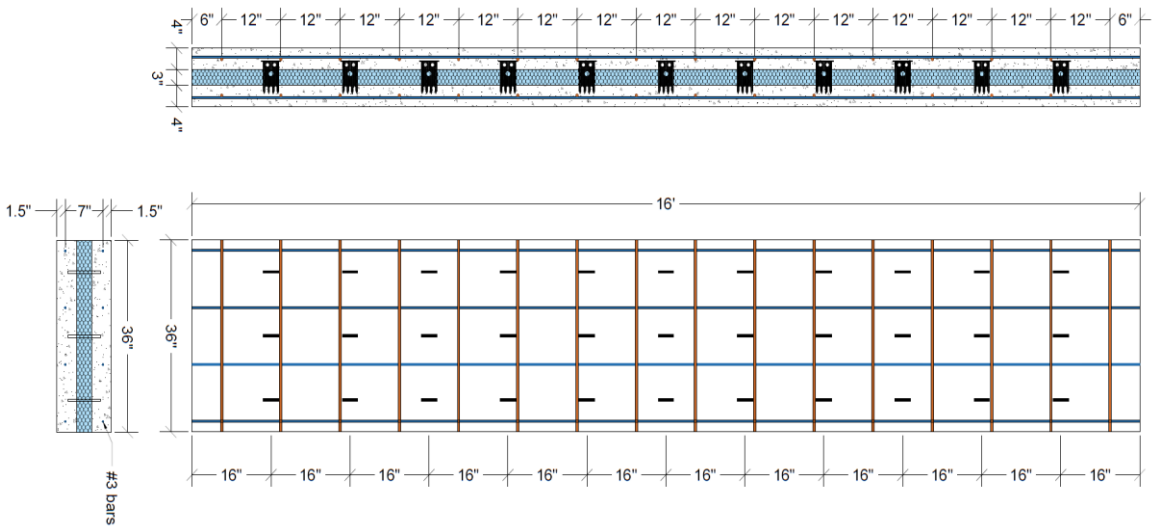

Solution

1. Find the forces in each connector using the load-slip relationship. Using an influence line, the ultimate slip (δ_{Ult}) that occurs at the maximum force is determined to be 0.12 in. In addition, the sum of the forces should be less than or equal to A_s * f_s in the bottom wythe. Calculate slip using Equation (6-11):

$$\delta(i) = \frac{\delta_{Ult}}{\frac{L}{2} - x_1} * \left(\frac{L}{2} - x_i\right)$$

$$\delta(i) = \frac{0.12\ in}{\frac{192}{2} in - 16\ in} * \begin{bmatrix} \frac{192}{2} - 16 \\ \frac{192}{2} - 32 \\ \frac{192}{2} - 48 \\ \frac{192}{2} - 64 \\ \frac{192}{2} - 80 \end{bmatrix} \text{in} = \begin{bmatrix} 0.12 \\ 0.0968 \\ 0.0726 \\ 0.0484 \\ 0.0242 \end{bmatrix} in$$

Find F_i at each connector by using Figure C-9.

$$F(i) = \begin{bmatrix} 3.13 \\ 3.52 \\ 3.91 \\ 2.97 \\ 2.03 \end{bmatrix} kips$$

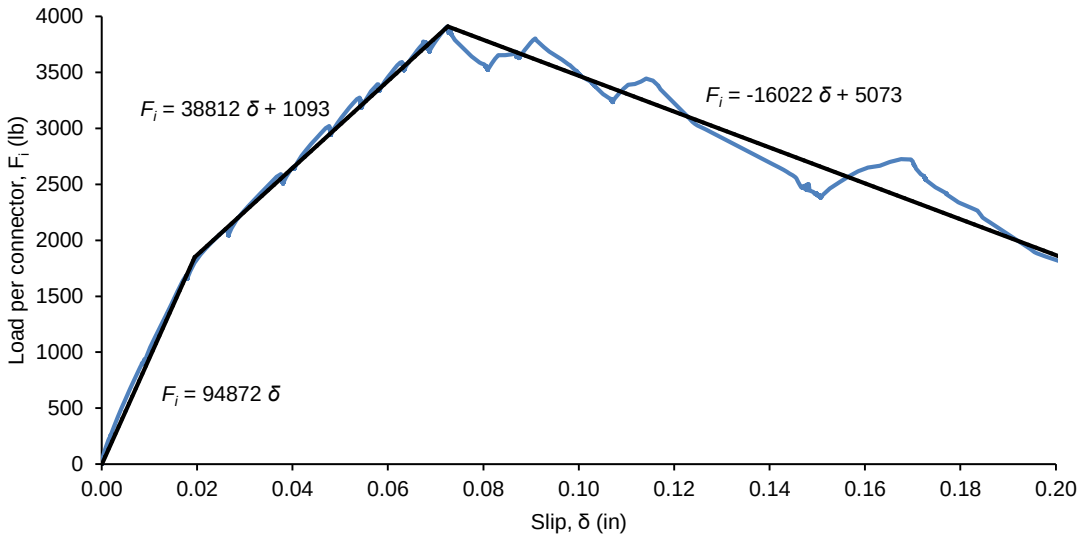

Figure C-9 Load-slip curve for HK

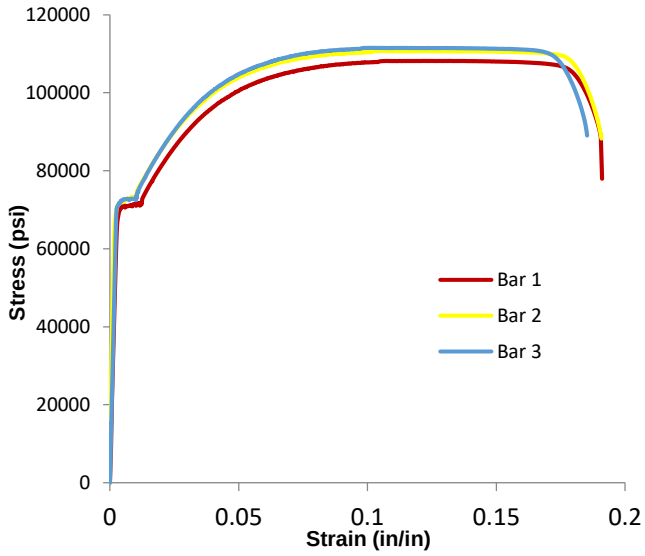

Figure C-10 Actual stress vs strain of HK and Thermomass panel

2. Find the total sum of the connector forces using Equation (6-12):

$$F_{sum} = N * \sum F_i = 46.7\ kips$$

$$F_{sum} \leq A_s * f_u = 0.44\ in^2 * 110\ ksi = 48\ kip \quad \therefore \quad OK$$

3. Find C_1 and T_1 for the first wythe

   a. Assume ε_c = 0.003.

   b. Assume a value of c_1. We will assume c_1 = 0.327 in.

   c. Calculate curvature using Equation (6-13):

$$\varphi_1 = \frac{\varepsilon_c}{c_1} = \frac{0.003}{0.327} = 0.00917$$

   d. Calculate the compressive force in the top wythe using Equation (6-15). This will incorporate Hognestad's Equation (6-14).

$$C_1 = b * f_c' * \frac{\varphi_1 * c_1^2}{\varepsilon_0} * \left(1 - \frac{\varphi_1 * c_1}{3\varepsilon_0}\right)$$

$$C_1 = 36\ in * 9.23\ ksi * \frac{0.00917 * 0.327^2}{0.002} * \left(1 - \frac{0.00917 * 0.327}{0.006}\right)$$

$$= 81.5\ kips$$

e. Calculate the strain and stress in the steel using Equations (6-17) and (6-18). The stress will come from a stress-strain curve for the actual steel used in the panel as shown in Figure C-10.

$$\varepsilon_s = 0.003 * \frac{2.0 - 0.327}{0.327} = 0.01535$$

$$f_s = 79.0\ ksi$$

f. Calculate the tension force in wythe 1 with Equation (6-20)

$$T_1 = 79.0\ ksi * 0.44\ in^2 = 34.8\ kips$$

g. Enforce force equilibrium for wythe 1 with Equation (6-21):

$$C_1 - T_1 = 81.5\ kips - 34.8\ kips = 46.7\ kips = F_{sum} \quad \therefore \quad OK$$

4. Find C_2 and T_2 for the second wythe

a. Assume both wythes will deflect equally, therefore assume $\varphi_2 = \varphi_1 = 0.00917$.

b. Assume a value of c_2. Assume $c_2 = -4.7$ (neutral axis in the foam, no compression force)

c. Calculate the compressive force in the bottom wythe, C_2, using Equation (6-22). The compressive force in the concrete will again utilize Hognestad's equation to estimate the concrete compressive strength, but it is critical here because Whitney's stress block is only valid when the top

fiber is at 0.003 strain and in the case of partial composite action, this will not be true.

$$C_2 = b * f_c' * \frac{\varphi_2 * c_2^2}{\varepsilon_0} * \left(1 - \frac{\varphi_2 * c_2}{3\varepsilon_0}\right)$$

$$C_2 = 0\ kips$$

d. Calculate the strain and stress in the steel using the actual stress strain relationship for the steel in the panel as shown in Figure C-10.

$$\varepsilon_s = \varphi_2\ (d_2 - c) = 0.00917 * \big(2 - (-4.7)\big) = 0.0614$$

$$f_s = 106.1\ ksi$$

e. Calculate the tension force in wythe 2 using Equation (6-24):

$$T_2 = f_s * A_s = 106.1\ ksi * 0.44\ in^2 = 46.7\ kips$$

f. Enforce force equilibrium for wythe 2 with Equation (6-25):

$$T_2 - C_2 = 46.7\ kips - 0\ kips = 46.7\ kips = F_{sum} \quad \therefore \quad OK$$

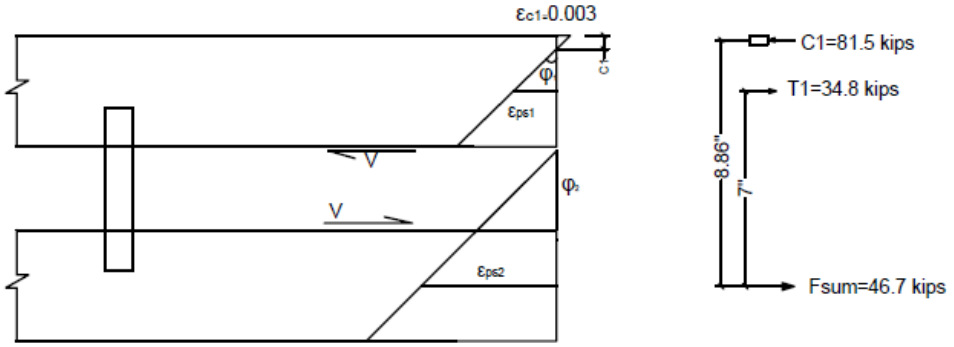

Figure C-11 HK Panel Design Example

5. Calculate the ultimate moment of the concrete sandwich wall panel using Equation (6-26). In addition, Using Equation (6-16) to calculate the centroid of C_1

$$x_{c1} = c_1 - \frac{c_1 * (8 * \varepsilon_o - 3 * \varphi_1 * c_1)}{12 * \varepsilon_o - 4 * \varphi_1 * c_1}$$

$$= 0.327\ in - \frac{0.327\ \text{in} * (8 * 0.002 - 3 * 0.00917 * 0.327)}{12 * 0.002 - 4 * 0.00917 * 0.327} = 0.1362\ in$$

$$M_1 = C_1 * (d_1 - x_{c1}) = 81.5\ kips * (2.0 - 0.1362) = 151.9\ kip * in$$

$$M_2 = C_2 * (d_2 - x_{c2}) = 0$$

$$M = M_1 + M_2 + F_{sum} * \left(\frac{t_{wy1} + t_{wy2}}{2} + t_{ins}\right)$$

$$= 151.9\ kip * ft + 0 + 46.7\ kips * \left(\frac{4\ in + 4\ in}{2} + 3\ in\right) = 478.8\ kip * in$$

$$= \mathbf{39.9\ \ kip * ft}$$

APPENDIX D.

Partially-Composite Strength Prediction Method Design Example

As with many design problems, an example may clarify the ultimate moment method described in this chapter. This example only takes into account a single load case, but illustrates the design method to achieve full-composite action at failure. There are two major stages to consider in this design of concrete sandwich wall panels. The first stage is to find the required area of steel, and the second stage is to determine the number and spacing of connectors needed. Figure D-1 depicts the sandwich panel used in this example.

Panel Properties

$L = 37\ ft$ $Span = 35\ ft$

$t_{wy1} = 3\ in$ $t_{wy2} = 3\ in$

$t_{ins} = 3\ in$ $b = 8\ ft$

$f_c' = 6.0\ ksi$ $f_y = 60\ ksi$

$Wind\ Load = W_L = 30\ psf$ Insulation Type: XPS

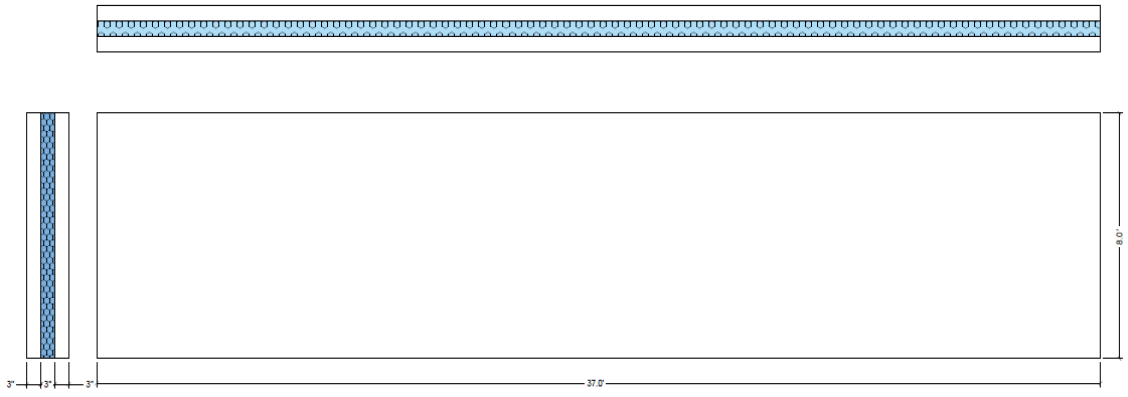

Figure D-1 Design example sandwich panel dimensions

Solution

a. First, assume the panel acts with full-composite action and find the required area of steel.

$$\phi = 0.9 \qquad d_1 = 1.5\ in \qquad d_2 = 1.5\ in$$

Nominal moment may be calculated using Equation (6-5) as

$$M_n = \frac{M_u}{\phi} = A_{s1} * f_{s1} * \left(d_1 - \frac{a}{2}\right) + A_{s2} * f_{s2} * \left(d_2 + t_{wy_1} + t_{ins} - \frac{a}{2}\right)$$

Ultimate factored moment is calculated as

$$M_u = \frac{1.6 * W_L * b * L^2}{8} = \frac{1.6 * 30\ psf * (8\ ft) * (35\ ft)^2}{8} = 58.8\ k.ft$$

Assume $As_1 = As_2 = 1.514\ in^2\ and\ (f_{s1}\ \&\ f_{s1})\ are\ yield$

$$a = \frac{(As_1 + As_2) * f_y}{0.85 * f_c' * b} = \frac{(1.514 + 1.514) in^2 * 60\ kis}{0.85 * 6\ ksi * 8\ ft * \frac{12in}{ft}} = 0.371\ in$$

Using strain compatibility, the stress in the steel is calculated as

$$f_s = E_s * \left(\varepsilon_c * \frac{\left(d - \frac{a}{\beta_1}\right)}{\frac{a}{\beta_1}} \right) \leq f_y$$

Where

$$\beta_1 = 0.85 - 0.05 * (f_c' - 4\ ksi) = 0.85 - 0.05 * (6\ ksi - 4ksi) = 0.75$$

Stress is then calculated as

$$f_{s1} = 29000 * \left(0.003 * \frac{\left(1.5 - \frac{0.317}{0.75}\right)}{\frac{0.317}{0.75}} \right) = 222\ ksi > f_y \quad \therefore f_{s1} = 60$$

$$f_{s2} = 29000 * \left(0.003 * \frac{\left(7.5 - \frac{0.317}{0.75}\right)}{\frac{0.317}{0.75}} \right) = 1457\ ksi > f_y \quad \therefore f_{s2} = 60$$

Substituting, we can solve for A_s:

$$\frac{58.8\ k.ft}{0.9} = A_s * 60\ ksi * \left(1.5\ in - \frac{a}{2}\right) + A_s * 60\ ksi * \left(7.5\ in - \frac{a}{2}\right)$$

$$A_s = 1.52\ in^2 = Assumed\ A_s \quad \therefore OK$$

Therefore, **use eight #4 bars in each wythe**.

Assume the shear force provided by the connectors at midspan is equal to the area of steel times the steel yield stress.

$$F_{sum} = A_s * f_y = (8 * 0.2\ in^2) * 60\ ksi = 96\ kips.$$

b. Find the ultimate moment of the panel:

   i. Find C_1 and T_1 for wythe 1

      a. Assume $c_1 = 0.523\ in$

      b. Calculate curvature as

$$\phi_1 = \frac{\varepsilon_c}{c_1} = \frac{0.003}{0.523} = 0.005736$$

      c. Using Whitney Stress block, we calculate compressive force of

$$C_1 = 0.85 * f_c' * b * \beta_1 * c_1$$

$$C_1 = 0.85 * 6\ ksi * 96\ in * 0.75 * 0.523\ in = 192\ kips$$

      d. Strain and stress of steel are calculated as

$$\varepsilon_s = \varepsilon_c \frac{d_1 - c_1}{c_1} = 0.003 * \frac{1.5 - 0.523}{0.523} = 0.056$$

$$f_s = \varepsilon_s * E_s = 0.056 * 29000\ ksi = 1624\ ksi >$$

$$60ksi \quad \therefore \quad f_s = f_y = 60\ ksi$$

e. Tension force in the wythe is calculated by

$$T_1 = f_s * A_s = 60\ ksi * (8 * 0.20\ in^2) = 96\ kips$$

f. Check for $C_1 - T_1 = F_{sum}$

$$C_1 - T_1 = 192\ kips - 96\ kips = 96\ kips = F_{sum} \quad \therefore \quad OK$$

ii. Find C_2 and T_2 for wythe 2

a. Assume $\varphi_2 = \varphi_1 = 0.005736$

b. Guess $c_2 = 0$ (neutral axis at *top* fiber of wythe 2)

c. It is recommended to facilitate design that there is zero compressive force in wythe 2, therefore

$$C_2 = 0\ kips$$

d. We also assume the steel has yielded, therefore

$$f_s = f_y = 60\ ksi$$

e. Tensile force in the bottom wythe will be calculated as

$$T_2 = f_s * A_s = 60\ ksi * (8 * 0.20\ in^2) = 96\ kips$$

f. Check for $C_2 - T_2 = F_{sum}$

$$C_2 - T_2 = 96\ kips - 0\ kips = 96\ kips = F_{sum} \quad \therefore \quad OK$$

iii. The moment is determined to be

$$M_1 = C_1 * \left(d_1 - \frac{a_1}{2}\right) = 192\ kips * \left(1.5 - 0.523 * \frac{0.75}{2}\right)$$

$$= 250.3\ kip * in$$

$$M_2 = C_2 * \left(d_2 - \frac{a_2}{2}\right) = 0\ kip * in$$

$$M_n = M_1 + M_2 + F_{sum} * \left(\frac{t_{wy1} + t_{wy2}}{2} + t_{ins}\right) = 250.3\ kip * in +$$

$$96\ kips * 6\ in =$$

826.3 k-in = **68.8 k-ft**

$$M_u = 58.8\ kip.ft < (\phi M_n = 0.9 * 68.8 = 61.92\ kip.ft) \qquad \therefore OK$$

c. Find the number of connectors and the spacing that provide the required shear force.

Assume 4 HK Composite connectors at 24 spacing. First calculate the slip using Equation (6-11).

$$\delta(i) = \frac{\delta_{Ult}}{\frac{L}{2} - x_1} * \frac{L}{2} - x_i$$

$$\delta(i) = \frac{0.0726\ in}{222\ in - 24\ in} * \begin{bmatrix} 222 - 24 \\ 222 - 48 \\ 222 - 72 \\ 222 - 96 \\ 222 - 120 \\ 222 - 144 \\ 222 - 168 \\ 222 - 192 \end{bmatrix} \text{in} = \begin{bmatrix} 0.0726 \\ 0.0638 \\ 0.055 \\ 0.0462 \\ 0.0374 \\ 0.0286 \\ 0.0198 \\ 0.011 \end{bmatrix} in$$

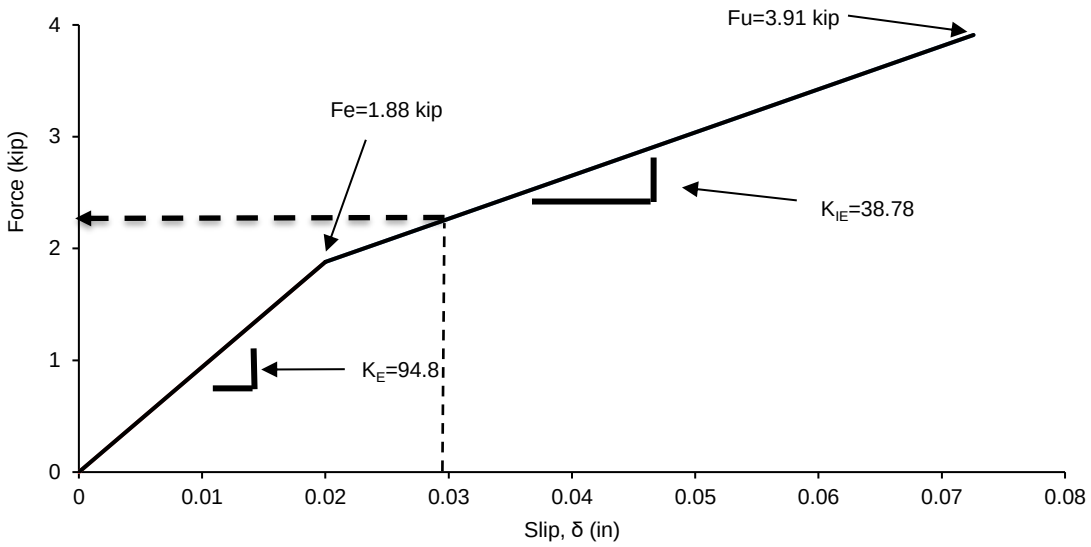

Figure D-2 Load-slip curve for D connector

Using Table 4-12, a design curve may be created for the recommended design. The force at each connector location can then be determined using the load-slip curve for the HK connector (see Figure D-2). Alternatively, the following equations may be used to calculate the force at each value of slip.

$$F(i) = \begin{cases} K_E * \delta(i) & if\ \delta \le \delta_E \\ (F_e - K_{IE} * \delta_E) + K_{IE} * Slip & if\ \delta > \delta_E \end{cases}$$

$$F(i) = \begin{cases} 94.8 * \delta & if\ \delta \le \delta_E \\ 1.11 + 38.78 * \delta & if\ \delta > \delta_E \end{cases}$$

$$F(i) = \begin{bmatrix} 3.91 \\ 3.57 \\ 3.23 \\ 2.89 \\ 2.55 \\ 2.21 \\ 1.861 \\ 1.0 \end{bmatrix} kip$$

These values can then be used with Equation (6-12) to calculate F_{sum}:

$$F_{sum} = 4 * 21.26\ kip = 85\ kip < A_s * f_y \qquad \therefore \qquad Not\ OK$$

Therefore, Assume 4 HK Composite connectors at 20 spacing.

Again, calculate the slip using Equation (6-11) as

$$\delta(i) = \frac{\delta_{Ult}}{\frac{L}{2} - x_1} * \left(\frac{L}{2} - x_i\right)$$

$$\delta(i) = \frac{0.0726\ in}{222\ in - 20\ in} * \begin{bmatrix} 222-20 \\ 222-40 \\ 222-60 \\ 222-80 \\ 222-100 \\ 222-120 \\ 222-140 \\ 222-160 \\ 222-180 \\ 222-200 \end{bmatrix} \text{in} = \begin{bmatrix} 0.0726 \\ 0.0654 \\ 0.0582 \\ 0.051 \\ 0.0438 \\ 0.0366 \\ 0.0295 \\ 0.0223 \\ 0.0151 \\ 0.008 \end{bmatrix} in$$

The force at each connector location can then be determined using the load-slip curve for the HK connector (see Figure D-2).

$$F(i) = \begin{bmatrix} 3.91 \\ 3.63 \\ 3.35 \\ 3.07 \\ 2.79 \\ 2.51 \\ 2.24 \\ 1.96 \\ 1.43 \\ 0.75 \end{bmatrix} kip$$

These values can then be used with Equation (6-12) to calculate F_{sum}:

$$F_{sum} = 4 * 25.65\ kip = 102.6\ kip > A_s * f_y \quad \therefore OK$$

Therefore, using 4 HK Composite connectors at 20 in. center-to-center spacing as shown in Figure D-3 is acceptable.

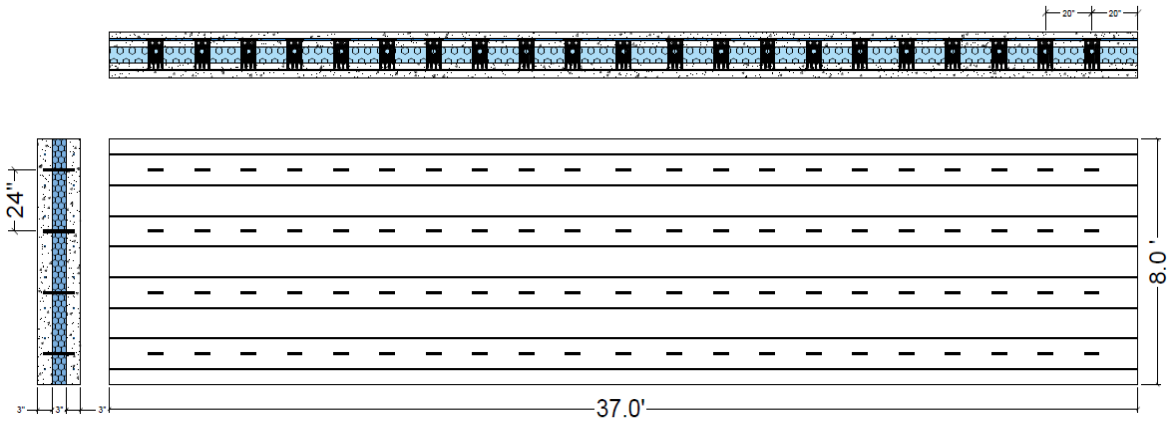

Figure D-3 Sandwich panel detail for Design Example